CATALYST AGING TESTS AND THE ROLE OF CATALYST WETTING ON HYDRODESULFURIZATION OF A COAL DERIVED LIQUID

By

DHIRENDRA CHHOTALAL MEHTA

Bachelor of Science
Banaras Hindu University
Varanasi, India
1970

Master of Science
Oklahoma State University
Stillwater, Oklahoma
1972

Submitted to the Faculty of the Graduate College
of the Oklahoma State University
in partial fulfillment of the requirements
for the Degree of
DOCTOR OF PHILOSOPHY
May, 1978

CATALYST AGING TESTS AND THE ROLE OF CATALYST WETTING ON HYDRODESULFURIZATION OF A COAL DERIVED LIQUID

Thesis Approved:

Billy L. Crynes
Thesis Adviser

Robert S. Treseder, Jr.

Don F. Kincannon

Jack H. Cleland

Kenneth J. Bell

Norman N. Durham
Dean of the Graduate College

ACKNOWLEDGMENTS

The subject of this study was the catalytic hydrodesulfurization of raw anthracene oil in a trickle bed reactor. Experiments were carried out at temperatures of 600, 650, 700 and 750 F (314, 343, 371 and 399 C), pressures of 500, 1,000 and 1,500 psig and liquid volume hourly space times ranging from 0.325 to 1.480 hours. The effect of catalyst wetting characteristics were investigated and the catalysts were also tested for their aging characteristics. Various reaction rate models were compared for their relative fit to the data.

I am deeply indebted to my thesis adviser Dr. B. L. Crynes for his expert guidance and valued suggestions during the course of my doctoral program. I would like to express my sincere gratitude to my examining committee which consisted of Dr. J. H. Erbar, Dr. R. L. Robinson, Jr., and Dr. D. F. Kincannon for their constructive criticism and suggestions. Discussions with other faculty members and fellow graduate students were also of considerable help.

Special thanks are due Dr. R. Sivasubramanian and Mr. Mushtaq Ahmed for their continued assistance during the course of my doctoral program. I am thankful to Richard Cavett, Donald Kennedy, Mohamed Ghaly, Kerry Scott, Nitin Mehta and Anthony Jones for the long hours they patiently spent operating the equipment. I am also grateful to my fellow graduate student, Mr. Kam Tong Wan, for his fortitude during the project.

The financial assistance from the School of Chemical Engineering at Oklahoma State University, Pittsburg and Midway Coal Mining Company and The U. S. - Energy Research and Development Administration is gratefully acknowledged.

The financial assistance from my present employer - Combustion Equipment Associates, Inc. - is gratefully acknowledged. Special thanks are due my supervisor, Mr. J. M. Falco, and colleagues, Mr. R. Davis, Mr. R. Rasbold, Mr. M. Kinkhabwala and Mr. H. Master, for their continued cooperation.

The editorial assistance from Mr. Ed Kelly is gratefully appreciated. I am also grateful to Ms. Rosalie LoBono and Mrs. Wanda Dexter for typing assistance. Special thanks to them for adhering to my schedule.

On a personal note, I shall always be thankful to all my family, relatives and friends who came to my mother's aid at the time of her greatest need. I am deeply grateful to Prof. and Mrs. Crynes and their entire family for extending to my wife and me the warmth of their friendship and making us feel like members of their family.

I shall always be indebted to my mother and sister, without whose personal sacrifices and encouragement this graduate study would not have been possible. I am eternally grateful to my father and brother for the guidance and provision they afforded their family. May their souls rest in peace.

Last, but in no ways least, I can never repay the debt I owe to my beloved wife, Rajul.

TABLE OF CONTENTS

LIST OF TABLES

LIST OF FIGURES

CHAPTER I

INTRODUCTION

The idea that the United States faced a critical shortage in energy supplies was first discussed some five years ago. At the time, neither the American people nor government gave the notion serious consideration. Sudden action, however, by the Organization of Petroleum Exporting Countries (OPEC) in 1973 made the Western industrial nations realize the great extent to which they depended upon imported oil. Authoritative projections of future energy requirements then began to forecast the serious crisis that lay ahead.

Energy consumption in the U. S. increased steadily from 1960 to 1974 at an average annual rate of about 4.1% (1). According to the reports of the U. S. Bureau of Mines (2), the energy consumption in the U. S. then showed successive declines in 1974 and 1975. The energy use in 1973 was at 74,555 trillion British thermal units (Btu) followed by 73,121 trillion Btus in 1974 and 70,580 trillion Btus in 1975. Despite the drop in 1974 and 1975, the projections for future energy requirements show a steady increase. The U. S. energy use in 1976 has already shown a rise of 4.8% over 1975. Jack Bridges (3) has summarized some of these projections in his report presented before the Joint Senate Commitee on Atomic Energy, March 1973. Figure 1 shows various energy consumption forecasts by different agencies in terms

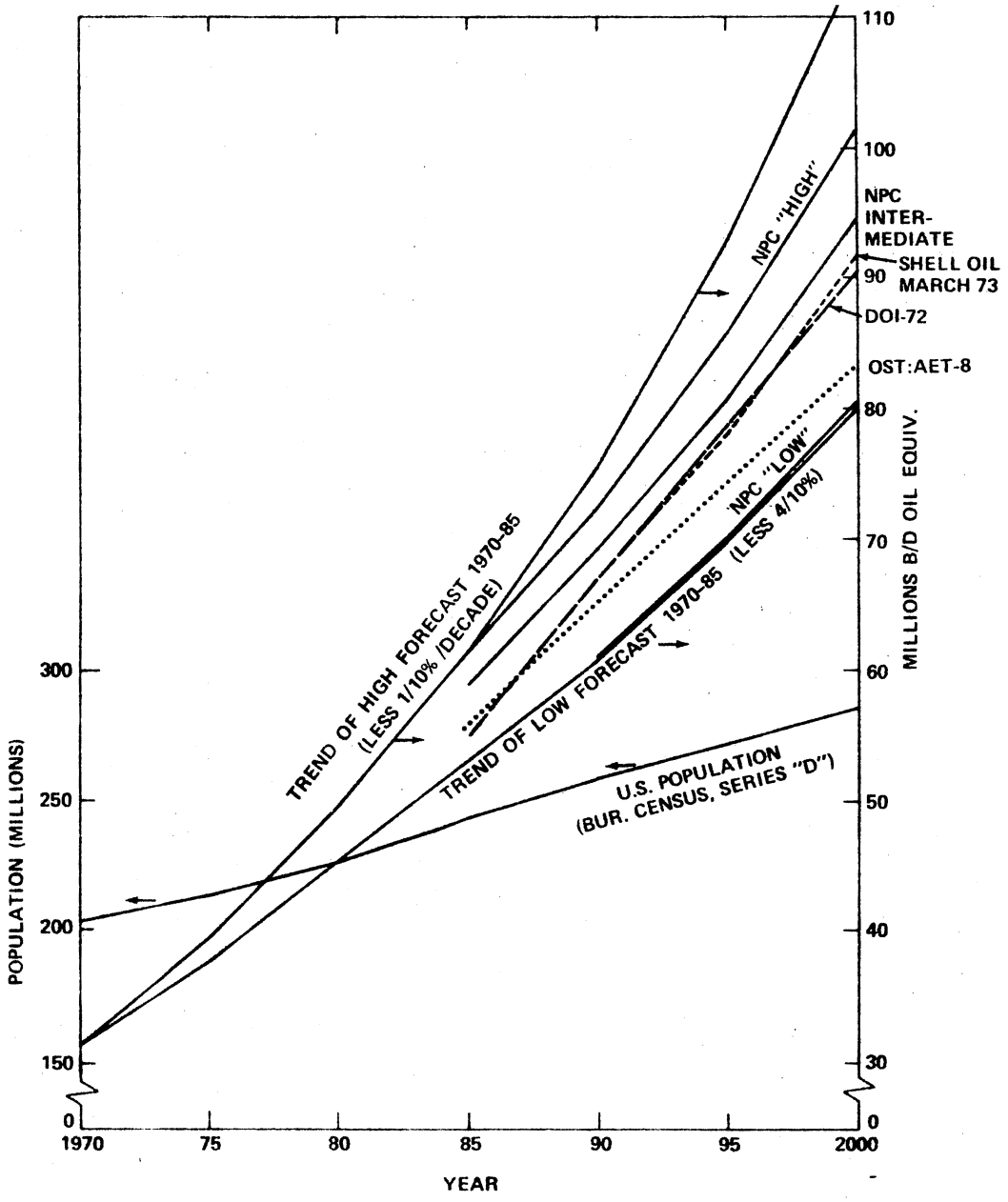

Figure 1. The Forecast of the Energy Demand up to Year 2000 (3).

of millions of barrels of oil equivalent (BOE*) per day. These forecasts show a distinct trend in energy consumption for any given year based on different annual growth rates. Figure 1 only demonstrates the projected consumption while not considering the source of energy. Based on recent trends and projected rates of development of resources, Jack Bridges indicated in Figure 2 what source of energy would possibly fill the demand in the years to come. Note that the energy from coal and nuclear will play an increasingly dominant role in the attempt to fulfill the high energy demand. Also noticeable are the contributions of oil and natural gas, which are expected to decline both quantitatively and in relation to other sources. Any delay in the development of the alternative energy sources (such as geothermal, Alaskan and offshore oil, solar, shale oil or even nuclear) could mean another round of energy shortages and/or increasing imports.

The OPEC unilaterally raised the price of their crude oil almost fourfold during October 1973 (4). At the same time, the OPEC also imposed an embargo on oil exported to the U. S. These drastic actions by the OPEC had a significant impact on the economy and stability of those nations depending heavily on the oil imports. The sudden jump in the crude oil price was a temporary disaster for Japan and continues to have lingering effects on many of the European nations and the U. S. (5). The crude price increase had the greatest immediate impact on the foreign balance of payment deficit. For example, the U. S. imported 5.7 million barrels per day (BPD) of crude oil in May 1973 at an

---

*Amount of energy produced from various energy sources converted in terms of barrels of oil producing equivalent energy.

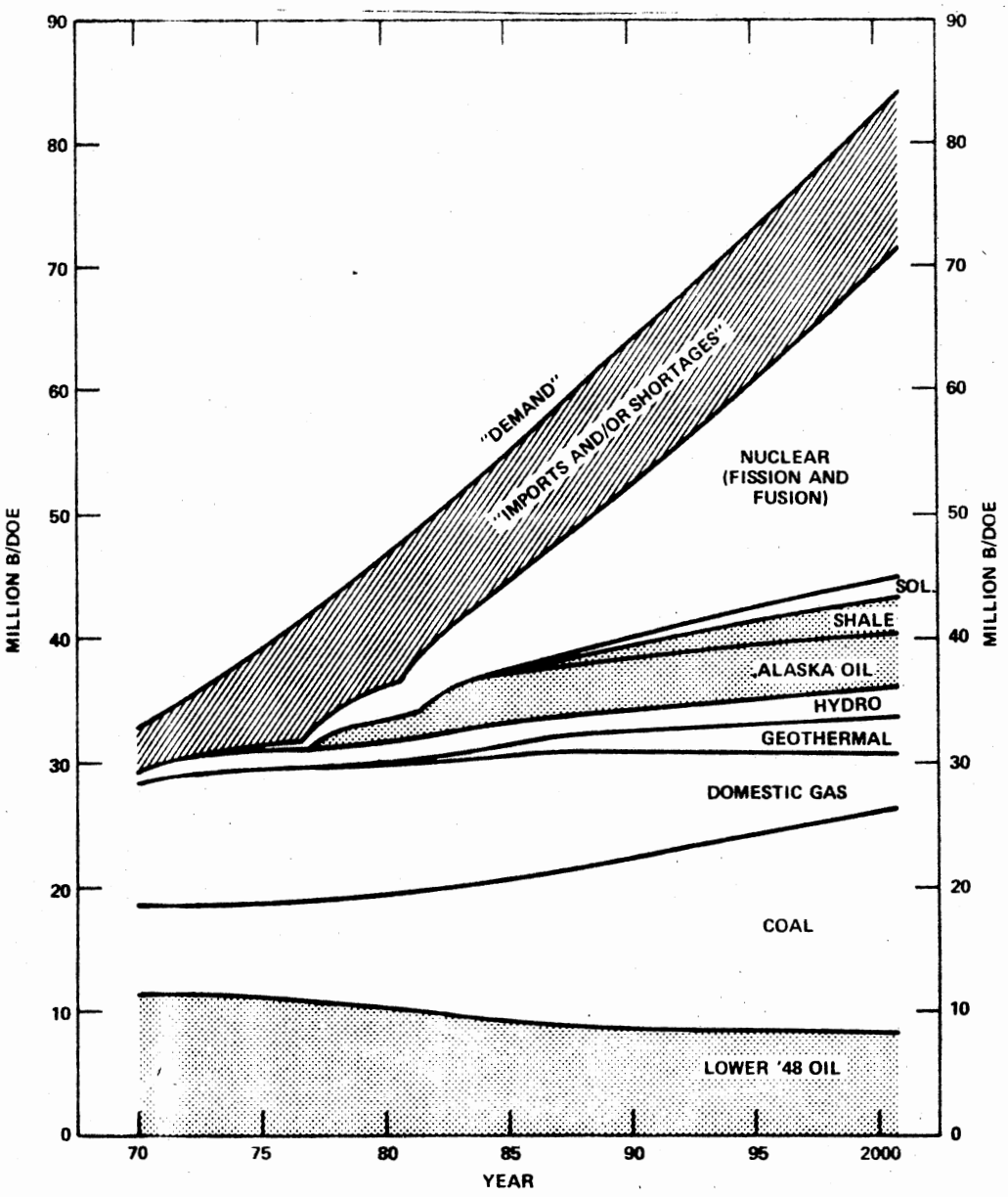

Figure 2. The Role of Various Energy Sources in Future Energy Situation (3).

approximate cost of $17 million daily or $6.2 billion annually (6). In November 1974, the crude oil imports were 6.5 million BPD, an approximate cost of $70 million daily or $25 billion annually. The crude oil imports in 1976 rose to 7.3 million BPD. At this rate, it is estimated that the reliance on the import of crude oil would cost the U. S. about $800 billion between 1974 and 1985.

Although the OPEC actions may have been the catalyst for the energy crisis in the U. S., other internal factors have also contributed greatly. The U. S. government's price control of natural gas is one such factor. These controls resulted in a downward trend in the natural gas prices from 23.25 cents per thousands cubic feet (¢/Mcf) in 1960 to 18.5 ¢/Mcf in 1968 (6), (7). The price of natural gas was controlled to such a great degree that in 1973 the average cost of natural gas was less than one-third the cost of oil for an equivalent amount of heating value. The result has been a reduction in exploration activities for natural gas. Developed reserves have dropped from 21.1 trillion cubic feet (Tcf) per year during 1964-1967 to 11 Tcf per year during 1967-1971 period. The controlled natural gas price has also resulted in depressing the prices of other energy sources. On a constant 1972 dollar basis the price of crude oil in the U. S. has declined from $3.93 per barrel in 1963 to $3.39 per barrel in 1972 (6). These lower costs also lessen the incentive for exploration and hinder the development of new reserves. A new analysis made by the Staff of the American Gas Association (AGA) (8) projects a continued decline in the overall production of natural gas under price controls. The AGA staff analysis shows that at a maximum wellhead price of 52 ¢/Mcf, the natural gas production would decline from 19.2 Tcf in 1975 to 12.5 Tcf

in 1990. They also conclude that at the deregulated prices, natural gas production would be maintained at a steady rate of 20.0 Tcf.

Other factors include actions of the Environmental Protection Agency (EPA). The stringent environmental regulations delayed or halted some of the exploration and production plans for additional sources of energy. EPA actions also hindered the leasing of public lands for exploration purposes. The drop in new reserve developments coupled with rising energy consumption brings us back to oil import to fill the gap between supply and demand. This is clearly shown in Figure 2.

Middle Eastern crude oil was abundant, at cheap rates, until October 1973. This supply was taken for granted and was assumed to be perpetual by its users. But the turn of events in the Fall of 1973 shattered these delusions. The situation in the U. S. became grave due to the threat of future crude oil embargoes at the whim of the OPEC. These chain of events prompted President Nixon (9) to announce major initiatives in a nationally televised speech on November 7, 1973:

> Let us unite in committing the resources of this nation to a major new endeavor. An endeavor that in this bicentennial era we can appropriately call Project Independence. Let us pledge that by 1980 under Project Independence we shall be able to meet America's energy needs from America's own energy resources (9, p. 92).

The energy experts do not believe that the U. S. could achieve independence from imported oil by 1980. But the concept of Project Independence (PI) is still conceivable and could be fulfilled by some later date. The appropriation by the Energy Research and Development Administration (ERDA) for research in the energy related areas for the year 1976 was $2.2 billion and the budget during 1977 has jumped to

$3.0 billion (10). ERDA is also lobbying for a law to provide $2.0 billion in loan guarantees for synthetic fuel productions from coal, oil shale and other sources. The details of the research activities will be discussed later in this chapter. The Federal Energy Administration (FEA) has completed a massive energy report that scrutinizes the concepts of PI. This 800-page document, released November 12, 1974, made non-conclusive but very specific remarks (9). The major remarks from the report include:

(i) Even though zero imports are possible by 1985, this course of action is not warranted economically or politically.

(ii) The U. S. will have to depend on the existing technology to raise any additional energy sources through 1985. New resources would play significant roles in the energy supply picture some time in future dates.

(iii) New exploration and research funding will depend primarily on the price of crude oil.

(iv) Although some environmental and economic dislocations will occur due to the energy crunch, major disruption may not be necessary and probably can be avoided.

(v) The U. S. economic resources will probably have greater influence on the accelerated supply strategy.

The principal goal of PI is to reduce the impact on the economy of future oil embargoes and balance of trade deficits. There are several alternatives at hand by which the goal of energy independence may be achieved. These are:

(a) Conserve energy,

(b) Explore for more oil and gas in the U. S.

(c) Convert coal by liquefaction and gasification processes.

(d) Develop new sources of energy.

A discussion of these alternatives follows:

(a) The days of wasteful use of energy are gone. Every effort must be made to use energy at a higher and higher efficiencies. As a matter of fact, the energy consumption in 1974 dropped about 2.2% from the 1973 level and it further declined another 3.5% in 1975 (2). This declining trend in energy consumption is the first since 1952. The Secretary of the Interior, Rogers C. B. Morton (1) attributed the decline in the energy consumption to (a) the Arab oil embargo during Fall 1973 and Spring 1974, (b) the escalation of fuel costs, which have had a direct influence on everybody's pocketbook, (c) the 1973 recession and slowdown of industrial production, (d) a relatively mild winter in 1973, which required comparatively less energy to heat our homes, and (e) the participation of government and private sectors in conservation efforts (such as lowering thermostat settings from 72 F to 68 F (22 C to 20 C) during winter, increased insulation of commercial and household buildings, reducing speed limit on highways from 70 miles per hour (mph) to 55 mph, etc.). The combination of all of these factors resulted in the decrease in energy consumption during 1974 and 1975. This decline boosted the morale of the proponents of Project Independence.

(b) Although every effort is and will be made to reduce energy waste, more oil and gas will have to be found to meet the growing energy demands of an expanding economy. A report of the Potential Gas Committee at Colorado School of Mines revealed that there is about 1,178 Tcf of gas yet to be discovered in the U. S., one third of which

is in Alaska (11). There is also an estimated 9.6 billion barrels of oil lying under the northern slopes of Alaska (12). The Alaskan oil and gas were discovered in 1968, but avid environmentalists forced delay in construction of the 789 mile trans-Alaska pipeline, citing possible ecological disruptions along the route. The construction of the pipeline was finally approved by Congress in 1974. The pipeline was completed recently and a complex system start-up operations began in the Summer of 1977 (13). The pipeline will handle 300,000 BPD of oil during the start-up stages and will later transport up to 2,000,000 BPD. The report by the Potential Gas Committee also indicated that most of the new reserves are deeper than 15,000 feet on the off-shores bordering the U. S. and Alaska. This is compared to the average well depth of 5,000 feet today. The operations on some of the oil wells were curtailed long ago due to unfavorable economics. Now that the oil and gas prices have gone up, these deep drilling operations can be resumed. In spite of the energy crisis, leases for drilling and exploring off-shore U. S. reserves are still delayed by the threats of environmentalists. (The exploration in the Gulf of Mexico is the only one in which small quantities of oil have been found (14).) These complications will certainly delay the accomplishment of PI. It is hoped that these obstacles will be overcome soon so that the goal of PI may be achieved.

(c) One of the major alternatives considered for supplementing the energy supplies of the U. S. is the increased use of coal. Since liquids and gases are more convenient and desired forms of energy, the efforts given to the concept of coal conversion to these forms have increased markedly. The U. S. coal reserves are estimated to be 3.2

trillion tons (15). A National Petroleum Council (NPC) study indicates that, based on present technology, approximately 150 billion tons (450 billion BOE) can be recovered economically from the total coal reserves.

In fact, the technology of coal processing to produce a synthetic liquid fuel is not new. The pioneering work by Bergius, a German scientist, earned him the Nobel prize for chemistry in 1932 (16). It is also believed that the Germans used the Bergius process to produce about 90 percent of their peak-time aviation and motor fuel during World War II. Another old process is the Fisher-Tropsch synthesis method. These processes must be further tested for use on the variety of U. S. coals. The economics of these methods must also be assessed. New investigations under the sponsorship of ERDA are developing new processes for the liquefaction of various U. S. coals. The details of these processes will be discussed later in this chapter.

Coal gasification technology is not new either. Gases such as water gas, producer gas, town gas, carburetted blue gas, and oil gas have been produced for over fifty years (17). The heat content of these gases has varied from 70 Btu per standard cubic feet (scf) to 420 Btu/scf compared to about 1,000 Btu/scf for natural gas. Therefore, these low-Btu gases became nearly obsolete once natural gas came into the energy market. The present drive for coal gasification requires gas from coal whose heat content can match that of the natural gas. With an abundant quantity of coal scattered throughout the U. S., the synthetic natural gas (SNG) can reach the diversified markets with less difficulty. ERDA (then Office of Coal Research) sponsored studies on different types of U. S. coals for gasification. Various private

industries also developed other processes to produce SNG. The status of the leading coal gasification processes is presented in Table I (15).

TABLE I

PRESENT STATUS OF LEADING COAL GASIFICATION PROCESSES

Process	Developer	Status
Hygas	Institue of Gas Technology	Operating a 100 T/D pilot plant. Planning a scale-up facility.
CO_2 acceptor	Consolidation Coal Company	Operating a 40 T/D pilot plant. Planning a scale-up facility.
Bigas	Bituminous Research Inc.	Operating a 120 T/D pilot plant.
Synthane	Bureau of Mines	Operating a 70 T/D pilot plant.
Lurgi	Lurgi Mineralol-technik GmbH	Process less methane synthesis in operation. A full scale plant is in design.
COGAS	FMC Corporation	Operated a pilot plant.
EXXON	Esso Research Inc.	Operated a pilot plant.

The previous studies have indicated that for a common basis of amount of SNG production, coal price, and the rate of return, the cost of SNG would vary from 90 ¢/Mscf to 135 ¢/Mscf (18). The shape of the

price structure has since changed and the current predictions state that SNG may cost in the neighborhood of $3.00/Mscf. But this latter price for SNG may still be competitive since imported oil and gas prices have also risen so sharply.

(d) The final alternative is to develop new sources of energy. With reference to the Project Independence, the FEA report suggests an ever expanding role of nuclear power (9). According to Thomas G. Ayers, Chairman and President of the Commonwealth Edison Co. of Chicago, the cost of generating electricity from different fuel sources is as illustrated in Table II.

TABLE II

COMPARATIVE COSTS OF GENERATING ELECTRICITY

Fuel Source	Cost of Electricity, ¢/kwh
Oil-fired peaking units	4.00
Conventional oil-fired	1.80
Western low-sulfur coal	0.80
Nuclear	0.25

The expansion in the role of nuclear power will largely depend upon federal policies toward granting of permits and licenses as well as federal funds for research and development.

Another new source of energy could very well be shale oil. The oil shale deposits are mixed hydrocarbon reserves. The world's largest deposits of the Green River formation are estimated to have a total recoverable product of up to 600 billion BOE (9). In a conventional oil production there is generally large initial investments followed by relatively low operating expenses. Oil shale, however, is feared to require both large initial investments and significantly higher operating expenses. Should oil prices drop, oil shale prices could be non-competitive. The risks involved in such investments may have to be protected by federal regulations.

There are also plans for harnessing energy from certain natural sources such as solar, wind, and geothermal and ocean thermal. The studies are underway to transform these energies to conventional forms for convenient usage.

Solar energy can be redirected from numerous sources to a central location to attain a temperature of up to 1200 F (649 C) (9). This absorbed heat can then be utilized to produce steam which in turn can generate electricity. Certain modifications in building designs can also capture solar energy for heating and cooling.

There are several areas in the U. S. where the prevailing wind velocities can generate significant amounts of power.

Likewise, there are numerous locations in the U. S. where there are geysers or hot springs (19). Energy from these hot springs can be transformed via an intermediate fluid to generate electricity. The same is the case for seawater. The key questions are when and how much of these naturally available energies can be converted economically to meaningful end uses. The National Science Foundation is sponsoring

several research studies to explore different design concepts that can produce favorable answers.

The Project Independence is a big challenge as is the decision of which of these alternatives is most economical and reliable for an extended use. Probably a combination of all or most of these alternatives must be used to ease the pressure from the current energy supply and demand situation. In spite of all this confusion, one of the fossil fuels is now getting a lot of attention. President Ford (20), in his speech before a group from The National Coal Association, proclaimed that coal is the ace in the hole for the U. S. Similarly the Director of the U. S. Bureau of Mines, Dr. Thomas V. Falkie (21), stated that there is a growing appreciation of the enormous stand-by energy wealth represented in the public and privately owned deposits of coal that are widely distributed throughout the country. With these remarks Dr. Falkie stressed that for the next 20 to 30 years all new fossil fuel power plants should use coal instead of petroleum products or natural gas to generate electricity. Figure 3 illustrates the unbalance in energy reserves and production (9). Up to 94.5% of the U. S. recoverable fossil fuel reserves are coal but only 18% of the energy production is shared by coal. Coal began to play an increasing role in the energy picture only since 1974. Coal has accounted for 17.6%, 17.8%, 18.1% and 18.4% of the total energy use during the years 1973, 1974, 1975 and 1976 respectively (1), (2). The gain does not appear significant but the trend is certainly important.

The technology and fuel resources may be available to make the U. S. independent of all foreign energy reliance. The financing, however, may become the limiting factor in expanding the U. S. supplies.

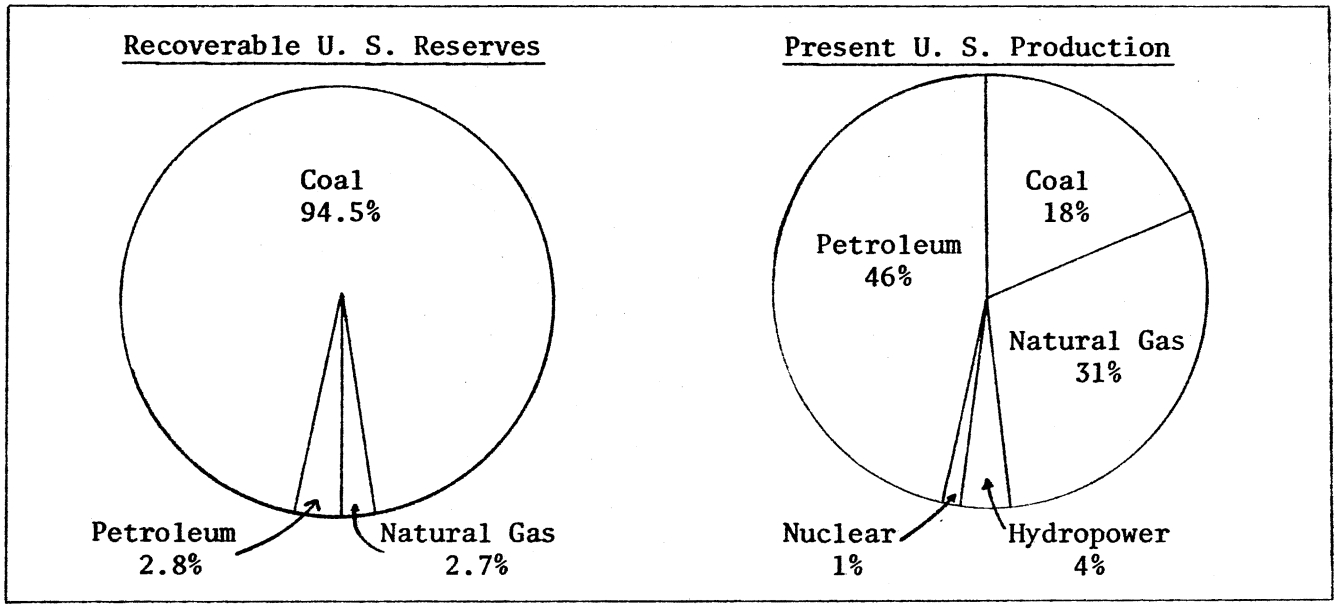

Figure 3. The Unbalance in the Energy Reserves and Production (9).

At the New York public hearings on PI, the chairman of AGA's finance committee mentioned that the U. S. might run out of money before running out of gas (9). Mr. Collado of Exxon Corporation estimated that the energy industry will have to invest about $500 billion (1973 dollars) between now and 1985 just to end the growth in the energy imports. The chairman of the board of directors of the New York Stock Exchange, Mr. Needham, commented that presently the U. S. corporations are heavily in debt and there is too much risk involved in investing so much money in the energy related areas.

Another possible obstacle to achieving the PI goal could be the danger of environmental pollution and safety problems. The increased burning of coal and other fossil fuels may increase air pollution. The hurried licensing of the nuclear power plants might overlook certain safety precaution measures. Some of the stiff anti-pollution legislation may have to be set aside temporarily in order to conserve energy and to improve the supply situation.

In spite of these obstacles, the efforts to explore new horizons of energy supply should continue at their peak. ERDA has numerous research projects underway at institutions across the U. S. Listing all the projects under the sponsorship of ERDA is probably beyond the scope of this work. The four major areas of research are listed here in Table III.

The subject of high-Btu gas was also discussed earlier in this chapter. Low-Btu gas and direct coal combustion processes have been in practice in the U. S. for decades. Coal liquefaction is the major area of research which is developing new processes. The basic concept of coal liquefaction is to produce a non-polluting liquid product from

coal at a reasonable cost. This coal derived liquid can not only replace petroleum as a power plant and industrial heating fuel but it can also act as a crude for hydrocracking and refining purposes. The present status of some of the leading coal liquefaction programs is presented in Table IV (15), (16).

TABLE III

MAJOR AREAS OF ERDA RESEARCH PROJECTS

Area of Research	Project Objectives
Coal liquefaction products	To be utilized for power generation, industrial, commercial, residential, and transportation requirements.
High-Btu gasification products	To supplement the industrial, residential, and commercial needs.
Low-Btu gas products	For power generation and industrial application.
Direct coal combustion products	For power generation and industrial application.

The U. S. has abundant coal reserves and some of the research programs for coal liquefaction have reached advanced stages. Capital investment and certain technical questions will be worked out during the upcoming pilot plant programs. The remaining major obstacle is pollution control. Sulfur content of coal is the primary concern. The distribution of the estimated U. S. coal reserves by sulfur

content as of Jan. 1, 1975 is shown in Figure 4 (22). This figure may be misleading. About 70% of the coal, including most of the low-sulfur coal, lies west of the Mississippi, while, over 90% of the coal production activity and major market have been in the areas east of the Mississippi. The distribution of the estimated reserves in states east of the Mississippi by their sulfur content is presented in Figure 5 (22).

TABLE IV

PRESENT STATUS OF LEADING COAL LIQUEFACTION PROCESSES

Process	Developer	Liquefaction Step	Status
SRC	Gulf-Pittsburg and Midway Coal Mining Company	Non-catalytic	Successfully operating a 50 T/D pilot plant since 1974.
H-Coal	Ashland Oil Company	Catalytic ebullating bed	Constructing a 600 T/D pilot plant.
SASOL II	South African Coal Oil & Gas Company	Fischer-Tropsch	Constructing 40,000 T/D Power Plant
Synthoil	Bureau of Mines	Catalytic fixed bed	Operating a 0.5 T/D pilot plant.
COED	FMC Corporation	Fluid bed hydrotreating	Operated a 0.5 T/D pilot plant undergoing further analysis.
Exxon	Esso Research & Engineering	Hydrogenated solvent	Operated a 0.5 T/D pilot plant. Building a 250 T/D unit.

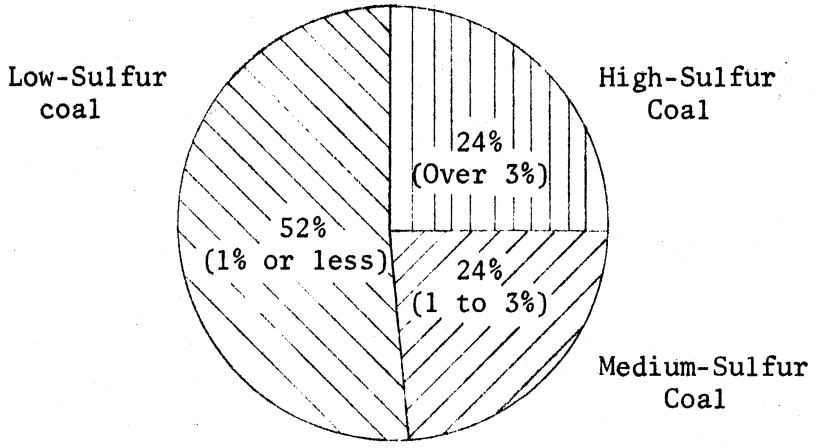

Figure 4. Distribution of U. S. Coal Reserves by Sulfur Content (22).

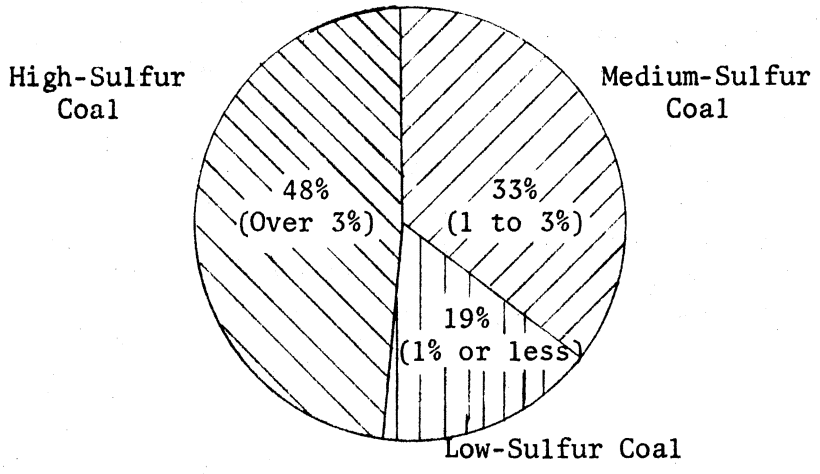

Figure 5. Distribution of Coal Reserves East of Mississippi by Sulfur Content (22).

Sulfur in coal is undesirable for two reasons. The first consideration is certainly air pollution. The second consideration is that higher sulfur content coal derived liquid will probably poison catalysts in any subsequent processing steps. Hence, the removal of sulfur from the coal derived liquids becomes more than essential. Predictably, part of the attention in the coal liquefaction program is focused towards sulfur removal from the coal derived liquids.

The present study is a part of a continuing investigative program at the Oklahoma State University directed towards developing hydrotreating catalysts for coal derived liquids. The hydrodesulfurization (HDS) of raw anthracene oil, a coal derived liquid, was investigated in a trickle-bed reactor in the presence of several commercially available Co-Mo-Alumina catalysts. These catalysts were also tested for their aging characteristics for the HDS of raw anthracene oil.

The objectives of the present study were as follows:

1. To provide useful information with regards to developing hydrotreating catalysts for coal derived liquids.
2. To determine the effects of the reactor operating conditions on the hydrodesulfurization of raw anthracene oil using selected catalysts.
3. To develop a reaction rate model for hydrodesulfurization of raw anthracene oil in the presence of selected catalysts.
4. To evaluate the aging characteristics of the hydrotreating catalysts.

There are a few techniques available in the literature for the sulfur removal from coal, petroleum feedstocks and coal dervied liquids.

The next chapter covers some of these techniques as well as the types of suitable reactors that can be employed, properties of the catalysts used and areas related to this investigation.

CHAPTER II

LITERATURE REVIEW

The catalytic HDS of petroleum distillates has been practiced for several years, but the chemistry of the process has not been fully understood. Recently, the research efforts in the area of HDS have increased sharply because of tough air pollution control standards requiring low sulfur fuel oils. Most of the current engineering research on the catalytic HDS is proprietary and hence the related information is not available in the open literature. At the same time, other related aspects of the reactor operation are reported quite extensively. The type of reactor used for research studies on the HDS is generally a trickle bed reactor. Therefore, the literature reivew related to the fluid flow characteristics is limited only to the trickle bed reactor. Ample information on the flow characteristics and other related subjects such as axial dispersion, backmixing and catalyst wetting is available in the open literature. Very limited research studies are available regarding the effects of reactor temperature, pressure and space time on the kinetics of HDS. A number of recent research studies are concentrated on the study of different HDS catalysts with a special attention to the Co-Mo-Alumina catalysts. These studies cover a wide range of catalyst characteristics such as pellet size, surface area, pore size, active life, etc.

There are a few industrial scale HDS techniques available in the market. But most of these techniques apply to a specific type of petroleum feedstock. With feedstock of varying physical and chemical properties, the type of sulfur containing compounds present in a particular feedstock may vary and, thus, the methods to attack the sulfur containing compounds also vary. At present, the methods to attack particular sulfur containing compounds in the coal-derived liquid are not reported.

This chapter is organized to take the reader step by step, through the reactor to the catalyst bed. The type of reactors used for the HDS is discussed first. The fluid flow characteristics of the trickle bed reactor are presented. Next, the effects of varying reactor operating conditions are examined. The current techniques for the HDS are outlined along with the type of feedstocks and respective sulfur containing compounds. Finally, the attention is concentrated on numerous catalyst characteristics including the studies on various HDS catalysts. The catalyst deactivation is also covered along with the reasoning behind such deactivation.

Although there are many chemical reactors, only trickle bed reactors are used extensively in the HDS studies. Very rarely is the reasoning behind such selection reported. A portion of the explanation is presented in the next chapter, certain specific aspects of the selection are briefly explored here.

Trickle Bed Reactor

Two of the most frequently used reactors in the hydroprocessing industries are fluidized bed and trickle bed reactors. In a fluidized

bed reactor, the catalyst particles stay in motion and the liquid and gas phases flow cocurrently upward while chemical reactions take place. In a fluidized bed reactor, the catalyst particles must be of very small size to remain in suspension. In a trickle bed reactor, the liquid phase flows downward through a fixed bed of catalyst particles and the gas phase may be flowing upward or downward. (The downward flow of both fluid and gas occurs most frequently.)

Both of these reactor types have their advantages and disadvantages. Some of the advantages of the fluidized bed reactors include good temperature control, convenient heat recovery, easier removal and replacement of short lived catalysts, and a significantly high rate of reaction per unit volume of catalyst for highly reactive catalysts (23). The disadvantages of the fluidized bed reactors include lower degree of conversion per pass because of the residence time distribution patterns approaching a continuous stirred tank reactor, difficulties in separation of the catalyst particles from the reaction products, and relatively greater chances of the occurrence of homogeneous side reactions. The advantages of trickle bed reactors consist of easier separation of the catalyst particles and the reaction products and higher conversion per pass due to the residence time distribution patterns approaching the plug flow reactors. The major disadvantage of the trickle bed reactor is the temperature control. Additionally, the factors that weigh heavily in favor of the trickle bed reactor are the easier construction and lower cost of operation than that of the fluidized bed reactor. The trickle bed reactor is the most frequently used reactor in the petroleum industry for hydroprocessing (24).

In spite of the extensive application of the trickle bed reactor for hydroprocessing, virtually no fundamental research has been published on the chemical aspects of its operation. This, in part, may be because of the operating complexities involved in the handling of three phases. Some nonconclusive inferences have been made from the experimental data that has been published, but none of these address the high pressure and high temperature operations in the HDS reactions.

Backmixing in Trickle Bed Reactor

The trickle bed reactor is designed on the assumption that the liquid flow through the packed bed is a plug flow. The plug flow condition is the ideal flow pattern for these catalytic reactors. Deviation from plug flow conditions requires additional reactor volume to attain the same level of chemical reaction at identical process conditions. Complete backmixing is the maximum nonideality from the plug flow condition. The disturbances at the entrance and exit of the packed bed reactor create liquid distribution problems. Several researchers attempted to establish a "critical" or a minimum packed column height to diameter (L/D) ratio above which any deviation from the plug flow conditions is negligible. The pioneering work on this subject was done by Partington and Parker (25) in 1919. They recommended that the L/D ratio should be at least 5 for adequate liquid distribution. The results of the subsequent work on the subject of backmixing by Scott (26) in 1935 demonstrated that the L/D ratio ought to be above 25 to limit the liquid distribution problems to a negligible level. Most of the early work on the trickle bed reactors, to include that of Scott, was performed with air and water systems.

While analyzing his results, Scott also observed that the critical L/D ratio lie somewhere between 10 and 20, depending upon the size of the packings used. Scott did not correlate the critical ratio to the packing size. The studies of Baker, Chilton, and Vernon (27) confirmed Scott's observation of a critical L/D ratio above 10 for adequate liquid distribution. The later studies on liquid backmixing attempted to incorporate particle diameter. The investigation by Schwartz and Smith (28) in 1953 revealed that the tube diameter to particle diameter ratio (D_t/d_p) should be above 30 to significantly limit the liquid distribution problems. The works by Schiesser and Lapidus (29) on air-water system and by Glaser and Lichtenstein (30) on brine-air and kerosene-hydrogen systems suggested that the D_t/d_p ratio must be above 16 to avoid significant deviation from plug flow conditions. All the above information does give a general idea of ways to avoid deviation from plug flow conditions, but the conclusions are still very vague. During the last fifteen years, a more exact mathematical model of liquid distribution has been developed.

Initially, the concept was to include the physical properties of the fluids. Two of the most frequently used non-dimensional numbers are Reynolds number ($d_pU\rho/\mu$) and Peclet number (d_pU/E) where d_p is the particle diameter, U is the liquid linear velocity, ρ is the liquid density, E is the dispersion coefficient, and μ is the liquid viscosity. While reviewing the work of Wilhelm (31), Satterfield (32) observed that the radial dispersion approaches a constant value above the liquid Reynolds number of 100, and the axial dispersion approaches a steady value above the liquid Reynolds number of 10. Examination of the definition of the Reynolds number indicates that, with other items

remaining constant, the Reynolds number rises as the liquid velocity increases. And therefore, as the liquid velocity ultimately increases the Reynolds number beyond 10 (or 100, as the case may be), the axial or radial dispersions make no significant contributions to the fluid flow situation.

Schwartz and Roberts (33) evaluated some of the most recent models representing the liquid flow in trickle bed reactors. The summary included a "dispersion" model of Levenspiel and Smith (34), which requires only one adjustable parameter to describe the deviation from plug flow. The other models developed tend to lean towards more exact mathematical modeling of residence time distribution (RTD) of the liquid phase, such as the "modified mixing-cell" model by Dean (35), the "crossflow" model by Hoogendoorn and Lips (36), and the "time delay" model by Buffham, et al. (37). All three of these models require two adjustable parameters to describe the liquid flow situations. A fourth model by Van Swaaij, et al. (38), requires three adjustable parameters. Schwartz and Roberts observed that the mathematical and experimental efforts required to estimate two parameters from the measured RTD data are greater than those required for the one parameter dispersion model. Moreover, correlations such as Furzer and Mitchell (39), Hochman and Effron (40), and Sater and Levenspiel (41), are readily available for estimating the axial Peclet number, but only one attempt has been made to develop general correlation for a two parameter model (40). All the above models were put to test by Schwartz and Roberts (33) for a first order reaction. They concluded that the simple dispersion model adequately represents the liquid flow

situation. However, it should be emphasized that the two-parameter models do offer a closer fit of the experimental RTD curves than the one-parameter dispersion model. They also suggested that in most laboratory trickle bed reactors, except for those that are very small, liquid backmixing is not of major significance.

The most effective model expressing the reactor design limitations to restrict the deviation from plug flow situation is proposed by Mears (42), (43). This model postulates that for the reactor length to be increased no more than 5% due to the axial dispersion effects over a minimum length required with plug flow, the criteria to be met is as shown in Equation (2.1).

$$\frac{L}{d_p} > \frac{20\ n}{Pe_m} \times \ln\ (C_i/C_f) \qquad (2.1)$$

where L/d_p is the ratio of the reactor length to the particle diameter, n is the order of reaction, Pe_m is the liquid Peclet number and C_i/C_f represents the ratio of reactant concentrations entering and leaving the reactor. The most significant contribution of Mears' work is that a portion of the investigation was applied to a bench scale hydroprocessing unit. The reactor operating conditions for the work were almost identical to the operating conditions selected for the HDS reactions, such as 700 F (371 C), 1,500 psig and a liquid volume hourly space velocity of 2.0 per hour. The minimum L/d_p estimated by Mears was 350. Mears' model also suggests that, for frequently occurring reaction conditions and most general length of a foot for reactor, the deviation from plug flow condition would be negligible for conversion roughly less than 90%.

The operation of a commercial reactor may be considerably different from a laboratory reactor. Because of the larger dimensions in the commercial units, the inability of the reactor to achieve the expected conversions may have nothing to do with the mass transfer effects or catalyst activity caused by increased liquid distribution problems. Most of the deviation from the plug flow situations could be avoided by adequate design and operation of the trickle bed reactor.

Catalyst Wetting and Mass Transfer Effects

The multiple reactant and product phases in the HDS reactions provide a very complex mass transfer situation. In the three phase situation that occurs in HDS reactions, there are several stages of mass transfer that can affect the rate of the overall reaction. These mass transfer stages are: (a) diffusion of the reactants in the gas and liquid bulk phases to the liquid film surrounding the catalyst pellet; (b) diffusion of the reactants to the catalyst surface; (c) diffusion of the reactants through the catalyst pores to the active sites; (d) adsorption of the reactants on the active sites; (e) chemical reaction between the reactive molecules on the catalyst surface; (f) desorption of product molecules from the active sites; (g) diffusion of the products through the catalyst pores; (h) diffusion of the products through the liquid film surrounding the catalyst pellet; and (i) the diffusion of products to the bulk gas and liquid phases. Any one or a combination of the above can be rate controlling steps. Because of the complexities involved in the three phase reactions, the results of an experiment on mass transfer effects can hardly be generalized for other systems. Occasionally, catalyst

wetting characteristics are incorporated in the mass transfer effects. The catalyst wetting characteristics are discussed later in this section. In a review of trickle bed reactors, Satterfield (23) discussed the mass transfer effects, among other aspects. He contended that the mass transfer phenomenon is a combination of two processes, a diffusional process predominating in the direction normal to the flow and a convective process predominating in the direction of the flow. Satterfield explained that the mass transfer in a catalyst bed occurs for a predominance of the particles. Several models available to estimate the overall mass transfer coefficient, K_{ls}, such as stagnant film model, non-mixed model, mixed model, and a model from penetration theory were compared by Satterfield (23) to hydrogen in an α-methyl styrene system. The comparison of these four models, when plotted for predicted K_{ls} against the liquid flow rate, offered general guidelines: (a) the predicted values of K_{ls} by the non-mixed model and the stagnant film model were almost identical and may be used at low liquid flow rates; (b) the model from penetration theory predicted reasonable K_{ls} values only when the liquid flow rates were above 0.7 cc/sec; and (c) the mixed model provided a better fit at high liquid flow rates. A significant conclusion drawn from the comparison of these models was that for a fixed average concentration in the bulk liquid, the observed rate of reaction changed little with large variations in the liquid flow rates, even if substantial mass transfer limitations prevailed in the liquid film.

Satterfield (23) also presented the criteria to predict the sensitivity of mass transfer through the liquid film. He stated that the mass transfer through the liquid film will be significant only if

the following relationship exists,

$$(10 \times d_p/C^*) \times r \times (1 - \varepsilon) > K_{ls} \qquad (2.2)$$

where d_p is the particle diameter, C^* is the saturation concentration of gas in liquid, r is the rate of reaction, ε is the void fraction, and K_{ls} is the overall mass transfer coefficient.

Another aspect of mass transfer in a trickle bed reactor is the diffusion within the catalyst pores. Generally, these internal diffusion limitations are expressed in terms of the catalyst effectiveness factor, η, defined as the ratio of the observed rate of reaction to the expected rate of reaction in the absence of any internal concentration or temperature gradients. The methods to estimate η are presented in reference (32) in detail. Satterfield (32) contends that, for a first order chemical reaction, the internal diffusion would be insignificant if the following inequality is true,

$$\frac{(d_p/2)^2 \times r \times (1 - \varepsilon)}{D_{eff} \times C_s} < 1 \qquad (2.3)$$

where d_p is the particle diameter, r is the rate of reaction, ε is the void fraction, D_{eff} is the effective diffusion coefficient and C_s is the reactant concentration at the catalyst surface. D_{eff} is defined as $D \times \theta/\tau$ where D is the diffusivity, θ is the catalyst void fraction, and τ is the tortuosity factor. The value of τ falls between 2 and 7, usually taking a value of 4. In one of the experiments by Ma (44), the estimated value of τ for hydrogen in an α-methyl styrene system was 3.9. The reported estimates of the effectiveness factor range from 0.36 to 0.8 for different systems. Van Deemter (45) used 0.5 cm diameter $CoO/MoO_3/Al_2O_3$ particles in an industrial desulfurizer and calculated an effectiveness factor of 0.36. Adlington and Thompson (46)

reported an effectiveness factor of 0.6 for the same catalyst of different size (0.32 cm pellets) in another desulfurizer. At the same time, Van Zoonen and Douwes (47) reported the results of their work on the HDS. They concluded that the effectiveness factor varied from 0.5 to 0.8 on 3 x 3 mm pelleted catalyst by merely changing their densities. No quantitative measurement of large solute molecule size versus pore size is available. Qualitatively, it is inferred that the rate of diffusion within the pores becomes less than expected because of the shorter distance between the molecules and the pore walls.

Other aspects of the mass transfer reported to be affecting the reaction kinetics are the liquid holdup and catalyst wetting. Based on various data on hydroprocessing, Henry and Gilbert (48) concluded that the catalyst activity was proportional to the liquid holdup, which in turn was proportional to $d_p^{-2/3}$ and $\nu^{1/3}$ where $\nu = \mu/\rho$. Therefore, they derived a correlation to express the catalyst activity as shown in Equation (2.4),

$$\ln (C_i/C_f) \propto L^{1/3} \times (LHSV)^{-2/3} \times d_p^{-2/3} \times \nu^{1/3} \qquad (2.4)$$

A close scrutiny of this correlation reveals that the catalyst activity will increase as the particle diameter decreases, which is contrary to the findings of many other researchers. But, in a recent study on the reduction of crotonaldehyde over a palladium catalyst, Sedriks and Kenney (49) observed that the prewetting of the catalyst bed caused substantially different behavior than if the catalyst bed was initially dry. Therefore, based on this and similar observations, Mears (43) suggested that, instead of the liquid holdup, the catalyst activity was proportional to the fraction of the outside catalyst surface which was effectively wetted by the fresh batch of the flowing liquid. Several

investigators have reported that the wetted area of the catalyst bed at moderate liquid flow rates is proportional to the 0.25 to 0.4 power of the mass velocity. A recent study by Puranik and Vogelpohl (50) indicated the wetted area to be proportional to 0.32 power of the liquid velocity. Mears included above results and the effectiveness factor to express the catalyst activity as shown in Equation (2.5),

$$\ln(C_i/C_f) \propto L^{0.32} x (LHSV)^{-0.68} x d_p^{0.18} x \nu^{-0.05} x (\sigma_c/\sigma)^{0.21} x \eta \qquad (2.5)$$

where σ_c/σ relates to the surface tension properties of the liquid phase.

After analyzing all the information concerning the rise in activity as the wetted area and liquid holdup increased, Sylvester and Pitayagulasarn (51) investigated the effect of the diffusion coefficient on the behavior of conversion and catalyst wetting. The results of their study demonstrated that Mears' concept of direct proportionality is true for a non-volatile liquid phase. However, the gas phase to liquid phase diffusivity ratio of the reactants determines the effects of catalyst wetting for a volatile liquid phase. Sylvester and Pitayagulasarn illustrated that the reaction rate is directly proportional to catalyst wetting for higher gas phase to liquid phase diffusion ratio of the reactants. Conversely, the reaction rate is inversely proportional to catalyst wetting for lower gas phase to liquid phase ratio of the reactant. Thus, it can be seen that the present status of the reported information on mass transfer in the heterogeneous systems is rather confusing, primarily because of the complexities of the system itself. Additionally, Satterfield (23) contended that the mass transfer through the liquid film did not appear to be of significant resistance under normal HDS

conditions.

Hydrogen Rate Effects

The results of most of the HDS investigations generally give greater emphasis to aspects other than the hydrogen flow rate. Very few really attempt to study the effects of hydrogen flow rates on the activity of an HDS catalyst. Since hydrogen is one of the reactants for HDS reactions, the hydrogen flow rates are certainly included in almost all the related reports. The hydrogen flow rates used in the HDS studies have ranged from 250 standard cubic feet (scf)/barrel (Bbl) of feed oil to 39,800 scf/Bbl. Wan (52) studied hydrogen flow rates of 3,980 scf/Bbl and 39,800 scf/Bbl of a raw anthracene oil and concluded that the variations in hydrogen flow rates, within the range tested, had insignificant effect on the desulfurization ability of the catalyst. The efforts of Jones and Friedman (53) concerning the Char Oil Energy Development project included work in trickle bed reactors at hydrogen flow rates of 5,700 scf/Bbl and 13,500 scf/Bbl of the feedstock. The results of their work did not demonstrate any difference in the HDS activity of the catalyst at identical operating conditions. Other hydrogen feed rates reported include 1,260 scf/Bbl of feed for gasoline desulfurization by Byrns, et al. (54), 1,500 scf/Bbl to 4,500 scf/Bbl by Gwin and coworkers (55) in the hydrogenation of asphalt, 3,000 scf/Bbl of feed rate by Berg (56) for the desulfurization of gas, approximately 90% hydrogen by Stevenson and Heinemann (57), and up to 6,000 scf/Bbl of feed used by Frost and Cottingham (58). Gregoli and Hartos (59) conducted experiments on a number of feedstocks with the sulfur concentration ranging from 3.2% to 5.4% by weight. The

consumption rate of hydrogen changed extensively depending upon the sulfur content in the feedstock as well as the product oil. Gregoli and Hartos reported that the hydrogen consumption rate varied from 400 scf/Bbl for Venezuelan atmospheric residual to almost 1,000 scf/Bbl for Khafji vacuum residual.

All the above experiements tend to emphasize that, within the range of hydrogen flow rates used, there was no measurable effect of changing the hydrogen flow rate on the rate of the HDS reaction. But the above mentioned findings can be partially explained by inspecting the rate of hydrogen consumption. Frost and Cottingham (58) reported the hydrogen consumption rates during the HDS of petroleum residuum ranging from 200 to 700 scf/Bbl, with higher consumption rates occurring at the most severe reaction conditions of 600 F (314 C) and 800 psig. Schmid (60) recorded the hydrogen usage rate ranging from 290 to 730 scf/Bbl feed, with maximum consumption rate at the most severe reaction conditions. Sooter (61) outlined different areas of the hydrogen consumptions which include sulfur removal (formation of H_2S), nitrogen removal (formation of NH_3), oxygen removal (formation of H_2O), gas making, and hydrocracking. Considering all these factors, Sooter estimated the average hydrogen consumption rate as 450 scf/Bbl feed with some 493 scf/Bbl feed at the most severe reaction conditions. With the hydrogen consumption rates in mind, it is evident that the effects of hydrogen flow rate would be noticeable when the flow rate would be less than the rate of its consumption. That is exactly what was observed by Hoog and his coworkers (62). During the experiments of desulfurization of petroleum oils, Hoog and his colleagues observed a slight effect on the HDS reactions of the hydrogen flow rates between

250 scf/Bbl and 1,500 scf/Bbl feed and no measurable effect beyond 1,500 scf/Bbl feed. This gives a lead value of 1,500 scf/Bbl feed for the hydrogen flow rate, which may be changed according to the estimates of the hydrogen consumption rates. The hydrogen flow rate of three times the rate of its consumption may be more than adequate for the HDS experiments.

Temperature Effects

The reaction temperature is one of the most frequently investigated operating variables in the desulfurization of the coal derived liquids and the petroleum residua. The three different criteria for which the temperature effects are studies are rate of reaction, activation energy of the HDS reaction, and catalyst life and stability. Numerous investigations have reported that the rate of the HDS reaction increases with an increase in the reaction temperature (52), (61), (63), (64), (65), (66). However, there is a wide spectrum of values reported for the activation energy ranging from 6,800 Btu/mole (3.8 Kcal/mole) to 101,200 Btu/mole (56.2 Kcal/mole) (56), (67). Even then, most of the reports have the activation energy ranging from 43,200 Btu/mole (23 Kcal/mole) to 61,200 Btu/mole (34 Kcal/mole) (58), (60), (68), (69). In a more recent work, Sooter (61) estimated the activation energies of an HDS reaction to be 80,370 Btu/mole (44.65 Kcal/mole) and 9,720 Btu/mole (5.4 Kcal/mole) for "slow" and "fast" reacting molecules, respectively. (The terms "slow" and "fast" refer to the sulfur containing molecules found in the heavy and light distillation fractions of the feed.) The diversity in the reported values of the activation energies of the HDS reactions may be attributed to the fact that these

experiments were conducted: (1) on a variety of feedstocks; (2) with different catalysts; (3) under different experimental conditions; and (4) with many HDS kinetic models, ranging from the simple first order, pseudo-second order, to the third order. For heavy petroleum feedstocks, the initial desulfurization reaction is chemically controlled. As the temperature increases, however, a suspected deviation in the reaction mechanism diverts the reaction to a diffusion controlled.

Many of the petroleum feedstocks contain a relatively high concentration of metals. Because of this high metal content, the catalyst activity tends to deviate due to the pore plugging phenomena (70), (71). Therefore, the reaction temperature is raised to such a degree that the rate of reaction will increase just enough to balance the deactivation due to pore plugging. The active life of a catalyst can then be improved considerably.

Normally, the HDS reactions are exothermic. These reactions, when conducted in the trickle bed reactors, could create a rather unstable temperature condition (72), (73). Although the overall reactor temperature may be stable, there can be significant interphase temperature variations that include momentary temperature runaways and hot spots. These unstabilities, though predictable, can make a significant impact on the rate of an HDS reaction.

Pressure Effects

The research of pressure effects is as diversified as that of temperature. Unlike temperature, the course of the pressure effect is not unanimous, since different investigators may vary the pressure ranges they are studying. There may also be a variety of feedstocks

and experimental conditions involved that can make a difference in the ultimate results. Hoog (62), working on a shale oil at 750 F (399 C) and pressure ranging from 735 psia to 2,200 psia, observed a slight increase in the extent of sulfur removal with increasing pressure. Schmid (60), on the other hand, experimenting on a petroleum vacuum in a trickle bed reactor, noticed a dramatic improvement in the sulfur removal for pressure increase up to about 1,000 psia. While studying the HDS of a coal derived liquid at 725 F (385 C), Jones and Friedman (53) did not observe any significant change in the rate of sulfur removal reaction in pressure range of 2,000 to 3,000 psia. Qader and Hill (64) demonstrated a trend of increasing sulfur removal with increase in pressure only up to 1,500 psia. Wan (52) and Sooter (61) used the same feedstock as the one used in this latter research. Wan worked within the pressure range of 1,000 psig to 2,500 psig and reported no significant increase in the sulfur removal with rise in reactor pressure. Sooter worked at pressures between 500 psig and 1,500 psig. His results demonstrate a substantial improvement in the sulfur removal for pressure increase from 500 psig to 1,000 psig, but hardly any increase after that. Combining these observarions, it appears that 1,000 psig is a limiting pressure. Below this level, an increase in the reaction pressure is acknowledged by an increase in the sulfur removal. Above 1,000 psig, the effect of changing pressure almost subsides.

Effects of Space Time and Kinetics of HDS Reaction

The effects of temperature and space time are established to follow an identical trend in the desulfurization of oil. Like temperature, both space time and sulfur removal decrease or increase correspondingly. These variations in the sulfur removal with respect to space time are generally attempted to fit a kinetic model. The numerous kinetic models reported to represent the desulfurization process vary significantly from pseudo-first order model (61), (74), (75), (76), (77), second order kinetic models (60), (78), (79), (80), (81), (82), pseudo-second order kinetic models (83), (84), (85) and up to a third order kinetic model (58). A more recent concept in explaning the desulfurization process is to derive reaction rate models for each sulfur containing compound in the feedstock (86). The diversity in the kinetic models and the subsequent confusion may be clarified following a study of the above mentioned articles.

Hoog (87) appears to have done the pioneering work in attempting to explain desulfurization in the trickle bed reactors. His data on the wide range of boiling distillates did not fit a first order rate model. But his similar data on the narrow range boiling distillates did fit the first order kinetic model. Hoog tried to describe that the higher molecular weight sulfur containing compounds may be shielded from the hydrogen atoms by the hydrocarbon groups. In other words, the possibility exists that different sulfur containing compounds may be following different reaction rates.

The various types of sulfur containing compounds in the feedstock are certainly very difficult to identify. However, work has been done to separate the sulfur containing compounds into different groups. These groups are listed later in this section. Cecil, et al. (74) worked on a Middle Eastern residuum at different hydrogen partial pressures and space velocities. They divided the sulfur containing compounds in the feedstock into reactive and nonreactive fractions. The data from their experiments showed that each of these fractions followed a first order kinetic reaction whereas the overall order of reaction turned out to be of the second order. Working along similar lines, Sooter (61) tried successfully to fit his data to a two parallel first order reaction model. The fractions of the feedstock were termed as low boiling fraction and high boiling fraction. However, the data fit the overall second, third or fourth order reaction rate models equally well. Sooter explained that the surface adsorption and desorption of the sulfur containing compounds in the higher boiling fractions could be the limiting step in the desulfurization process.

Yitzhaki and Aharoni (75) studied the HDS of gas oil over Co-Mo-Alumina catalyst bed at 450-700 psig pressure and 662 F (350 C). They fractionated the feedstock and product at temperature intervals of 38 F (20 C) and analyzed each fraction for its sulfur content. The results indicated that the HDS reaction for the corresponding fractions in feedstock and product follow first order rate models. Qader, Wiser and Hill (76) investigated the HDS of low temperature coal tar at varying operating conditions. The authors demonstrated that the overall HDS reaction followed a first order rate model with respect to sulfur concentrations. The authors went on to mention that, if hydrogen

concentration were considered, the HDS would be a pseudo-first order reaction. Aboul-Gheit and Abdou (77) also demonstrated that the results from the HDS study of an Egyptian crude oil best fit a pseudo-first order rate model.

Yergey et al. (86) worked extensively on the sulfur containing compounds in coal. These sulfur containing compounds are likely to eventually appear in the coal derived liquids. The sulfur containing compounds in 10 different coals were sub-divided into eight groups, such as Organic I, Organic II, Pyrite, Sulfide, Organic III, Sulfur with Fe, Sulfur with C, and Sulfur with CaO. Their kinetic data presented a mixed bag of orders of reactions. The sulfur containing compounds in Organic I, Organic II and Pyrite group followed one-half order. The remaining groups followed first order, except for Organic III, which followed a second order reaction rate model. This represents that each and every sulfur containing compound in a feedstock may be following its own reaction rate. Therefore, the overall rate of the HDS reaction can vary depending upon the concentrations of various sulfur containing compounds in the feedstock.

The second order kinetic models have been reported to be successfully fit to data by Schmid and Beuther (60) and Massagutov, et al. (88). While working on a petroleum vacuum distillate from a crude oil, Massagutov and coworkers demonstrated that the activation energy of the desulfurization reaction dropped dramatically from 60,000 Btu/mole (33 Kcal/mole) to 9,500 Btu/mole (5.3 Kcal/mole) with an increase in reaction temperature from 662 F (350 C) to 806 F (430 C). This observation helped them to conclude that diffusion must be playing a significant role at the higher reaction temperatures. To substantiate

the claim of the diffusion control, they further demonstrated that the rate of desulfurization reaction increases more than four-fold with a decrease in the catalyst particle size from 5/64 inch to 1.25/64 inch (0.2 cm to 0.05 cm). The experiments by Schmid and Beuther (60), besides showing a second order fit of the data, also showed that the removal of higher boiling fractions (such as asphaltenes) from the feedstocks increased the rate of desulfurization reaction almost four-fold. Schmid and Beuther also attempted to incorporate the effects of catalyst surface area, pore radius, and pore volume in the kinetic model.

The HDS of specific sulfur containing compounds, such as thiophene, benzothiophene and dibenzothiophene, have been investigated by Lee and Butt (78), Hargreaves and Ross (79) and Bartsch and Tanielian (80). Lee and Butt studied the kinetics of the HDS of thiophene on a representative Co-Mo-Alumina catalyst. Their kinetic results fit a second order rate model. The HDS reaction was first order with respect to each of the reactants, thiophene and hydrogen, and the reaction was shown to be inhibited by the presence of thiophene and H_2S. The investigation by Hargreaves and Ross (79) was directed towards the mechanism of the HDS of thiophene over several sulphided Co-Mo-Alumina catalysts. The overall kinetic results were successfully fit to a second order rate model. From the results of the HDS tests on several catalysts, Hargreaves and Ross observed that the catalyst activity increased over four-fold with an increase in the Co-Mo atomic ratio from 0.29 to 0.81 at 11% by weight of Mo. Bartsch and Tanielian (80) examined the HDS of benzothiophene and dibenzothiophene. The overall kinetic data were successfully fit to a second order reaction rate

model. Bartsch and Tanielian reported the activation energies of the HDS of benzothiophene ranging from 8,820 to 25,200 Btu/mole (4.9 to 14.0 Kcal/mole) and the HDS of dibenzothiophene ranging from 9,540 to 25,400 Btu/mole (5.3 to 14.1 Kcal/mole), respectively.

Bruijn (81) tested the HDS of vacuum gas oil from Kuwait in a bench scale and a pilot scale plant. Bruijn also tested the effect of diluting the packed bed, in which, the packed bed of large catalyst particles was mixed with smaller inert particles to improve the liquid distribution patterns. Most of the HDS activity data sets were shown to fit rate models ranging in order from 1 to 2 and averaging 1.65. Bruijn also found that the catalyst activity improved about 50% at 680 F (360 C) because of the dilution of the packed bed. Marooka and Hamrin (82) studied, in separate experiments, the HDS of thiophene over Nalco 471 catalyst and low temperature ashes. The activity data successfully fit a second order rate model. The activation energies of the HDS reaction were estimated to range from 17,100 to 36,000 Btu/mole (9.5 to 20.0 Kcal/mole) for Nalco 471 catalyst, and from 18,000 to 19,800 Btu/mole (10 to 11 Kcal/mole) for the low temperature ashes, respectively.

Johnson, et al. (84) investigated the desulfurization mechanism of a Kuwait feed. When blanketing all the sulfur containing compounds in a single group, the experimental data fit a second order reaction rate model more closely than any other model. The grouping of all the sulfur containing compounds was probably what prompted them to call it a pseudo-second order reaction. The flexibility of the H-oil process is that additional desulfurization stages can be included for feedstocks that are difficult to desulfurize. The experiments by Johnson, et al.

were conducted on Kuwait feed at temperatures ranging from 700 F (371 C) to 800 F (427 C). Hisamitsu and coworkers (85) studied the HDS of two heavy distillates in a trickle bed reactor over a commercially available Co-Mo-Alumina catalyst. The data from the tests on both the feedstocks fit different rate models at different reaction temperatures. For both the feedstocks, the data obtained at 644 F (340 C), 680 F (360 C), and 716 F (380 C) fit 2.1, 1.8, and 1.6 order of reaction rate models, respectively.

In addition to all these, there are reports that describe a third order fit of the kinetic data. Frost and Cottingham (58) conducted a series of experiments on a residual fuel. Their results showed different kinetic model fit to data at different reaction temperatures, such as, pseudo-third order fit at 600 F (314 C), pseudo-second order at 740 F (393 C), and almost first order at 800 F (427 C). Sooter (61) also found his data to fit second, third, and fourth order kinetic models equally.

Very limited attempts have been made to represent the HDS reaction mechanism, and even fewer have verified any of the proposed paths. One of the two reaction networks is by Owens and Amberg (89), which desulfurizes thiophene. Satterfield and Roberts (90) used commercial cobalt-molybdate catalyst (3% Co and 7% Mo) with reaction conditions of slightly above atmospheric pressure and the reaction temperature falling between 508 F (264 C) and 538 F (281 C). Their results were consistent with Owens-Amberg network. The other reaction network is by Givens and Venuto (91), which starts from benzothiophene. They show four different paths to be followed in the reaction and, not surprisingly, hardly any of these are well established paths.

Even with all these diversified kinetic models, certain things can be derived very clearly. Individual sulfur containing compounds can be said to follow a first order reaction model and that the overall HDS reaction can follow varied rate models, depending upon the reaction temperature and the concentrations of the various sulfur containing compounds.

Organic Sulfur Containing Compounds in Feedstocks

The studies of desulfurization have been conducted by different investigators. Invariably, the feedstocks used for study have also been different. But, since recent reports state that the rate of the HDS reaction depends more on the type of sulfur containing compound than any other factor, a thorough knowledge of the sulfur containing compounds present in all of these feedstocks is necessary. A few of the investigators have tried to isolate and identify the sulfur containing compounds in oils using high resolution mass spectrometry. The most complete and thorough identification work has been published by the U. S. Bureau of Mines (92). This report identified about 200 sulfur containing compounds in petroleum feedstocks. The primary building blocks of most of these sulfur containing compounds are sulfides and dibenzothiophenes. Akhtar and his coworkers (93) attempted to identify the sulfur containing compounds in two of the coal derived liquids. These are identified in Table V. Their desulfurization experiments revealed that dibenzothiophenes were the most difficult to decompose, followed by benzothiophenes and naphthobenzothiophenes. Greenwood (94), using mass spectrometry, attempted to isolate organic and organo-metallic compounds in the

TABLE V

ORGANIC SULFUR CONTAINING COMPOUNDS IN COAL DERIVED LIQUIDS

Coal Derived Liquid	m/e*	Molecular Formula	Identification
Light oil	134	C_8H_6S	Benzothiophene
	98	C_5H_6S	Methylthiophene
	114	$C_6H_{10}S$	Diallylsulfide
	148	C_9H_8S	Methylbenzothiophene
	162	$C_{10}H_{10}S$	Dimethylbenzothiophene
Heavy oil	98	C_5H_6S	Methylthiophene
	138	$C_8H_{10}S$	Tetrahydrobenzothiophene
	174	$C_{11}H_{10}S$	Benzylthiophene
	184	$C_{12}H_8S$	Dibenzothiophene
	198	$C_{13}H_{10}S$	Methyldibenzothiophene
	208	$C_{14}H_8S$	Benzo(def)dibenzothiophene
	234	$C_{16}H_{10}S$	Naphthobenzothiophene
	248	$C_{17}H_{12}S$	Methylnaphthobenzothiophene
	284	$C_{20}H_{12}S$	Dinaphthothiophene
	298	$C_{21}H_{14}S$	Methyldinaphthothiophene

*equivalent molecular weight

feedstock of the present study, anthracene oil. Among other numerous compunds, Greenwood identified the presence of benzothiophene, dibenzothiophene and naphthobenzothiophene in the anthracene oil. Dibenzothiophene was shown to be the most frequently occurring sulfur containing compound in the anthracene oil. In their work on Kuwait gas oil and Venezuelan gas oil, Jewell, et al. (95) isolated benzothiophenes, dibenzothiophenes, and naphthobenzothiophenes. Many other researchers have identified these three sulfur containing compounds in their work on different feedstocks. Hammer (96) reported that the major sulfur containing compounds in shale oil gasoline were thiophenes. Similarly, the work done by Qader, Wiser and Hill (76) indicated that the single most frequent fundamental structure of sulfur containing compounds found in coal tar was dibenzothiophene. Wilson, et al. (67) worked with dibenzothiophene in naphtha for their desulfurization studies. Thus, in spite of the diversity in the feedstocks, very few of the sulfur containing compounds are present, in a measurable quantity, in all of the feedstocks put together. This represents a thin similarity among different desulfurization studies. However, it must not be overlooked that even within the small group of sulfur containing compounds, the rate of reaction is likely to vary appreciably, depending upon the operating conditions.

Selection of Catalysts

There are many catalysts accelerating various chemical reactions. Checking each one of them for hydroprocessing would become too time consuming and expensive. In this fast and ever changing world, the industry can not wait for decades for the results from the research

on all the available catalysts. Thus, the selection of the right type of catalysts for the research purpose is a very important aspect of an investigation.

Sinfelt (97) summarized the influence of a closely related group of substances which catalyze different heterogeneous reactions. Although the factors determining the catalytic specificity were not well understood for the heterogeneous reactions, the patterns of variations in the catalytic behavior from one substance to another were very well established. His review considered such patterns of variations in the catalyst behavior for hydrogenation, hydrogenolysis, isomerization, and many other types of reactions.

The hydrogenation reactions reviewed in detail by Sinfelt (97) were hydrogenations of ethylene, benzene and acetylene. The results from these and other reactions revealed that the substances in Group VIII of the Periodic Chart such as rhodium, cobalt, nickel, platinum, ruthenium, and palladium were relatively more reactive than substances in the other groups. The higher activity of Group VIII substances may be explained in terms of the strength of the adsorption of the reactants on the catalyst surface. However, Sinfelt also mentioned that the substances in Group VA and VIA such as tantalum, chromium, molybdenum, and tungsten, have strong adsorption bonds between the reactants and the catalyst surface.

One of the most thorough and extensive catalyst evaluation studies was conducted at the Bureau of Mines by Kawa and his coworkers (98). In their experimental study, they tested 85 different combinations of catalysts and supports for the HDS and liquefaction of coal. The comparison of the activity for liquefaction and desulfurization

revealed that a high-surface area silica-promoted catalyst containing 2.4% and 10% Mo on alumina support performed best in the batch study. From the catalysts with simple components of Mo, Sn, Ni, Co or Fe, the catalysts with Mo were best for sulfur removal, whereas the catalysts with Sn were best for coal to oil conversion. Their study also showed that the sulfur removal rate appeared to increase with the high-surface area catalysts.

Kushiyama and coworkers (99) studied the effects of chemical composition of catalysts on the HDS of residual oil. Their results illustrated that the HDS of Khafji residual oil increased with an increase in the Co-Mo atom ratio at constant Mo concentration, and the level of HDS was maximum at the Co-Mo atom ratio of 0.5-0.6:1, regardless of Mo concentration. Parsons and Ternan (100) tested the HDS activity of some supported binery metal oxide catalysts. One of the metal oxides in all catalysts was MoO_3. The secondary metal oxides tested by Parsons and Ternan were Ti, V, Cr, Mn, Fe, Co, Ni, Cu and Zn. Their results showed that promotion with Co at 1:1 atomic ratio increased the HDS activity more than any other promoter.

Trifiro and coworkers (101) studied the behavior of four component catalyst containing Mo and Co oxides supported on alumina and any one of the Fe, Zn, or Ca as a fourth component in the HDS study of a Kuwait residual oil. All these catalysts were compared with the activity of a commercially available Co-Mo-Alumina catalyst. Trifiro and coworkers found that the commerical catalyst, which had 4% CoO compared to 2% CoO in their catalysts, performed better than any other for desulfurization.

All these studies of the catalyst components for desulfurization indicate that Co and Mo probably have greater influence on the removal of sulfur than the other components. Furthermore, higher catalyst surface area tends to enhance desulfurization. These HDS studies also indicate that diffusion of sulfur containing compounds through the liquid interphases and the catalyst pores is probably the rate controlling step in the desulfurization reaction.

Effects of Catalyst Characteristics

The three catalyst characteristics studied after establishing the chemical components of the catalyst are its pore size, surface area, and the pellet size. Of these three, the catalyst pore size has probably been the subject of greatest research. However, it should not be overlooked that numerous flow characteristics are likely to change with any changes in catalyst properties, and therefore, research studies on an isolated catalyst characteristic is very difficult, if not impossible. Sooter (61) extensively researched the literature on the effects of catalyst pore size, and therefore, it is only summarized in the following. Sooter presented a first order reaction model by Van Zoonen and Douwes incorporating the pore size effects. The desulfurization reactions were experimentally found to be anything other than first order reactions and a more complex model reflecting pore size effects may be desirable. Even then, the Van Zoonen and Douwes model did give a general idea of how pore size and other physical characteristics are related.

The experiments by Sooter (61) confirmed one of the well founded effects of pore size, i. e., higher pore size catalyst removed more

sulfur containing compounds than the smaller pore size catalyst. Sooter's experiments were conducted on anthracene oil and Co-Mo-Alumina catalysts having pore radii ranging from 25 Å to 33 Å. The larger pore size catalysts help in dealing with larger sulfur containing organic molecules. There are numerous U. S. patents which reflect similar results. One of the patents (102) recommended 60 Å as the most frequent radius (d_f) and a spread of at least 10 Å for more frequent pore radii (Δd). The patent went on to suggest a pore distribution factor (PD) of at least five was preferable, where PD was defined as

$$PD = (d_f)^2 \times (\Delta d) \times 10^{-4} \qquad (2.6)$$

These parameters are estimated from the pore distribution curves which are obtained from the mercury penetration porosimeter experiments. Other patents suggest the pore radius be distributed evenly from 0 to 120 Å. The literature on the pore size effects is abundant but almost all of it falls in the general framework of what has been covered so far in this section.

The catalyst surface area effects do not appear to be well established. However, the experiments with changes in the surface area, as well as some other catalyst characteristics, show that the catalyst with higher surface area provides higher desulfurization and vice versa. The experiments with changing catalyst pellet size demonstrate that smaller pellet size improve the sulfur removal ability of the catalyst, suggesting that the desulfurization reaction is a diffustion controlled. But the experiments by Sooter (61) with catalyst particle size changing from 8-10 mesh to 40-48 mesh did not make any difference in the sulfur removal ability of the catalyst.

The results of the effects of the catalyst characteristics on desulfurization reaction can be summarized very briefly. Large size pores are necessary to desulfurize the large organometallic molecules. In addition, wider pore size distribution is desirable than narrow more frequent pore size. Increased catalyst surface area improves its ability to remove sulfur. The experiments with changing pellet size indicate the desulfurization reaction to be diffusion controlled but 8-10 mesh appears to be the limiting smallest catalyst particle size.

Catalyst Aging Characteristics

The discussion so far has centered around the effects of various reaction parameters on the activities of different catalysts to remove sulfur from various feedstocks. All these activities are short lived and mention very little of how long the catalyst will perform at that level of activity. In other words, a possible deactivation of the catalyst can hardly be judged from the results of experiments presented thus far. The long term effects on the active life of the catalysts are more important from the commercial standpoint.

Newson (103) developed a model to include several variables affecting the catalyst deactivation. The model was later compared with commercial data and showed reasonable agreement. Newson explained that the organometallic constituents of the feedstock, primarily nickle, vanadium, and iron containing compounds reacted with hydrogen sulfide to form solid deposits of the metal sulfides. These metal particles can be deposited inter or intra-particle. The intra-particle deposits reduce the effective diffusivity of the catalyst particles by plugging the catalyst pores. Other authors suggested the pore plugging phenomena

as the primary cause for catalyst deactivation (84), (104), (105). Richardson (104) also included the possibility of coke deposits to explain the deactivation.

The catalyst deactivation model by Newson (103) incorporated the effects of process conditions and catalyst characteristics. He successfully compared his model with experimental results. The process variables studied by Newson were liquid hourly space velocity (LHSV), percent desulfurization, and the reactor pressure. Only a rise in LHSV from 0.5 per hour to 1.0 per hour increased the catalyst life from 600 hours to 3,400 hours. Whereas, reducing desulfurization from 75% to 63% increased the catalyst life from 600 hours to about 1,500 hours. The effect of pressure was just the opposite. Reducing the reactor pressure from 1,500 psig to 800 dropped the catalyst life from 800 hours to 400 hours. As for catalyst characteristics, changing pore size distribution had very little effect on catalyst life as long as the average pore diameter was same. Newson demonstrated that by changing the average pore diameter from 40 Å to 65 Å, he could increase the catalyst life from 400 hours to 1,200 hours. Johnson and his coworkers (84) showed the effect of metallic content in the crude on the catalyst life. Using a Venezuelan atmospheric residuum having 200 ppm of vanadium, the weight percent sulfur in the product oil increased from 0.37% to 1.4% in just 4.0 Bbl of oil per pound of catalyst (about 700 hours). Whereas, using the same feedstock with only 40 ppm of vanadium, the weight percent sulfur in the product oil increased from 0.3% to only 0.5% in 9.0 Bbl of oil per pound of catalyst (about 1,600 hours).

There are two solutions that the hydroprocessing industry has developed to handle catalyst deactivation. One solution is the offshoot of the effect just explained - demetallization. The demetallization process reduces the metal content of the feedstock, thereby increasing catalyst life. The other solution is to increase the inlet temperature of the feedstock. Many publications demonstrate very distinctly the effect of raising inlet temperature over a range of operation of up to 40 months (70), (71), (106).

The survey of catalyst deactivation illustrates that the process conditions play a significant role in determining catalyst life. The LHSV and the metal content in the feedstock appear to have the most dramatic effects on catalyst life.

CHAPTER III

EQUIPMENT SELECTION AND SET UP

The equipment for this study consisted primarily of a catalytic reactor and a sulfur analyzer. The coal derived liquid was treated with hydrogen in the catalytic reactor at the desired reaction conditions and the liquid products from the reactor were then examined for their sulfur content in the analyzer. This chapter will explain the selection of the type of reactor and related equipment and discuss the set up of the experiment.

This project was basically an extension of the work started by Sooter (61). The equipment set up designed and erected by Sooter, with the necessary modifications, was employed in this project. This explanation essentially justifies the type of equipment used by Sooter, and its subsequent adaptation for this project. Most of the emphasis on the equipment selection is devoted to the reactor because of its prime importance.

Accurate and reliable laboratory data is, of course, necessary for the design of an industrial reactor. Laboratory studies which include both the design and construction of laboratory reactors and other equipment items, and the subsequent experimental programs are invariably expensive and time consuming. Therefore, the entire reaction kinetic study must be carefully planned to minimize expenses and time and to generate the most useful data possible. A primary

concern would be the selection of a suitable reactor for the kinetic study.

The selection of the reactor type is clarified once the goals of the study are appropriately defined. Generally, the experimental catalyst work is divided into four major classes. These classes include comparative performance testing, developing kinetics for the reactor design, simulation of plant operation, and determining reaction mechanism. The first three of these are comparatively simple. The determination of reaction mechanism requires extensive research and is highly complex. The investigation becomes more detailed when there are simultaneous reactions coupled with heat and mass transfer effects.

Weekman (107), based on his industrial experience, developed a concept of comparative suitability for a particular type of reator in a given reaction. His concept is summarized in Table VI. The types of reactors covered in Table VI demonstrate certain advantages and disadvantages of the various operation encountered during an experimental study. The fixed bed, stirred-contained, and pulse type reactors are most convenient for the sampling and analysis of products. These types of reactors also offer least resistance in the separation of the catalyst and the sample. But the temperature control in these reactors becomes inadequate for highly exothermic or endothermic reactions. Because of thorough mixing, the stirred type reactors and the recirculating transport type reactors offer better temperature control, and also provide higher residence-contact time to catalysts and reactants. Generally, one additional item of equipment is required for separating the catalyst and the product samples in these reactors. The catalyst batch must be changed more frequently for a fast decaying

TABLE VI

COMPARATIVE REACTOR RATING FOR GAS-LIQUID, POWDERED CATALYST, AND NONDECAYING SYSTEM (107)

Reactor Type	Sampling and Analysis	Isothermality	Residence-Contact Time	Selectivity Disguise-Decay	Construction Problems
Differential	P-F[a]	F-G	F	G	G
Fixed bed	G	P-F	F	G	G
Stirred batch	F	G	G	G	G
Stirred-contained solids	G	G	F-G	G	F-G
Continuous stirred tank	F	G	F-G	G	P-F
Straight-through transport	F-G	P-F	F-G	G	F-G
Recirculating transport	F-G	G	G	G	P-F
Pulse	G	F-G	P	G	G

[a]P = Poor
F = Fair
G = Good

catalyst. The types of reactors offering better leverage against fast decaying catalyst are the stirred tank and the transport type. The relative ease of construction is also a significant factor in the selection of a laboratory reactor. Because of the comparative simplicity in design, differential, fixed bed, stirred batch, and pulse type reactors are relatively easier to construct. The information presented here clearly indicates that some previous knowledge of the reaction mechanism is necessary before Table VI can be of much value.

The experimental data from Sooter's (61) work suggested that the HDS reaction is not highly exothermic. His research also indicated that the catalyst was not a fast decaying type, especially within the time duration of his experiments (up to 250 hours).

Some of the reactor types such as differential, stirred batch, pulse would be eliminated at the first glance because these do not reasonably simulate the industrial hydroprocessing plant operation. The cost consideration and construction problems would tend to eliminate the rest of the reactor types except fixed bed. Isothermality in the fixed bed reactor can be maintained by using a long and narrow reactor with appropriate controls. Thus the fixed bed type reactor was selected for the proposed experimental program.

Oil and hydrogen were fed to the fixed bed reactor from the top and were allowed to flow cocurrently downward. The fixed bed reactor was packed with catalyst and inert particles. The HDS reaction products were collected in the SS containers. The gaseous product rates were measured and the gases were scrubbed with NaOH solution prior to venting to the hood. The liquid product samples were periodically transferred to bottles for analysis.

Experimental Equipment

Reactor

The reactor used for the experimental study was a 1/2" O. D., 18 BWG, SS 316 tubing. The high quality steel was desirable to withstand possible corrosion effects due to the presence of hydrogen sulfide in the heterogeneous reaction mixture. The reaction itself was conducted at elevated temperatures (up to 800 F or 427 C) and elevated pressures (up to 1800 psig). The thickness of the reactor walls must be above the safe limit to sustain the dual load of high pressure and packing weight. Previous work by Wan (52) was conducted in a reactor 20" in length. Of these 20", only 10 to 12" of the reactor were actually available for the catalyst bed. The remainder of the reactor length was packed with inert particles to minimize any entrance or exit effects. The small reactor would have a larger scaling factor when designing a pilot plant. A larger reactor, capable of holding more catalyst and allowing higher liquid and gas flow rates, was more desirable. The reactor length selected in this project was 33". The reactor length surrounded by the heating blocks was 28 to 29". The remainder was used for connections and supports. This reactor could hold up to 20" of catalyst bed before encountering possible entrance effects. Figure 6 illustrates the reactor and the related measurements used in a typical experiment. The catalyst bed contained a different Co-Mo-Alumina catalyst for each experiment. The catalysts were received from the vendor and were crushed to desired size and packed in the reactor. Details concerning the catalyst will be presented in later chapters. The inert particles were berl saddles

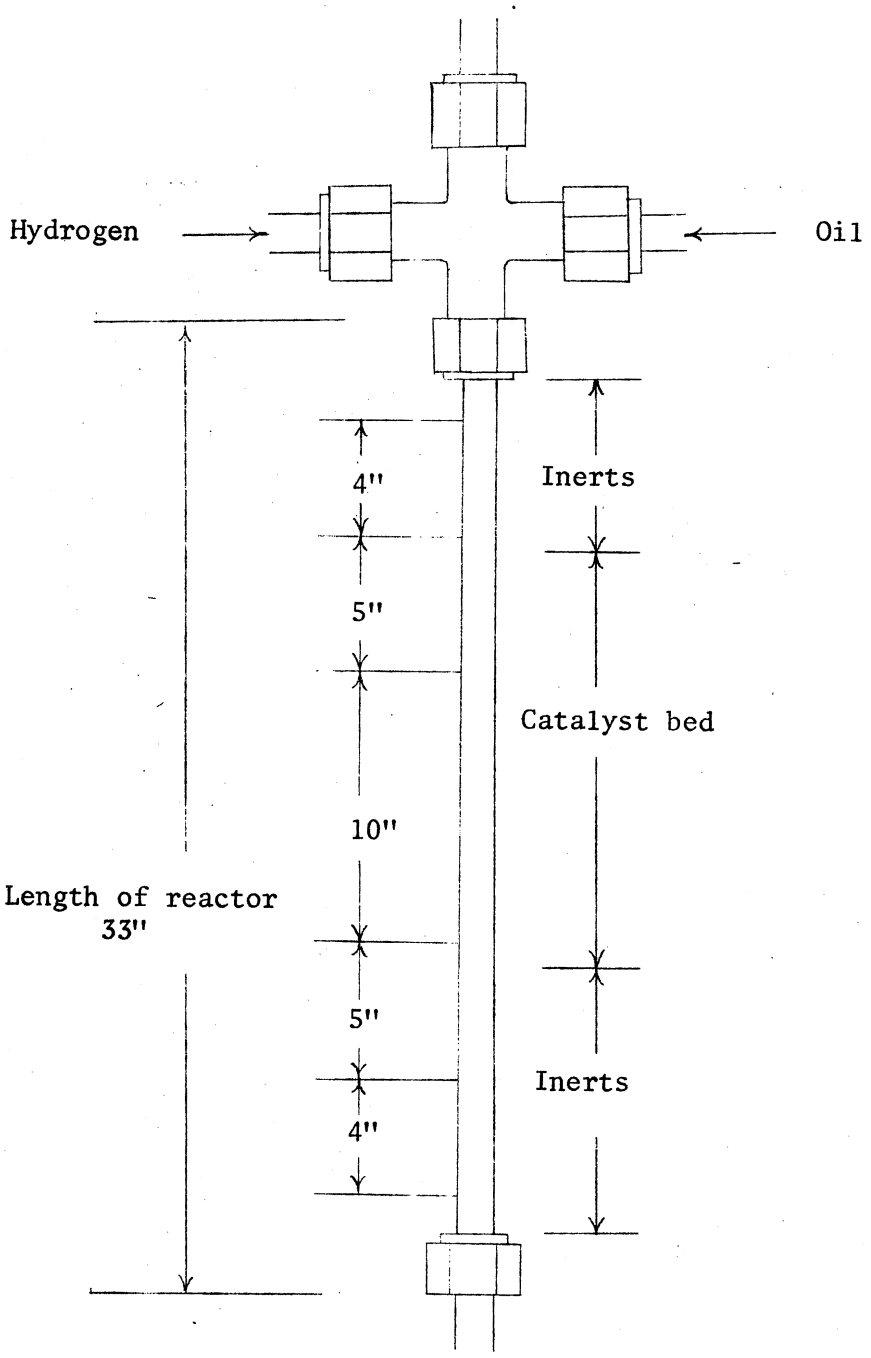

Figure 6. Trickle Bed Reactor and the Related Measurements

crushed to the same size as that of the catalyst particles. Initially, a fine screen was placed at one end of the reactor. A thermowell measuring 1/8" O. D. and 4" longer than the reactor was connected to the screen. Care was taken to ensure that the thermowell coincided with the central axis of the reactor during packing. The reactor was conveniently packed upside down. The reactor was tapped continuously during packing to ensure settling. The packed bed was finally capped with another fine screen to hold the packing in place. The parts list for the reactor and other equipment items is tabulated at the end of this chapter.

Reactor Heating System

The HDS reactions were conducted at elevated temperatures ranging 600 to 800 F (314 to 427C). The reactor was electrically heated to maintain these high temperatures. Five separate heating blocks were employed to achieve and maintain the reactor at the desire temperatures. The heaters were square aluminum blocks grooved to hold beaded resistance wires. Different views of the heating block are shown in Figure 7. The top view of all heating blocks is identical. Each was a 4" square with grooves of 5/8" depth and 3/16" width. These heating blocks were of three different lengths. Two blocks were 4" long, two blocks 5" long, and one block was 10" long. Greater heating control was needed at the entrance and exit of the reactor as well as at the beginning and end of the catalyst zone. The 10" block was then placed in the middle, and the 5" and 4" blocks were placed on either sides. There was a 1/2" diameter hole drilled through the center along the length of each of the heating blocks to place the reactor. The heating

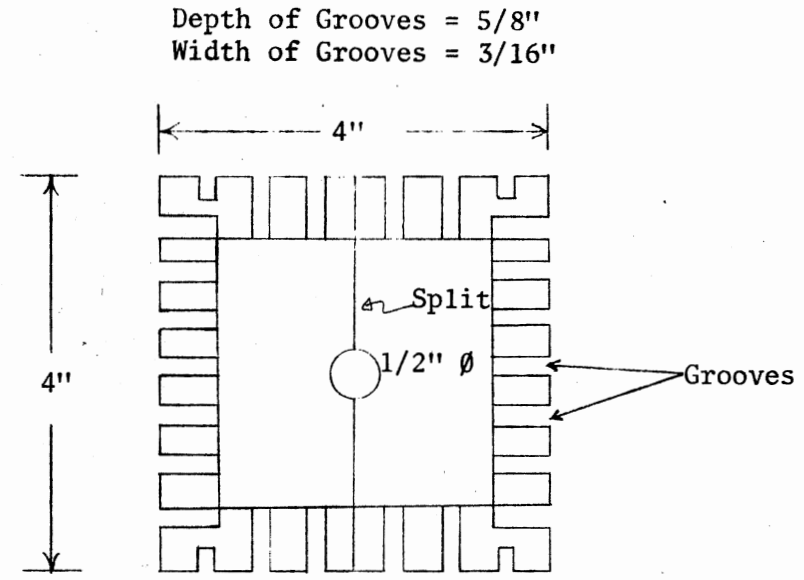

(i) Top View of the Heating Block

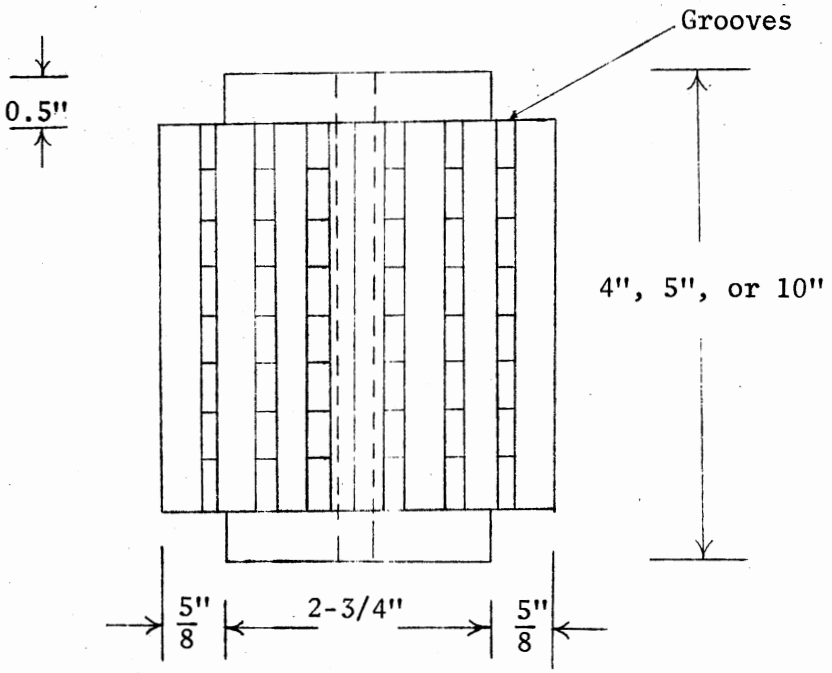

(ii) Side View of the Heating Block

Figure 7. Different Views of the Aluminum Heating Block

blocks were split through the center and hinged on one side for convenient removal.

Beaded resistance wires were passed through the grooves of each heating block and were then connected to five different electrical sources. The beaded resistance wires used in this experimental study were Marsh beeded heaters each having an output of 400 watts. The electrical sources employed were of two types. One type was F & M Scientific 240 temperature programmer supplied by Hewlett Packard, Inc. The temperature programmers were capable of adjusting the heat load to their corresponding reactor zone and maintaining the temperature in that zone at a preset value. (Consult Hewlett Packard manual for detail mechanism and operational procedure of the temperature programmer (108)). The other type of heaters were manually operated variacs. These variacs were Powerstats, supplied by The Superior Electric Co., and were capable of handling loads from 0 to 140 volts. The central 10" heating block was generally connected to the temperature programmer; the four smaller heating blocks were connected to the variacs. The arrangement of the reactor heating system is illustrated in Figure 8.

Reactor Insulation

The reactor and the heating blocks would reach high temperature during the course of any experiment. To preclude heat loss and the threat of personal injury, the heating blocks were insulated by layers of asbestos and fiber glass. The asbestos layer was 1/2" thick and was wrapped around the heaters in two pieces. Three to four metal straps held the asbestos layers in place. The second insulation layer

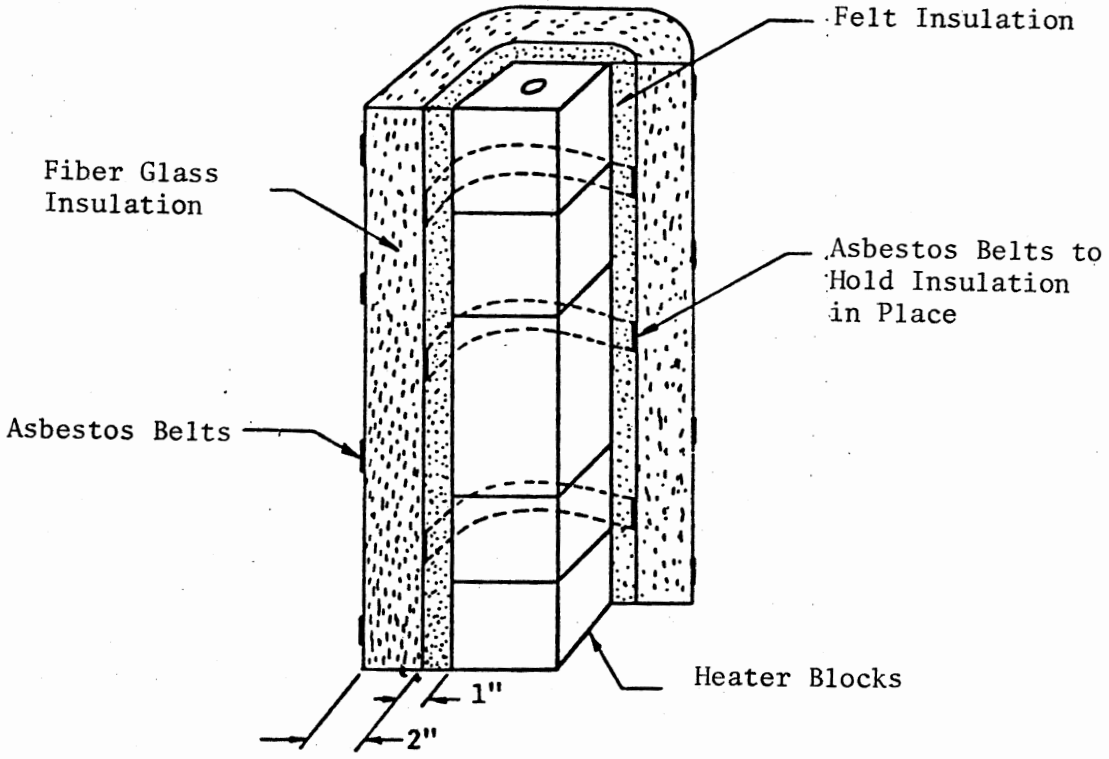

Figure 8. Heater Blocks Showing Insulation (61)

was 2" thick fiber glass. This, too, was wrapped around heaters in two pieces and were held in place with the help of metal straps. The heating blocks were also covered from top to bottom to minimize heat loss. The insulation at the top of the reactor was critical since the operator would be in this area during the measurement of the reactor temperature.

Temperature Measurement

An iron-constantan thermocouple was employed to measure the reactor temperature. The thermocouple was about 36" long and slipped into the thermowell resting along the central axis of the reactor. The lead wires of the thermocouple were connected to a Numatron numeric display. The Numatron was calibrated according to the procedure explained in Leeds & Northrup manual (109) to read temperatures from 0 F to 1000 F (-18 C to 538 C) with an interval of 0.1 F. In the event of an emergency, such as digital readout malfunction during the course of an experiment, the lead wires of the thermocouple were then connected to a millivolt potentiometer. The potentiometer readings would be in millivolts and those could be converted into F by using the charts for respective thermocouples provided by the vendors (Leeds & Northrup Co.).

Pressure Holding and Measurement

The HDS reactions were conducted at reactor pressures ranging from 500 psig to 1,500 psig. The pressure in the system was held steady by a 'Mity Mite' pressure regulator. The block diagram of the reactor system, along with the locations of 'Mity Mite' and pressure

guages, is shown in Figure 9. The primary function of the 'Mity Mite' was to maintain a constant delivery pressure when the inlet pressure or flow volume fluctuated. The 'Mity Mite' model used in these experiments was internally loaded and hence available only for gas loading. The diaphram in the 'Mity Mite' acted as a balancing tool, with dome unit, to adjust the inlet flow and maintained constant downstream pressure. Once the 'Mity Mite' dome was loaded, the system pressure did not exceed the dome pressure.

The pressure holdup in the system was assisted by a needle valve (V-19) at the opposite end of the system. The pressure of the system was measured by three gauges. The main pressure gauge, called 'Heise', had a range of up to 5,000 psig. The 'Heise' gauge was more precise because it had subdivisions of up to 5 psi. The 'Heise' guage possessed a fine needle indicator and mirror along the back panel, which greatly facilitated accurate measurements. The 'Heise' pressure gauge primarily recorded the reactor pressure. The other two pressure indicators were Autoclave gauges and had a range of up to 3,000 psig, with markings at an interval of 20 psi. One of the Autoclave gauges (G-II) was used to measure the oil pump pressure. The oil pump was always pressurized up to the reactor pressure separately to eliminate the possibility of gases flooding the pump space during pressurizing. The other Autoclave gauge (G-III) was employed to measure the pressure of the container in which liquid sample was collected. The operational sequence for sample collection included separation of the sample container from the system, depressurization, and, finally, repressurization.

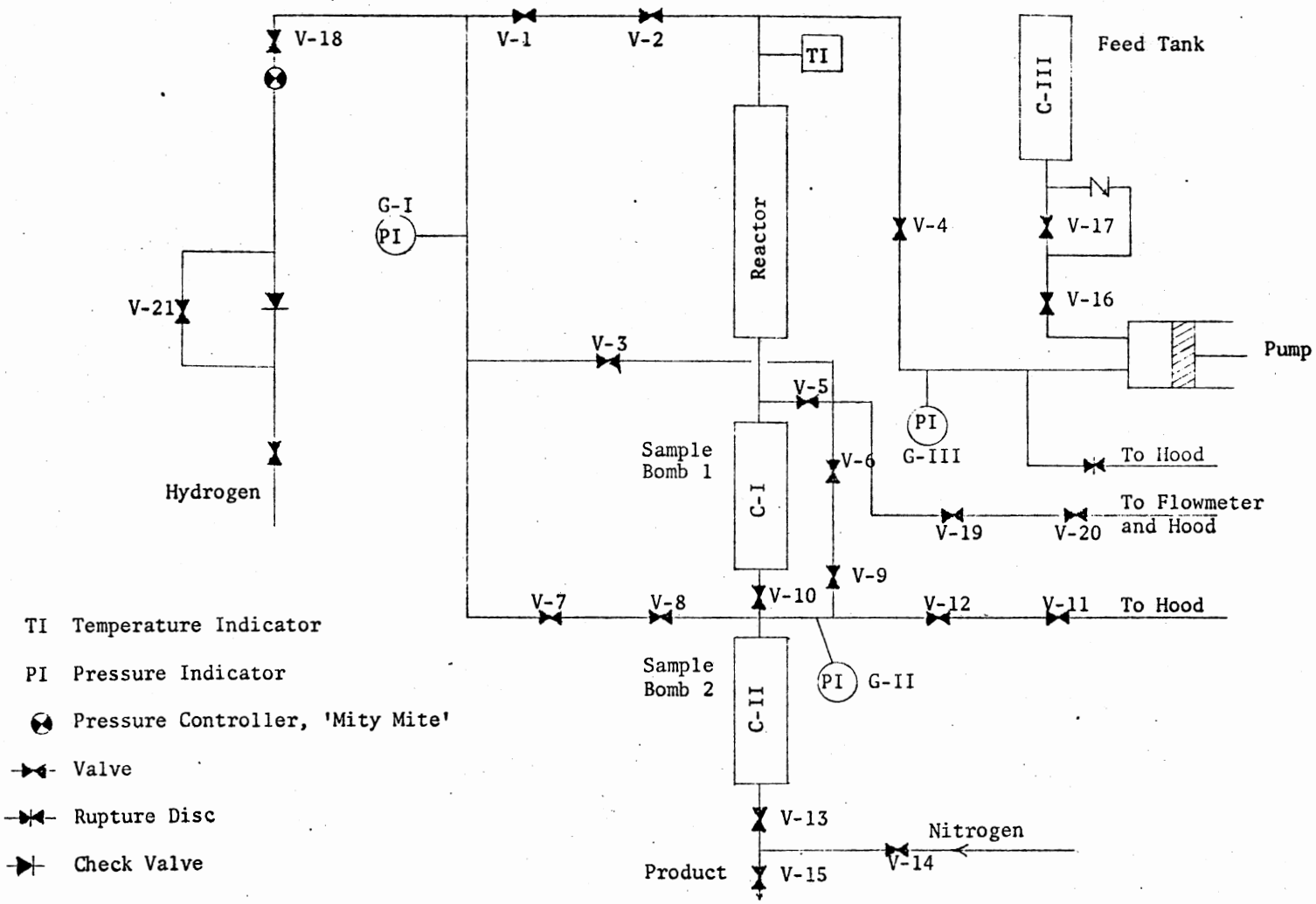

Figure 9. Equipment Setup for the Experimental Program

Sample Collection System

Hydrogen gas and oil flowed cocurrently over the catalyst bed during the HDS reactions. The liquid product, along with the gases, went to stainless steel (SS) containers via SS tubing. The containers were rated up to 5,000 psig at 70 F (21 C). The liquid product was the only one that was finally transferred into the sample bottles and analyzed. Therefore, the liquid product had to be separated from the gas-liquid mixture. The separating mechanism is demonstrated in Figure 10. The gas-liquid mixture came all the way to the bottom of the container through SS tubing. The liquid formed a pool at the bottom of the container and allowed the gases to bubble through it before escaping to the atmosphere. This mechanism eliminated the escape of liquid droplets with the gases by: (1) trapping the droplets in the pool itself; and (2) decelerating and forcing the droplets to remain in the large empty space above the liquid pool.

Another feature of the sampling system was the series arrangement of two sample containers. When a sample needed to be transferred to a bottle, the container holding the sample oil must be depressurized. The next sample was then collected in the other container while the transfer was taking place.

Oil and Hydrogen Feed Systems

The two feed materials for the HDS experiments were oil and hydrogen. The sulfur in oil was removed with the help of hydrogen. The oil was filled in a displacement pump made by Ruska Company. The flow of oil to the reactor could be regulated by the pump controls. The oil

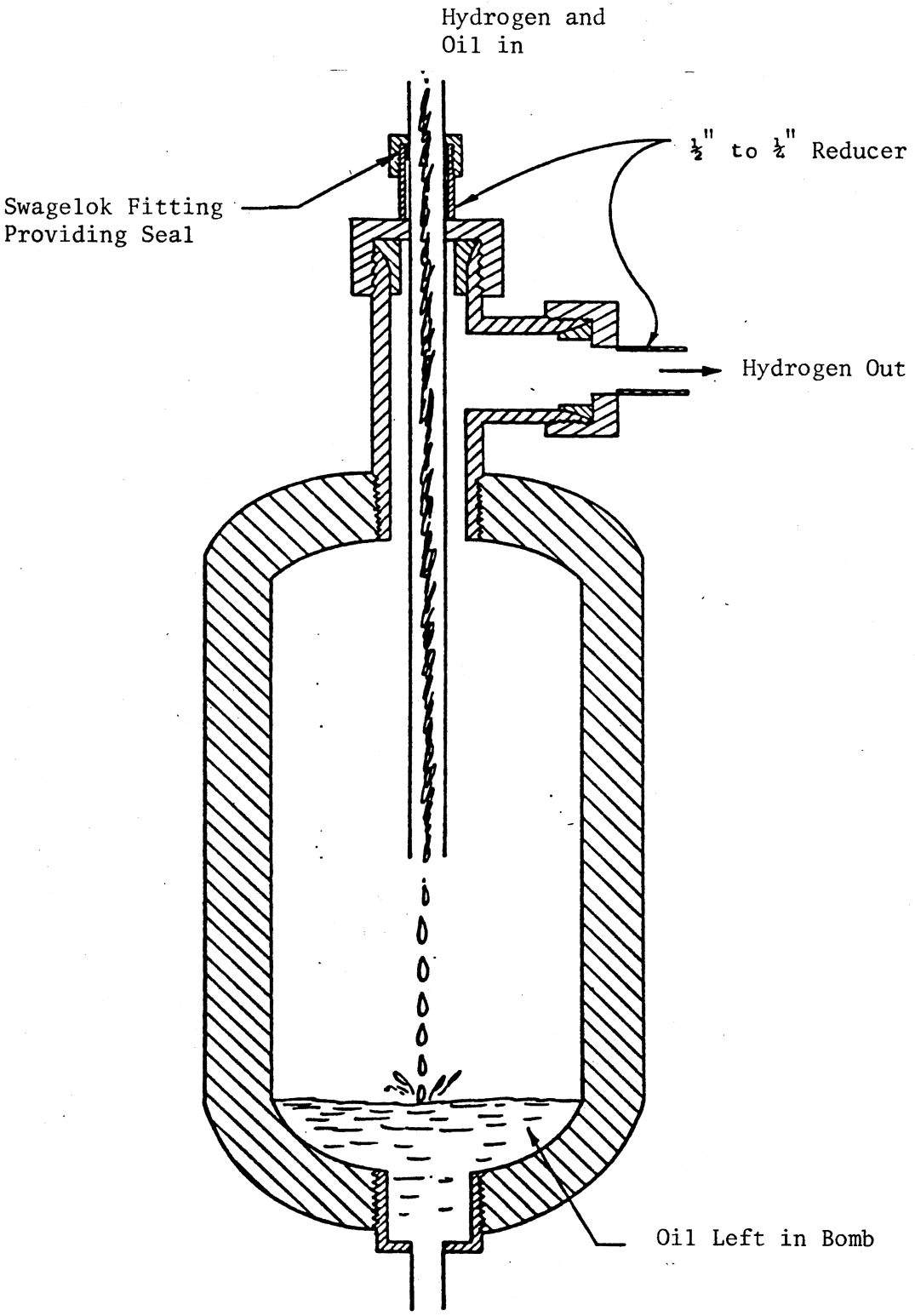

Figure 10. Exploded View of Bomb (61)

was delivered to the top of the reactor via a 1/4" SS tubing.

The hydrogen delivered by various vendors was supplied at varied cylinder pressure. The hydrogen cylinders were connected to the system using a manifold, as shown in Figure 11. The manifold was designed so that three hydrogen cylinders could be connected to it simultaneously. Empty cylinders could be replaced without appreciably disturbing the hydrogen flow to the reactor. A regulator at the cap of the cylinder controlled the hydrogen delivery pressure from the cylinder. The hydrogen flow rate was controlled by a needle valve (V-20) at the opposite end of the system.

Material of Construction

The product gas mixture coming from the reactor and a mixture that was passed through the reactor during pretreatment both contained H_2S. The experiments were conducted at reactor pressures up to 1,500 psig. The material of construction for the equipment must be able to withstand the corrosion effects of H_2S and also sustain the elevated pressures. This material must be readily available at reasonable prices. To fulfill these requirements, SS 316 was employed for all the equipment items, delivery tubes, fittings and valves. To preclude corrosion in the diaphram, 'Mity Mite' must be disconnected during any pretreatment with H_2-H_2S mixture.

Safety Measures

The feed materials - oil and hydrogen - required in the experiments are highly inflammable. The handling of both required extreme caution before and during the experiments. Certain safety devices

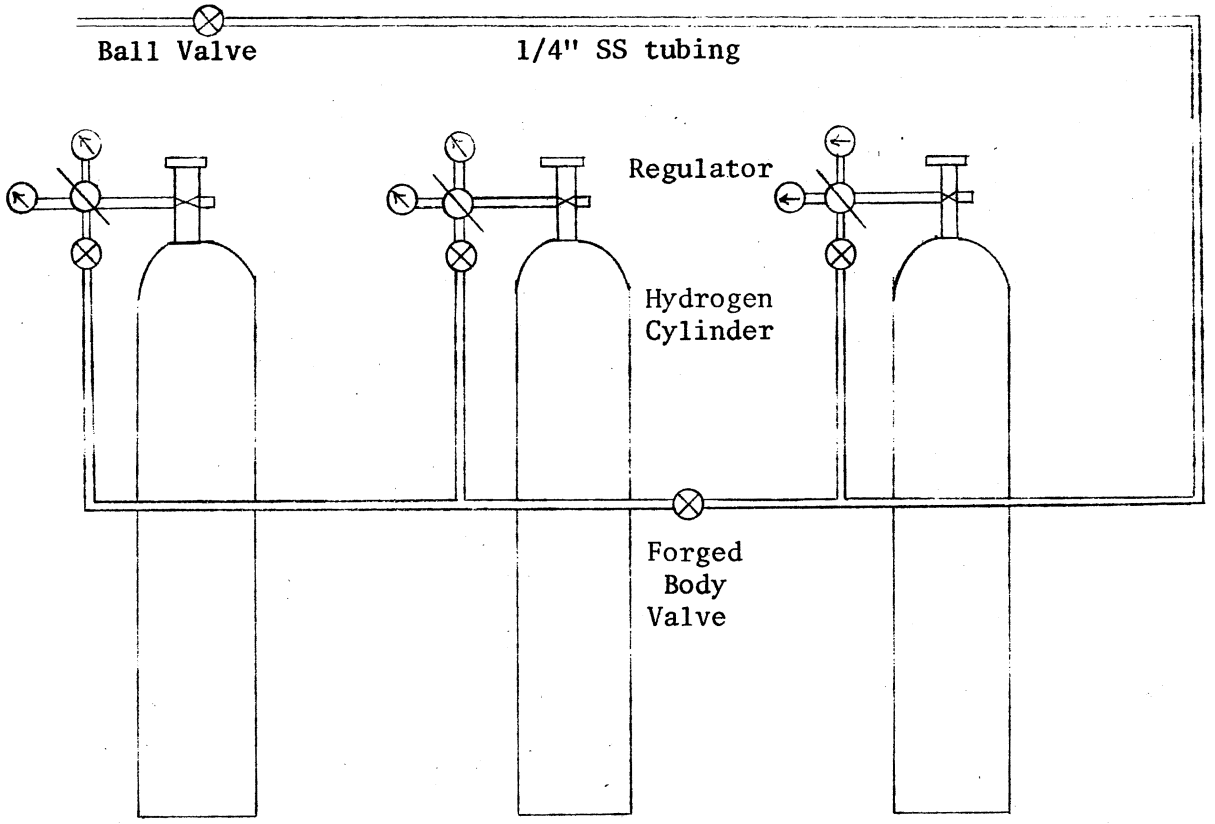

Figure 11. Hydrogen Manifold System

were employed to minimize the danger. The most important precaution was the rating of each equipment item during its design. All the equipment items, tubes, valves and fittings were rated for more than 3,000 and up to 5,000 psig at 70 F (21 C). This rating was more than twice the desired reaction pressures.

The system was repeatedly checked for hydrogen leaks prior to startup of the experiment. The system was pressurized with nitrogen to the highest desired reaction pressure and checked for leaks with soap solution. The soap solution was poured liberally on all the connections and joints. The soap solution would form bubbles at the point of leak. Leaky joints were either tightened or the fittings replaced. The system must be absolutely leak-proof prior to and during the experiments. Hydrogen in the surrounding atmosphere and in the laboratory was continuously monitored during the course of the experiment. The monitoring device gave visual warnings in the event excessive hydrogen concentrations were present in the atmosphere. Should the system malfunction and hydrogen surge to the reactor, a check valve would stop the hydrogen flow immediately. Any drastic fluctuation in the hydrogen flow rate would also shut this check valve. The check valve could only be opened manually to restore the hydrogen flow.

The Ruska pump was filled with oil from a storage tank located above the pump. Any hydrogen gas trapped in the Ruska pump (at high pressure levels) will spill oil into the laboratory when the valve connecting the pump and the storage tank was opened. To prevent such spillage, a unidirectional valve was placed between the pump and the oil storage tank. The oil pump was never pressurized with hydrogen,

as the gas may seep into the pump and disrupt the oil flow rate. To preclude damage from runaway pressure during the charging stage, a rupture disc was placed in an SS tube connecting the pump and hood. The rupture disc would break when the pump pressure became excessive.

The heaters were always checked for short circuits before operation. The resistance of the beaded heating wires from each of the heating blocks was measured. Normal readings would be between 15 and 50 ohm; the resistance of a short circuited wire would read above 100,000 ohms. If a short circuited wire was not repaired, the temperature in the section of the reactor that lies within this heating block would rise from 70 F (21 C) to 1,000 F (538 C) in a matter of minutes, as compared to a controlled heat rise of about 100 F (56 C) per hour.

As an additional safety measure, an attendant contiually monitored the equipment during the course of an experiment. In the event of an emergency, he would depressurize and shut down the system. The laboratory was equipped with an explosion-proof telephone to immediately notify the proper authorities of any emergency condition.

Analytical Apparatus

The liquid product from the reactor was examined for sulfur content in an analyzer. A brief outline of this analytical apparatus is presented in this chapter. The operational procedure will be discussed in the next chapter. Refer to the Laboratory Equipment Company (LECO) manual for detail schematics of the equipment (110).

The basic concept of the LECO method for sulfur analysis was oxidation of sulfur in the sample oil to sulfur dioxide (SO_2), and

titrate SO_2, using potassium iodate (KIO_3). The block diagram of the analytical apparatus is illustrated in Figure 12. A LECO induction furnace, designed to evaluate the sulfur content in hydrocarbons, was employed to warm the sample oil for oxidation. Oxygen gas from cylinders passed through a purifying train before entering the oxidation zone, thereby removing any suspended impurities and ensuring a consistent quality of O_2 for oxidation. LECO crucibles and covers were used to place the sample oil in the oxidation zone. The gases were transferred to the titrator through a glass delivery tube after oxidation. A resistance wire was spiralled around the glass to warm the tube and so prevent the partial condensation of gases passing through it.

The LECO analyzer used for the titration was an 'automatic' model. The operator had only to start the titration. The analyzer would automatically stop the flow of reactants at the end of the process. The only additional equipment required for the titration was a wide-mouth hose, which was connected to a blower and extended all the way to the top of the titrating vessel. This hose vented all product gases directly to the hood. The equipment items, fittings and parts required for this experiment and analysis are listed in Table VII.

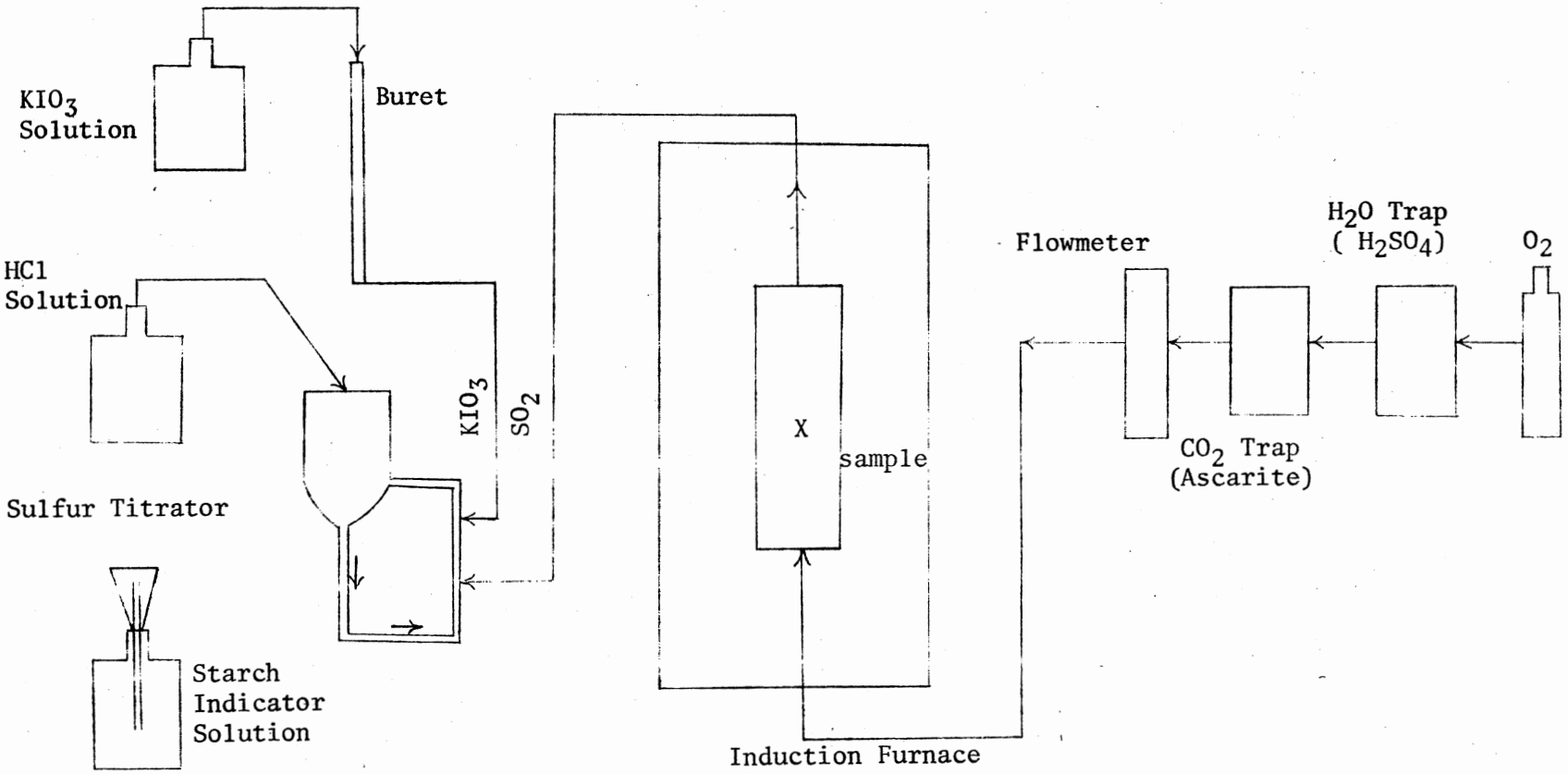

Figure 12. Schematic Diagram of Apparatus for the Determination of Sulfur

TABLE VII

LIST OF EXPERIMENTAL AND ANALYTICAL EQUIPMENT ITEMS

Equipment	Specifications[a]	Vendor
SS tubing	1/8" OD, 18 BWG, 30'	Metal Goods Corp.
SS tubing	1/4" OD, 18 BWG, 30'	"
SS tubing	1/2" OD, 18 BWG, 30'	"
Reactor	1/2" OD, 18 BWG, 33"	"
Female connector (5)[b]	1/2", Swagelok	"
Reducer (9)	1/2" to 1/4", Swagelok	"
Reducing union (3)	1/4" to 1/8", Swagelok	"
Union tee (2)	1/8", Swagelok	"
Union tee (6)	1/4", Swagelok	"
Union cross (2)	1/2", Swagelok	"
Union cross (3)	1/4", Swagelok	"
Cap (3)	1/8" & 1/4", Swagelok	"
Plug (3)	1/8" & 1/4", Swagelok	"
Union (2)	1/8", Swagelok	"
Union (5)	1/4", Swagelok	"
Union	1/2", Swagelok	"
Elbow union (2)	1/4", Swagelok	"
Male run tee (2)	1/2", Swagelok	"
Male adapter	401-A-8-316, Swagelok	"
Forged body valve (5)	1VS4-316, Vee tip	Whitey Res. Tool Co.
Union bonnet valve (3)	3TS4-316, Teflon tip	"
Micrometering valve (3)	22RS4-316, Needle tip	"

TABLE VII (Continued)

Equipment	Specifications[a]	Vendor
Ball valve	43S4	Whitey Res. Tool Co.
Lift check valve	53S4-316	"
Speed valve (6)	10V-4001, straight 2-way	Autoclave Engineers
Check valve	SK-4402, Autoclave	"
Pressure gauge (2)	0-3000 psig, P-480	"
Rupture disc	3000 psig	"
Pressure regulator (2)	Model 8	Matheson Scie, Inc.
Pressure regulator	Model 11-330, H_2S	"
Receiving bomb (2)	1000 cc, SS 316	"
Feed tank	2250 cc, SS 316	"
Pressure regulator (3)	Model 105, No. 63-3143	"
Pressure regulator	'Mity Mite', Model 94	Grove Valve & Reg. Co.
Pressure gauge	Heise-Bourdon, 0-5000 psig	Heise Corp.
Positive displacement pump	1000 cc, proportionating with transmission	Ruska Inst. Co.
Thermocouple	J-SS4-G-T3-36" 8ft lead wire	Conax Corp.
Numatron numeric display	Model 900	Leeds & Northrup Corp.
Temperature programmer	Model 240, 0-1000 C	Hewlett-Packard Corp.
Powerstat (5)	No. 9-521	Fisher Engineering
Hydrogen detactor	Model I-501, wall mount dual diffusion head	MSA Inst. Divn.

TABLE VII (Continued)

Equipment	Specifications[a]	Vendor
Pressure regulator	No. E11-F-N115G	Air Products Inc.
Felt insulation fabric	No. 9326P5	McMaster-Carr Inc.
Fiberglass insulation	No. 9356M13	"
Induction furnace	Model 521	Laboratory Equip. Co.
Automatic titrator	Model 532	"
Purifing train	Model 516	"
Crucibles	No. 528-036	"
Crucible covers	No. 528-042	"

[a]Unless otherwise specified, the material for the equipment is SS 316.

[b]These numbers represent the number of times that identical item is used in the system.

CHAPTER IV

EXPERIMENTAL PROCEDURE

Reactor Operation

The basic principles of the reactor operation are simple. The coal derived liquid and hydrogen were allowed to flow cocurrently downward over the packed bed of catalyst at the controlled flow rates. HDS reactions in this study were carried out at different reaction conditions. The ratio of the hydrogen flow per barrel of oil fed was maintained at a constant, preset value. The oil flow was regulated by appropriately setting the gear box of the Ruska pump. The hydrogen required for the reaction came from the cylinders. After the reaction, the unreacted hydrogen and hydrogen sulfide produced during the reaction were scrubbed by sodium hydroxide solution and then vented. This was a 'once through' operation and thus the unreacted hydrogen was not recovered for recycling. The liquid products from the reactor were collected and transferred to the sample bottles at designated time intervals. These liquid product samples were later analyzed for sulfur content.

Reactor Preparation

The reactor was first cleaned and dried to remove any deposits remaining from previous experiments. The catalyst received from the

vendor was crushed and sized to 8-10 mesh. A specific amount (usually about 20 grams) of a fresh batch of catalyst was weighed in preparation for packing the reactor. Berl Saddles (inerts) were also crushed and sized to 8-10 mesh. A small retaining screen was placed at one end of the reactor. When the reactor was empty, the thermowell coincided with the radial axis of the reactor. The thermowell was held in this position while packing the reactor to ensure that the thermocouple will accurately measure the catalyst bed temperature. The inerts were distributed evenly at the top and bottom of the catalyst bed so as to reduce the end effects of entrance and heat loss. Another retaining screen was placed at the other end of the packing to hold the packed bed in place. The reactor was connected to the system after packing.

The system was then pressure tested overnight and checked for any pressure losses after 12 hours. Leaks causing pressure drops of more than 5 psi were sealed before any further connections were made.

The HDS reactions were conducted at temperatures ranging from 600 to 800 F (314 to 427 C). To maintain these temperatures, the reactor was electrically heated. Five separate aluminum heating blocks were employed to achieve and maintain the reactor at a specified temperature. All five heaters were placed around the reactor and controlled individually using a temperature programmer or a variac. The electrical connections must be checked for any short circuits prior to operation. The resistance of the beaded heating wires from each of the heating blocks was measured using a volt-ohmeter. The resistance reading of a properly connected heating wire would be between 15 and 50 ohms, whereas a short circuited wire would be over

100,000 ohms. The short circuited heating wires were fixed prior to operation. The heating blocks were then doubly insulated with layers of asbestos and fiber glass. While applying the insulation, care was taken that the thermocouple wires coming from the temperature programmers were properly placed. The catalyst was now ready for pretreatment.

Catalyst Pretreatment

The pretreatment stage was comprised of calcining and sulfiding. The calcining was performed to remove any moisture trapped in the packed bed of the reactor. The moisture was vaporized and eventually carried away by nitrogen. During calcining, the packed bed of catalyst and inert particles was heated to 450 F (233 C). During pretreatment, the 'Mity Mite' pressure regulator and 'Heise' pressure gauge were disconnected from the system and the open ends were capped to preclude corrosion in their diaphrams during sulfiding. The nitrogen gas entered the system just below the 'Mity Mite', flowed over the packed bed, passed through containers C-I and C-II, and left the system through valve V-20, which also maintained the flow rate at about 30 cubic centimeter per minute (cc/min). Such a low nitrogen flow was sufficient to carry away the moisture trapped in the packed bed. The valve positions during pretreatment are summarized in Table VIII. The valve positions presented in Table VIII would ensure desired route of the nitrogen flow. The catalyst was calcined for about 12 hours.

The other step in the catalyst pretreatment was sulfiding. The cobalt and molybdenum molecules in the catalyst were partially sulfided during the HDS reactions. But the fresh batch of catalyst

contained interlinked molybdenum, cobalt tetra and octahedra (111). These interlinking bridges are broken and the open anion vacancies filled by sulfur during sulfiding. It is also observed that the substitution of bridging oxides occurs in preference to the terminal oxides. Thus, sulfiding helps activate the cobalt and molybdenum molecules in the catalyst and initiate the HDS reactions. After calcining, the nitrogen flow was stopped and the system was switched to H_2-H_2S mixture (about 5% H_2S) for sulfiding. The catalyst bed was again maintained at 450 F (233 C) and the flow route for the H_2-H_2S mixture during sulfiding was the same as that for nitrogen. The H_2-H_2S mixture flow rate was kept low at about 30 cc/min. The catalyst was sulfided for about 90 minutes.

TABLE VIII

VALVE POSITIONS DURING CATALYST PRETREATMENT

Valve Number	Valve Postion
V-1, 2, 6, 9, 10, 18, 19 and 20.	Open
V-3, 4, 5, 7, 8, 11, 12, 13, 14, 15, 16, 17 and 21.	Closed

Reactor Feed Preparation

The two feed materials - oil and hydrogen - must be made available for the reactor operation. The hydrogen cylinders were connected to the system via manifold as shown in Figure 11 in the previous chapter. The 'Mity Mite' regulator and the 'Heise' gauge that were disconnected during the catalyst pretreatment must be reconnected prior to starting the hydrogen flow.

Oil to the reactor was supplied from a Ruska pump of 1,000 cc capacity. The pump itself was filled with oil from storage tank C-III. Since C-III is filled with more than 1,000 cc of oil, the pump must be disconnected from the system before the filling procedure was started to prevent gas backup and oil overflow, as previously discussed on page 66. Therefore, valve V-4 must be closed and the pump must be depressurized prior to connecting it with C-III. To depressurize the pump, the gear stem on the pump was shifted to the "traverse" position and the "traverse" switch was flipped to the "out" position. Any slight expansion of the liquid would sharply reduce the pump pressure. Once the pump pressure reached one atmosphere, the unidirectional valve between the pump and C-III was opened. The pump position was brought all the way out to the "0" cc mark to allow for the inflow of oil. The pump filled to the 1,000 cc level in less than two minutes, at which time the unidirectional valve was closed. The pump was then pressurized by flipping the "traverse" switch to the "in" position. The pump pressure would rise immediately. The system was ready for operation when the pump had reached the desired pressure level. Indentical procedure was followed for any refilling necessary during

the course of the experiment.

Startup Procedure

The steps involved in startup included pressurizing the system to the desired reaction pressure, establishing hydrogen flow, starting oil flow, and attaining desired reaction temperature. The HDS reactions were conducted at temperatures ranging from 600 F to 800 F (314 C to 427 C), pressures of 500, 1,000, 1,500 psig and the liquid volume hourly space times ranging from 0.3 to 1.8 hours. The startup steps were performed in the order they were presented above. As a precautionary measure, the entire system was not pressurized in a single step. Instead, successive pressurization of small segments were performed so that only a small part of the system was checked for leaks at any time. The hydrogen cylinder was opened and the discharge pressure at the regulator was set at a level slightly higher than the desired reaction pressure in order to maintain a steady flow. The segment of the system pressurized thus far lied between hydrogen cylinder and the 'Mity Mite' only (as seen in Figure 9, previous chapter). During 'Mity Mite' loading, some hydrogen gas did escape to the atmosphere and, therefore, the hydrogen monitoring device must be carefully observed to avert possible hazards. The next segment pressurized lied between 'Mity Mite', pressure gauge G-I, and valves V-1, V-3 and V-7. Therefore, valve V-18 was opened and valves V-1, V-7 were closed. The 'Mity Mite' was now loaded and discharge pressure was checked by watching G-I. The loading was discontinued after G-I read the desired reaction pressure. (Consult 'Mity Mite' manual for its loading technique (112).) Each segment was checked for leaks before

proceeding to the next segment. As mentioned earlier, the pump was pressurized separately and, therefore, V-4 remained closed until the start of oil flow to the reactor was required. The next segment pressurized fell between valves V-1, V-3, V-5, V-7, V-9, V-12 and V-13. This segment included the reactor, containers C-I and C-II, pressure gauge G-II and valves V-2, V-8 and V-10. Therefore, valves V-5, V-9, V-12 and V-13 were closed and V-2, V-8 and V-10 were opened. Valve V-1 was then opened gradually and the pressure reading on G-II observed. V-1 was opened completely once the reading on G-II matched that on G-I. At this stage, valves V-6 and V-9 were opened to pressurize the entire system up to valve V-19.

The next step in the startup procedure was to establish hydrogen flow. V-19 was opened partially and valve V-20 was maneuvered very carefully to establish hydrogen flow. The gases coming from V-20 passed through two sodium hydroxide scrubbers in series to trap H_2S and then moved through a buret. The time required for the soap film to travel the buret length corresponding to 25 cc was measured and was used as a basis for measuring hydrogen flow rate. The desired hydrogen flow rate was established by successively maneuvering of V-20.

Generally, the oil flow was not started immediately after establishing hydrogen flow. The reactor temperature at this stage would be about 450 F (233 C). The settings on the temperature programmer and all the variacs were now increased to attain a higher reactor temperature. The oil flow was started when the reactor temperature was about 30 F (18 C) below the desired value. The HDS reactions were exothermic and so once the oil flow was started, the reactor temperature would automatically move to the desired value. Before starting oil flow, the

pump was charged to the reactor pressure using the technique covered in an earlier section. The gear stem on the pump was shifted to the "feed" position, the feed switch on the pump was flipped to the "on" position, and V-4 was opened to establish the oil flow to the reactor. The reactor had been warming all this time and the exact reactor temperature was attained by adjusting the settings on the temperature programmer and/or the variacs.

Normal Operation

The coal derived raw anthracene oil and hydrogen came to the top of the reactor via 1/4" SS tubing from their respective feed storage tanks. The oil flowed from the pump through V-4 to the reactor, whereas, hydrogen flowed from the cylinder through V-21, the 'Mity Mite', V-18, V-1 and V-2 before reaching the top of the reactor. In the reactor, sulfur containing compounds in oil reacted with hydrogen in the presence of a catalyst to form hydrogen sulfide. The hydrogen flow rate, oil flow rate, reactor temperature, and reactor pressure were held constant for a certain length of time (ranging from two to six hours) during normal operation. The fluctuations encountered in each of these categories will be presented later in this chapter.

The reaction products in liquid and gas phases flowed to container C-I and on down to container C-II through V-10. The liquid and gas phases were separated in C-II by the mechanism illustrated in Figure 10 of the previous chapter. The liquid product collected in C-II was later transferred to sample bottles and finally analyzed for sulfur content. The gaseous mixture from C-II flowed through V-9, V-6, V-19, V-20, hydrogen sulfide scrubbers, and the flowmeter before

it was vented. In large scale industrial operations, the unreacted hydrogen must be recycled for economic and safety considerations. The system pressure was held at one end by the 'Mity Mite' regulator and at the opposite end by V-19. Therefore, the pressure beyond V-19 was essentially atmospheric. V-20 controlled the hydrogen flow rate.

Some of the valves in the system performed no apparent function. These valves were present as back-up valves and were used in the event of lead valve malfunction during the course of an experimental run. These valves, viz. V-2, V-6, V-8 and V-11 were, therefore, kept open all the time. The summary of the valve positions during the normal operation is presented in Table IX.

TABLE IX

VALVE POSITIONS DURING NORMAL OPERATIONS

Valve Number	Valve Position
V-1, 2, 4, 6, 8 9, 10, 11, 18, 19, 20 and 21.	Open
V-3, 5, 7, 12, 13 14, 15, 16 and 17.	Closed

Sample Collection

The most frequent cause of system disturbance was for sample collection. The liquid was first collected in C-II within the system.

This product must now be transferred to sample bottles. There was a sequence of steps involved in transferring the liquid product. These steps, along with necessary explanations, are outlined below:

1. Since the system was at an elevated pressure, C-II must be isolated and depressurized before V-13 and V-15 could be opened for sample transfer. During the time C-II was isolated, the next sample was collected in C-I. V-9 and V-10 were closed to isolate C-II and V-5 was opened to ensure continuity in gas flow.
2. C-II was brought to atmospheric pressure by gradually opening V-12 and simultaneously observing pressure in G-III. V-12 was left open once C-II reached atmospheric pressure.
3. Invariably, some H_2-H_2S gas mixture became trapped in the liquid product. Nitrogen gas was then purged through the sample to carry away the unwanted trapped gas mixture. V-15 must be closed before opening V-13. In case of an error, the entire sample in C-II would drain out on the floor. Nitrogen flow was started by the partial opening of V-14. Too high a nitrogen flow would entrain a portion of the liquid product. The nitrogen flow rate was kept at about 100 cc/min. The sample was purged with nitrogen for about 30 minutes.
4. V-12 and V-14 are closed once purging with nitrogen was stopped. The sample could be transferred from C-II to a bottle.

5. A sample bottle was placed below the opening of V-15 and V-15 was opened. The liquid product from C-II flowed through V-13 and V-15 and was collected in the sample bottle. V-13 and V-15 were closed when all the product had drained from C-II. The sample bottle was capped, labelled, and stored for later analysis.
6. C-II could be reconnected to the system after it was repressurized to the same level of the system. C-II was generally pressurized with hydrogen. V-1 was closed to avoid any drastic pressure disturbances in the reactor. If V-7 was opened at this stage, the check valve (V-21) would become clogged due to the sudden surge of hydrogen flow. Therefore, V-21 in the bypass line was partially opened (just one turn was enough). V-7 was now opened partially to allow slow build up of pressure in C-II. Any sudden fluctuations in pressure could damage the gauge G-II. When C-II reached the system pressure (as read in G-II), V-7 and V-21 were closed and V-1 was opened to reestablish the hydrogen flow to the reactor.
7. Thus far the next sample had been collecting in C-I. Since C-II was back again at the system pressure, the sample could now be transferred and collected in C-II. Therefore, V-9 and V-10 were opened and V-5 was closed to allow the liquid sample collection in C-II. At this stage the flow situation was identical to that of normal operation. Generally, it took 40 to 45 minutes to perform steps 1 through 7.

Control of Operating Conditions

There are four experimental variables that must be controlled during the experimental study, viz. reactor temperature, pressure, hydrogen flow rate, and oil flow rate. In any normal operation, these four variables must be observed, recorded, and readjusted if necessary. For a particular set of operating conditions, there would be a fixed value for each of these variables. Any deviation from these desired values must be monitored and corrected as quickly as it occurs.

One such operating variable was reactor temperature. Previous investigations by Sooter (61) and Wan (52) had noted that the effect of reactor temperature on reaction kinetics was significant. Therefore, a thorough control of temperature was essential. The temperature in the inert bed before catalyst zone was kept lower than the desired value so that the exothermic heat of reaction would be absorbed and still keep the catalyst zone at the desired reactor temperature. A typical reactor temperature profile is shown in Figure 13. The temperature was controlled with the help of five different heat sources. The reactor bed temperature was measured at least once every hour at points not more than 1" apart along the length of the reactor. The supply voltage on variacs and the setting on the temperature programmer were changed when necessary. Increasing such input would increase bed temperature and vice versa. It took 10 to 15 minutes for the reactor temperature to stabilize after any change in setting was made.

Another operating variable was reactor pressure. The observed effect of pressure on reaction kinetics was not as significant as that of temperature. Besides, fluctuations in reactor pressure were hardly

Test Series: SP
Nominal Temp: 750 F (399 C)
Nominal Press: 1,000 psig

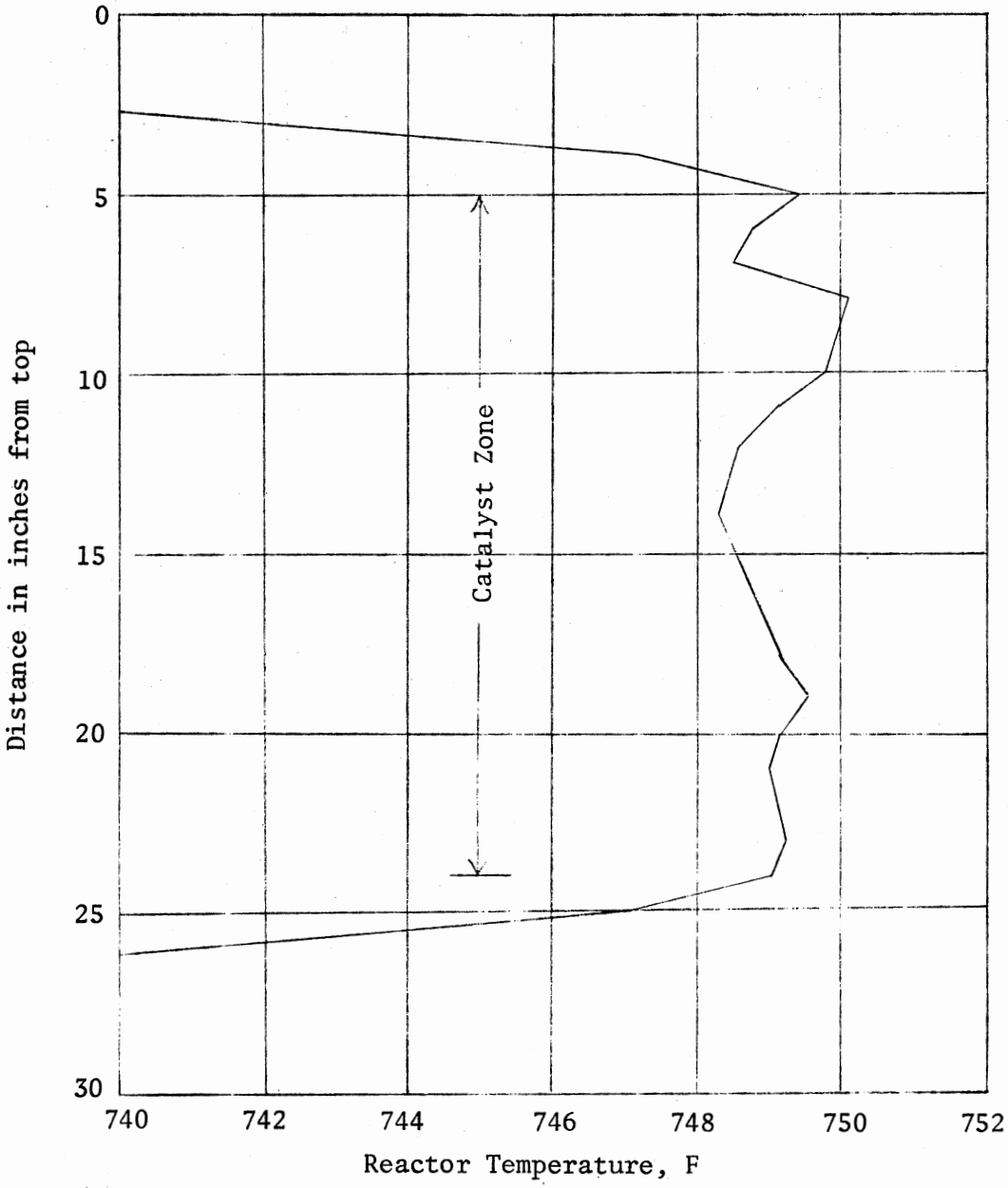

Figure 13. A Typical Temperature Profile

noticeable. Any sudden change in the hydrogen flow rate would affect the reactor pressure because of momentary adjustment, but the reactor pressure remained generally constant.

Hydrogen flow rate was one of the most important operating variables. In their experiments, Wan (52) and Sooter (61) observed that the effect of changing flow rate was negligible for hydrogen flow rates above 1,500 scf/Bbl, whereas below 1,500 scf/Bbl of oil the effect was significant. Therefore, the hydrogen flow rate was always maintained above 1,500 scf/Bbl of oil. The difficulties experienced in controlling the hydrogen flow rate were enormous and the rate had to be checked at least every 30 minutes, and sometimes every 15 minutes. The valve controlling the hydrogen flow rate was replaced more than any other in the entire system.

The final variable, the oil flow rate, caused the least amount of problems. The oil flow rate remained at the desired value throughout the experimental run. Difficulty could only occur if a portion of the Ruska pump was occupied by hydrogen gas. This problem could be eliminated by carefully filling and pressurizing the pump.

An experienced operator would facilitate the control of these variables. His presence could be extremely helpful when the operating conditions were changed.

Changing Operating Conditions

Some of the experiments were conducted at only one set of flow and reactor conditions (i.e. oil and hydrogen flow rates), reactor temperature, and pressure. Other programs did require these factors to vary. The reactor temperature or pressure could be changed

independently, whereas oil and hydrogen flow rates had to be changed simultaneously for a particular space velocity.

The oil flow rate was changed by appropriately setting the gears on the pump. First the pump was isolated and turned off by closing V-4 and turning the feed switch to the "off" position. The gear stem was then brought to the "neutral" position before changing gear settings. (Consult Ruska manual to find appropriate setting corresponding to the desired oil flow rate (113).) The gear stem was returned to the "feed" position and the feed switch was flipped to the "in" position. V-4 was opened and the oil flow rate change was complete. The hydrogen flow rate must also be changed to maintain constant H_2/oil ratio going to the reactor. The hydrogen flow rate was changed by adjusting V-20. This was a trial and error procedure, making adjustments and then checking the measured flow rate. Changing oil and hydrogen flow rates did not take more than five minutes.

The reactor pressure was changed by operating the regulator at the outlet of the hydrogen cylinder, the 'Mity Mite' regulator and the pump. To avoid any hydrogen seeping into the pump, the pump was pressurized or depressurized separately. Thus, before changing system pressure, the pump was isolated and turned off by closing V-4 and turning the feed switch to the "off" position. The outlet pressure of the regulator at the hydrogen cylinder was then set at a pressure approximately 100 psi higher than the desired reactor pressure. This extra 100 psi acted as a driving force and ensured smooth flow of hydrogen. The next step was to adjust the 'Mity Mite'. Prior to this, V-1 was closed so that the reactor did not receive abrupt pressure variations. (Consult 'Mity Mite' manual for the procedure of changing reactor pressure (112).)

V-1 was opened gradually and the reactor pressure was allowed to reach the desired value. V-1 was opened completely once the entire system (except the pump) attained the desired pressure level. The pump pressure was changed by flipping the feed switch to the "on" position without opening V-4. The pump pressure increased very slowly and V-4 was opened once it reached system pressure. Hydrogen flow rate was always checked after changing system pressure which normally took about 10 minutes.

Changing reactor temperature was time consuming but simple. One needed only change the settings on all the variacs and the programmer. The time required to change the reactor temperature by 50 F had varied from four hours to eight hours, depending upon operator skill. The reactor temperature measurements were more frequent (at least every 30 minutes) during the transition period.

Other adjustments necessary during the course of the experimental run were refilling the pump and switching hydrogen cylinders. The refilling was almost identical to the method explained earlier in this chapter except that the pump must be isolated and depressurized before it was ready for refilling. The design of the manifold allowed for isolating and switching the hydrogen cylinders without appreciably disturbing the system.

Shutdown Procedure

The duration of the experimental runs on the reactor had ranged from 100 to 250 hours. Once the experiment was complete, the shutdown procedure was started immediately. The steps involved for the shutdown procedure were as follows:

1. The hydrogen supply was turned off by closing the valve at the hydrogen cylinder.
2. The oil pump was isolated by closing V-4. Next, the feed switch was turned to the "off" position and over to the "out" position. Very slight expansion of the oil would drop the pump pressure down to one atmosphere. Once depressurized, the feed switch was brought back to the "off" position.
3. The heat supply to the reactor was cut off by turning the switches on all the variacs and the temperature programmer to the "off" position.
4. After the final sample was transferred to a bottle, all outlets from the system except V-12 were closed. V-12 was gradually opened and the system was depressurized very slowly. Some residual pressure, about 100 psig, was left in the system to sustain and absorb any contraction of gases due to cooling.
5. The reactor was then allowed to cool. The amount of time required to cool the reactor from about 700 F (371 C) to room temperature was approximately 12 hours.

The above covers all the major aspects of the reactor operation. The samples collected were labelled and stored to be analyzed later for sulfur content. The sulfur analysis of the liquid products was a measure of performance of the catalyst at the specific reactor conditions. Relative performances of the various catalysts could be studied after all the samples from different experimental runs were analyzed.

Analyzer Operation

Sulfur Analysis

A brief outline of the analytical method is described in the following. (Consult LECO manual for the detail procedure and schematics of the equipment (110).) The chemicals used during the analysis are listed at the end of this chapter in Table X.

The basic concept in the sulfur analysis could be summarized in reactions (4.1) and (4.2).

$$KIO_3 + 5KI + 6HCl \longrightarrow 6KCl + 3I_2 + 3H_2O \qquad (4.1)$$

$$I_2 + SO_2 + 2H_2O \longrightarrow H_2SO_4 + 2HI \qquad (4.2)$$

Potassium iodate (KIO_3) and potassium iodide (KI) would react in the presence of hydrochloric acid (HCl) to release iodine (I_2), reaction (4.1). I_2 would give distinct blue color in presence of a starch solution. The sulfur dioxide (SO_2) gas coming from the oxidizing sample oil, when passed through this mixture, would react with I_2 and thereby gradually fade the blue color, reaction (4.2). Additional KIO_3 solution would be required to attain the original level of blue coloration. This additional amount of KIO_3 was the measure of SO_2 and, in turn, the sulfur level in the sample oil.

Some chemicals must be prepared before the analytical procedure could be performed. The preparation of these chemicals is explained in the following:

1. The HCl solution was prepared by adding 15 ml of the concentrated HCl to distilled water to make a one liter solution. Enough HCl solution could be prepared for one month's use.

2. The KIO_3 solution was prepared by adding 0.111 gm of KIO_3 powder to one liter of distilled water. The KIO_3 buret range could be changed by adding different amounts of KIO_3 powder to one liter of distilled water. (Consult LECO manual for determining the amount of KIO_3 to be added to a liter of water corresponding to the sample size and its level of sulfur content.) Enough KIO_3 solution could be prepared to last for a month.
3. The starch solution must be fresh daily for consumption. First, 150 ml of distilled water was brought to boiling. Then, 2.0 gms of Arrowroot starch, mixed with 50 ml of distilled water, was added to the boiling water. The mixture was brought to and allowed to boil for about two minutes. The mixture was then cooled to room temperature. 6.0 gms of KI was added to the mixture and stirred well to make the desired starch solution.

The general set up of the LECO furnace and the analyser is as shown in Figure 12 of the previous chapter. There are certain maintenance steps that must be performed prior to the analysis. These are outlined as follows:

1. The KIO_3 level in the buret was checked. The KIO_3 level in the buret was set at 0.000 after everyday's analytical work. Thus, when checking, the level should read 0.000. If not, leak must be located and sealed.
2. The second check was for possible plugging of the gas line. The oxygen flow was started and the pedestal in the furnace was raised. If there was sudden rise in the back pressure in

the rotometer, the gas line was cleaned and rechecked.

3. Another very important item to check was the photocell alignment. The photocell housing would become dirty due to blue coloration of the reaction mixture, thereby increasing the photocell resistance. The photocell housing was cleaned prior to each day's analytical work and realigned so that the resistance read between 30,000 and 50,000 ohms.
4. The combustion tube was also cleaned everyday and the igniter was replaced if necessary.

After all these maintenance and checkup procedures were completed, the equipment was ready for analysis.

The sample should be prepared first for the analysis. The product oil from the reactor was oxidized in the furnace and the generated gases were sent to the anayzer for sulfur analysis. The oxidizing reaction was catalyzed by magnesium oxide (MgO). About 0.282 gm of MgO was first placed in the crucible. Then between 0.09 and 0.11 gm of oil sample was accurately weighed and placed over MgO in the crucible. Another 0.282 gm of MgO was added to the crucible on top of the sample. About 1.50 gms of iron chips and 0.77 gm of tin metal were added to the crucible as catalyst promoters. The crucible was then covered and was ready for oxidizing.

The furnace and the analyzer needed to be warmed up for the analysis. The analytical operation began with turning the power switches on the furnace and the analyzer to the "on" position. The analyzer was preset for a specific level of blue color as the end point. The equipment was allowed to warm for about 30 minutes. Oxygen flow was then

started at the rate of about 1.2 liters/min and the pedestal was raised into the combustion zone of the furnace. Simultaneously, the glass tube connecting the furnace and the analyzer was started to be warmed. The equipment was ready for analysis after about 15 minutes of oxygen flow. The titration vessel was then filled with HCl solution to a specific level. The amount of HCl solution used in each analysis must be same. Next, 5 ml of starch solution was added to the titration vessel and oxygen was allowed to bubble through the solution for thorough mixing. After about one minute of mixing, the double throw switch on the titrator was set to the "end point" position. Once the end point was established, the double throw switch was brought to the "neutral" position and the buret was refilled with KIO_3 solution to the 0.000 mark. The crucible loaded with sample, catalyst, and the promoters, was then placed on the pedestal and raised into the combustion tube. The double throw switch on the analyser was now set on the "titrate" position and about 0.777 gm of sodium azide was added to the reaction mixture to inhibit any side reactions due to the presence of chlorine in the sample oil. Chlorine replaced iodine in the KI, thereby forming more free iodine which, in turn, gave a darker blue color. The ultimate effect was that less KIO_3 was required to produce the preset level of blue color and thereby registering an erroneous lower value for the sulfur content in the sample oil. Sodium azide had been found to be successful in sufficiently eliminating the effect of chlorine. The plate voltage on the furnace rose sharply during the combustion of the sample oil and returned to the non-fluctuating initial value, once the combustion was complete. The reaction time could be controlled with the help of a timer. The amount of KIO_3

consumed in the reaction was recorded. The titration vessel was drained and thoroughly rinsed with distilled water. The analytical operation could be started all over again for the next sample.

All the samples were analyzed at least three times to check the consistency of the sulfur content. The buret readings and the calculation procedure for estimating sulfur content in the sample oil are presented in the next chapter. Results of the analysis of all the samples from the experimental runs are also presented in the next chapter and are examined for relative performances of the HDS catalysts.

TABLE X

LIST OF CHEMICALS USED IN EXPERIMENTS AND ANALYSIS

Chemical	Specifications	Vendor
Hydrogen	99.95%, prepurified, 3500 psig	Matheson Gas Products
Nitrogen	99.997%, prepurified, 3500 psig	"
H_2-H_2S mixture	5% hydrogen sulfide, 3500 psig	"
Hydrogen	99.95%, prepurified, 2200 psig	Union Carbide Corporation
Nitrogen	99.997%, prepurified, 2200 psig	"
Potassium iodate	ACS Reagent	Fisher Scientific Company
Arrowroot starch	ACS Reagent	"
Sodium hydroxide	ACS Reagent	"
Potassium iodide	"Baker Analyzed" Reagent	J. T. Baker Chemical Company
Hydrochloric acid	37%, ACS Reagent	DuPont Company
Sodium azide	Practical	Eastman Kodak Company
Magnesium oxide	ACS Reagent	MCB Manufacturing Chemists
Iron chips	No. 501-077	LECO Corporation
Tin metal	No. 501-076	"
Oxygen	99.5%, 2200 psig	Union Carbide Corporation

CHAPTER V

EXPERIMENTAL RESULTS

The HDS experiments conducted on raw anthracene oil had a wide range of objectives. However, since this project was a continuation of the research initiated by Sooter (61), some of the objectives investigated by him were not explored in this study. The major ones not considered among those of Sooter were the particle size effects, the start up effects, the equipment precision, etc. The results of Sooter's investigations indicated that, for the HDS of raw anthracene oil, the changes in the particle size range from 8-10 mesh to 48-60 mesh did not result in any noticeable change in the extent of the sulfur removal. Consequently, 8-10 mesh was the size selected for both the catalyst and inert particles in this investigation. Since frequent start ups and shut downs during an experiment were found to have unfavorable effects on the catalyst activity, all data collected was from the same run. Equipment performance for sulfur removal at identical reactor conditions for different runs was found to be quite satisfactory in Sooter's work. Therefore, the study of the equipment precision was omitted from this research program. Certain other goals may appear to be overlapping in this work but, in effect, those were the continuation of the research project.

The primary goals of the experimental study were to investigate the effects of (a) reactor temperature, (b) pressure, (c) hydrogen flow

rate, (d) space time, (e) catalyst wetting, and (f) catalyst aging characteristics on the rate of HDS reactions. The active life of various catalysts for HDS was investigated more extensively than any other factor. The kinetic data from the related runs was then studied to explain a possible rate model for the HDS reaction.

The results of the experimental runs are presented in this chapter along with an explanation of the objectivity of the experiment. The results are presented in a tabular form for each run and are analyzed for discussion in the next chapter. Since the general objective of these experiments was to remove sulfur from the feedstock, the results of the experiments are presented in terms of the ramaining wt % sulfur in the product oil and also the percent sulfur removal from the feed oil. Each of these terms is explained as,

$$\text{wt \% S} = \frac{\text{wt of S in sample}}{\text{wt of sample}} \times 100 \qquad (5.1)$$

$$\text{and \% S removal} = \frac{\text{wt \% S in feed} - \text{wt \% S in product}}{\text{wt \% S in feed}} \times 100 \qquad (5.2)$$

A smooth curve was drawn through the data points to prepare the figures. The curve fits of the data for comparing rate models were achieved by applying a least squares technique. The amount of catalyst used for all the experimental runs was constant, 20 grams. Which meant that reporting of the space time would be more convenient in liquid weight hourly space time (LWHST). In keeping with the trend in the literature, the space times are reported in terms of liquid volume hourly space time (LVHST). The LVHST was calculated as the volume of catalyst bed per unit volume of feed oil per hour. The reaction conditions are presented as the nominal temperature and pressure. The actual reactor temperature was controlled to within $\pm$ 5F (3 C) of the

nominal temperature and the actual temperature of the catalyst zone was controlled within ± 2 F (1 C) of the nominal temperature. The actual pressure was always controlled and adjusted, if necessary, to within ± 20 psi of the nominal pressure. The liquid flow remained essentially constant and, therefore, the LVHST was always considered as having a constant value. The hydrogen flow rate did fluctuate and, thus, was monitored very closely and adjusted if necessary.

Analytical Precision

The analytical equipment had been tested earlier in Sooter's work for precision (61). The feed oil was only analyzed to compare its analytical precision with Sooter's results and to determine a consistent value for the sulfur content of feed oil. The feed oil was analyzed eight times for sulfur content. The deviation of the sulfur concentration in feed oil from the predetermined value (by Sooter) of 0.470% was 0.001 and the standard derviation was calculated to be 0.00903. The detailed calculation steps are presented in Appendix A.

In addition to the test of the feed oil, each sample collected from all the experimental runs was analyzed at least three times for sulfur content. The imprecision within each sample was estimated according to the student t-test as presented in Appendix B. The details of the analytical results are also included in Appendix B. The average deviations and the standard deviations from the average value were then separated according to the mean sulfur content. The average deviations and the standard deviations from each group were then compared with the degree of imprecision achieved by Sooter (61). The results of the comparison are presented in Table XI.

TABLE XI

COMPARISON OF THE ANALYTICAL PRECISION OF THE SAMPLES WITH THAT OF THE EQUIPMENT

Wt % S	Std. Deviation, Equipment[a]	Std. Deviation, Sample[b]	% Deviation[c]
over 0.20	± 0.00838	± 0.00588	2.9
0.15 - 0.20	± 0.00525	± 0.00738	4.2
0.10 - 0.15	± 0.00581	± 0.00705	5.6
0.08 - 0.10	± 0.00692	± 0.00591	6.6
0.06 - 0.08	± 0.00491	± 0.00493	7.0
0.04 - 0.06	± 0.00370	± 0.00540	10.8
0.02 - 0.04	± 0.00400	± 0.00629	20.9
0.00 - 0.02	-	± 0.00332	33.2

[a]From Sooter's work.

[b]From the present study.

[c]% based on the average % S of the group.

The results presented in Table XI show that the standard deviations of the samples analyzed in the present study were essentially consistent with those found in Sooter's work. Furthermore, the sulfur content of about 85% of the product samples collected in the present study ranged from 0.06% to 0.15%. The percent deviation for the samples having higher sulfur content was relatively lower than those having low sulfur content.

Study of Catalyst Aging Characteristics

The major emphasis during the research program was given to the determination of the aging characteristics of the catalysts. Five of the catalysts were studied for their active life. The basic concept of this study was to determine if there was any activity decay of the catalyst during the study. Observing the effects from the earlier studies (52), (61), a continuous experimental run of 200 hours duration was considered adequate. The reactor operating conditions for all the runs were kept identical so that a relative performance of the catalysts could also be made. The reactor conditions were 700 F (371 C) temperature, 1,000 psig pressure, 1,500 scf/Bbl hydrogen flow rate and 40 cc/hr oil flow rate. The amount of catalysts used by weight were the same in all five cases. Therefore, the LWHST would be the same in all five runs, but the LVHST would vary. The MCM 1 catalyst having the least density in the lot had the highest LVHST. The amount of MCM 1 required to fill 20 inches (50.8 cm) catalyst bed was used as reference, and then the same amount of each of the other catalyst was weighed for the respective experimental runs. The results of the sulfur analyses of Runs 2, 3, 4, 6, and 8 are presented in Tables XII through XVI and illustrated in Figure 14. The time period of the first 48 hours of each run was considered to be the stabilization period. Consequently, the samples collected after the initial period were the only ones included in establishing possible catalyst deactivation.

In addition to the five experimental runs explained above, several samples were collected during other runs at certain time intervals and repeat reactor conditons to check possible deactivation. These samples

TABLE XII

EXPERIMENTAL RUN 2, MCM 1 CATALYST

Sample Number	Wt % S in Product Oil	Sample Number	Wt % S in Product Oil
ASP 1	0.086	ASP21	0.110
ASP 2	0.114	ASP22	0.135
ASP 3	0.113	ASP23	0.077
ASP 4	0.120	ASP24	0.103
ASP 5	0.098	ASP25	0.054
ASP 6	0.115	ASP26	0.121
ASP 7	0.127	ASP27	0.072
ASP 8	0.116	ASP28	0.157
ASP 9	0.064	ASP29	0.124
ASP10	0.112	ASP30	0.101
ASP11	0.160	ASP31	0.104
ASP12	0.124	ASP32	0.108
ASP13	NA	ASP33	0.059
ASP14	0.098	ASP34	0.110
ASP15	0.099	ASP35	0.069
ASP16	0.134	ASP36	0.130
ASP17	0.108	ASP37	0.112
ASP18	0.104	ASP38	0.120
ASP19	0.103	ASP39	0.113
ASP20	0.118	ASP40	0.087

Note: The operating conditions during the entire experimental run were as follows.

(a) Nominal temperature = 700 F (371 C)
(b) Nominal pressure = 1,000 psig
(c) Hydrogen flow rate = 1,500 scf/Bbl
(d) LWHST = 0.440 per hour
(e) LVHST = 0.925 per hour

TABLE XIII

EXPERIMENTAL RUN 3, MCM 2 CATALYST

Sample Number	Wt % S in Product Oil	Sample Number	Wt % S in Product Oil
ANA 1	0.165	ANA21	0.128
ANA 2	0.156	ANA22	0.125
ANA 3	0.142	ANA23	0.111
ANA 4	0.155	ANA24	0.109
ANA 5	0.163	ANA25	0.151
ANA 6	0.189	ANA26	0.109
ANA 7	0.180	ANA27	0.137
ANA 8	0.123	ANA28	0.120
ANA 9	0.183	ANA29	0.139
ANA10	0.103	ANA30	0.115
ANA11	0.105	ANA31	0.136
ANA12	0.112	ANA32	0.095
ANA13	0.096	ANA33	0.135
ANA14	0.126	ANA34	0.115
ANA15	0.110	ANA35	0.107
ANA16	0.101	ANA36	0.125
ANA17	0.102	ANA37	0.141
ANA18	0.110	ANA38	0.117
ANA19	0.137	ANA39	0.106
ANA20	0.122	ANA40	0.097

Note: The operating conditions during the entire experimental run were as follows.

(a) Nominal temperature = 700 F (371 C)
(b) Nominal pressure = 1,000 psig
(c) Hydrogen flow rate = 1,500 scf/Bbl
(d) LWHST = 0.440 per hour
(e) LVHST = 0.640 per hour

TABLE XIV

EXPERIMENTAL RUN 4, MCM 3 CATALYST

Sample Number	Wt % S in Product Oil	Sample Number	Wt % S in Product Oil
NLA 1	0.118	NLA21	0.080
NLA 2	0.119	NLA22	0.074
NLA 3	0.081	NLA23	0.081
NLA 4	0.143	NLA24	0.070
NLA 5	0.084	NLA25	0.072
NLA 6	0.110	NLA26	0.101
NLA 7	0.115	NLA27	0.075
NLA 8	0.111	NLA28	0.107
NLA 9	0.107	NLA29	0.087
NLA10	0.107	NLA30	0.081
NLA11	0.115	NLA31	0.088
NLA12	0.117	NLA32	0.088
NLA13	0.080	NLA33	0.074
NLA14	0.098	NLA34	0.076
NLA15	0.075	NLA35	0.099
NLA16	0.100	NLA36	0.095
NLA17	0.081	NLA37	0.078
NLA18	0.096	NLA38	0.096
NLA19	0.093	NLA39	0.098
NLA20	0.089	NLA40	0.086
		NLA41	0.152

Note: The operating conditions during the entire experimental run were as follows.

(a) Nominal temperature = 700 F (371 C)
(b) Nominal pressure = 1,000 psig
(c) Hydrogen flow rate = 1,500 scf/Bbl
(d) LWHST = 0.440 per hour
(e) LVHST = 0.616 per hour

TABLE XV

EXPERIMENTAL RUN 6, MCM 4 CATALYST

Sample Number	Wt % S in Product Oil	Sample Number	Wt % S in Product Oil
HRW 1	0.177	HRW21	0.131
HRW 2	0.136	HRW22	0.150
HRW 3	0.165	HRW23	0.141
HRW 4	0.197	HRW24	0.142
HRW 5	0.182	HRW25	0.133
HRW 6	0.173	HRW26	0.140
HRW 7	0.131	HRW27	0.135
HRW 8	0.156	HRW28	0.136
HRW 9	0.151	HRW29	0.133
HRW10	0.155	HRW30	0.135
HRW11	0.145	HRW31	0.128
HRW12	0.149	HRW32	0.121
HRW13	0.153	HRW33	0.127
HRW14	0.148	HRW34	0.128
HRW15	0.142	HRW35	0.128
HRW16	0.131	HRW36	0.124
HRW17	0.138	HRW37	0.123
HRW18	0.123	HRW38	0.137
HRW19	0.149	HRW39	0.125
HRW20	0.140	HRW40	0.159

Note: The operating conditions during the entire experimental run were as follows.

(a) Nominal temperature = 700 F (371 C)
(b) Nominal pressure = 1,000 psig
(c) Hydrogen flow rate = 1,500 scf/Bbl
(d) LWHST = 0.440 per hour
(e) LVHST = 0.650 per hour

TABLE XVI

EXPERIMENTAL RUN 8, MCM 5 CATALYST

Sample Number	Wt % S in Product Oil	Sample Number	Wt % S in Product Oil
NAC 1	0.100	NAC21	0.089
NAC 2	0.077	NAC22	0.086
NAC 3	0.064	NAC23	0.086
NAC 4	0.071	NAC24	0.070
NAC 5	0.077	NAC25	0.083
NAC 6	0.073	NAC26	0.070
NAC 7	0.086	NAC27	0.090
NAC 8	0.108	NAC28	0.075
NAC 9	0.083	NAC29	0.089
NAC10	0.086	NAC30	0.059
NAC11	0.081	NAC31	0.053
NAC12	0.072	NAC32	0.059
NAC13	0.128	NAC33	0.053
NAC14	0.073	NAC34	0.060
NAC15	0.078	NAC35	0.065
NAC16	0.078	NAC36	0.054
NAC17	0.083	NAC37	0.096
NAC18	0.076	NAC38	0.063
NAC19	0.065	NAC39	0.079
NAC20	0.094	NAC40	0.073

Note: The operating conditions during the entire experimental run were as follows.

(a) Nominal temperature = 700 F (371 C)
(b) Nominal pressure = 1,000 psig
(c) Hydrogen flow rate = 1,500 scf/Bbl
(d) LWHST = 0.440 per hour
(e) LVHST = 0.740 per hour

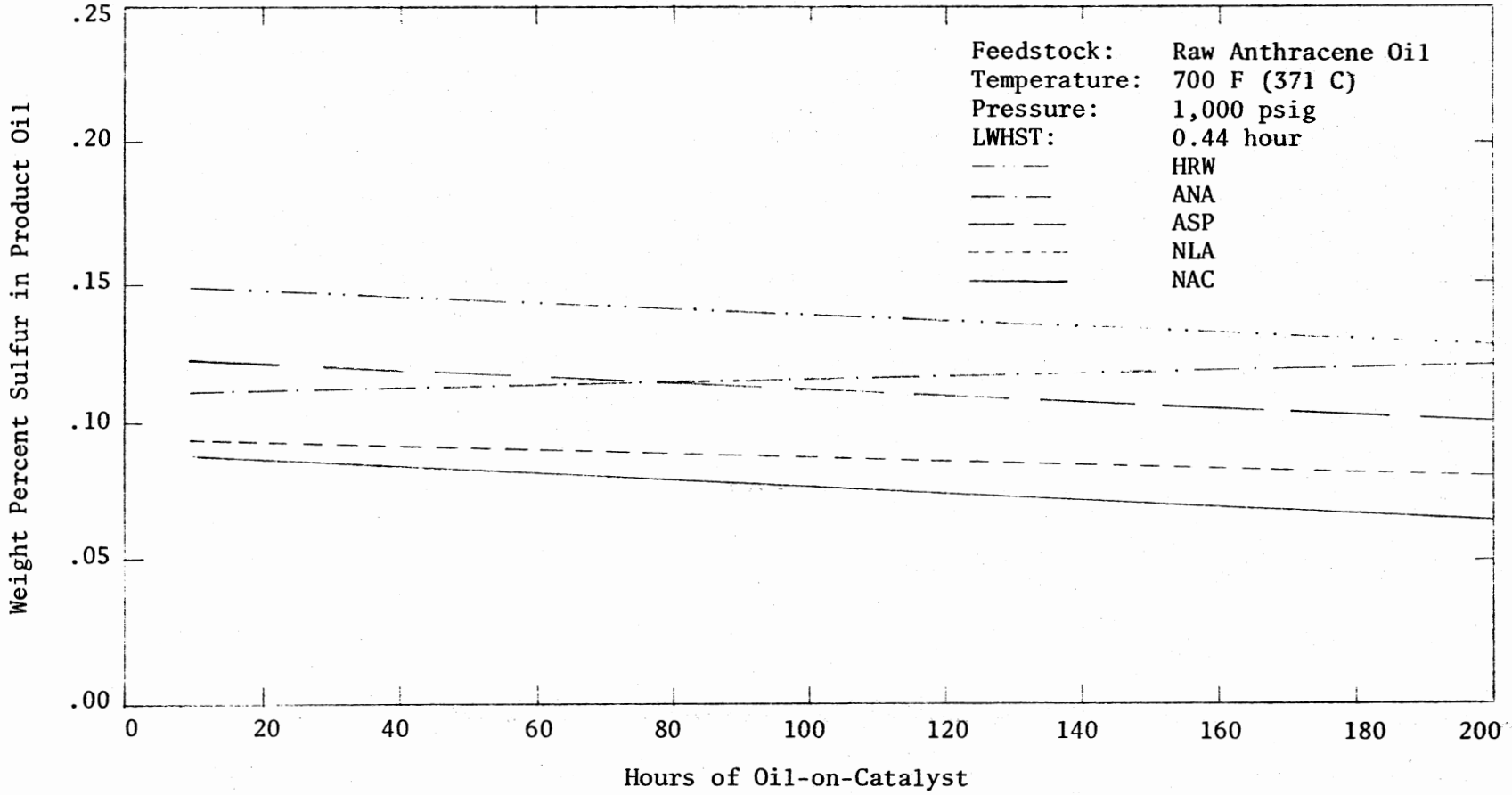

Figure 14. Results of the Catalyst Aging Tests

were collected at the reactor conditions which were already encountered during the earlier segment of the respective runs. These samples are identified later in this chapter.

Pressure Effects

One of the three operating variables studied was the effect of reactor pressure on the HDS reaction. Run 5 was the only one conducted to investigate the pressure effect. Run 5 was conducted at pressures of 500, 1,000 and 1,500 psig. All three pressures were tested at temperatures of 650, 700 and 750 F (343, 371, and 399 C respectively). Three different space times were also included at each of these operating conditions. The results of Run 5 are presented in Table XVII. Figure 15 illustrates a typical pressure effect on the extent of the sulfur removal from the anthracene feedstock. The effect of pressure from this table appears to be mixed at different reactor temperatures. Similar runs on other catalysts were not made since the effect of pressure was found to be insignificant when compared to that of temperature and space time on the HDS reaction rate. From the results of his work on another catalyst, Sooter (61) observed that the HDS reaction rate increased as the reactor pressure went up from 500 to 1,000 psig but no effect of any further pressure rise.

Temperature Effects

The other major operating variable investigated during this test program was the reaction temperature. The concept of high sulfur removal at higher reaction temperature was almost a maxim. But the extent of sulfur removal varies with the type of catalyst. The

TABLE XVII

EXPERIMENTAL RUN 5, MCM 4 CATALYST

Sample Number	Nominal Temp., F	Nominal Press., psig	LVHST Hour	Wt % S in Product Oil
HSW 1	650	1000	1.300	0.152
HSW 2	650	1000	1.300	0.154
HSW 3	650	1000	1.300	0.128
HSW 4	650	1000	1.300	0.135
HSW 5	650	1000	1.300	0.174
HSW 6	650	1000	1.300	0.160
HSW 7	650	1000	1.300	0.122
HSW 8	650	1000	1.300	0.149
HSW 9	650	1000	1.300	0.110
HSW10	650	1000	1.300	0.127
HSW11	650	1000	1.300	0.114
HSW12	650	1000	1.300	0.104
HSW13	650	1000	0.650	0.194
HSW14	650	1000	0.650	0.157
HSW15	650	1000	0.325	0.198
HSW16	650	1000	0.325	0.182
HSW17	650	1500	0.325	0.205
HSW18	650	1500	0.325	0.170
HSW19	650	1500	0.650	0.221
HSW20	650	1500	0.650	0.156
HSW21	650	1500	1.300	0.121
HSW22	650	1500	1.300	0.104
HSW23	650	500	1.300	0.141
HSW24	650	500	1.300	0.114
HSW25	650	500	0.650	0.175
HSW26	650	500	0.650	0.159
HSW27	650	500	0.325	0.217
HSW28	650	500	0.325	0.192
HSW29	650	1000	1.300	0.133
HSW30	650	1000	1.300	0.102
HSW31	700	1000	1.300	0.089
HSW32	700	1000	1.300	0.086
HSW33	700	1000	0.650	0.140
HSW34	700	1000	0.650	0.119
HSW35	700	1000	0.325	0.156
HSW36	700	1000	0.325	0.124
HSW37	700	1500	0.325	0.175
HSW38	700	1500	0.325	0.112
HSW39	700	1500	0.650	0.116
HSW40	700	1500	0.650	0.088
HSW41	700	1500	1.300	0.160
HSW42	700	1500	1.300	0.049
HSW43	700	500	1.300	0.059

TABLE XVII (Continued)

Sample Number	Nominal Temp., F	Nominal Press., psig	LVHST Hour	Wt % S in Product Oil
HSW44	700	500	1.300	0.060
HSW45	700	500	0.650	0.087
HSW46	700	500	0.650	0.126
HSW47	700	500	0.325	0.116
HSW48	700	500	0.325	0.143
HSW49	700	1000	1.300	0.091
HSW50	700	1000	1.300	0.045
HSW51	750	1000	1.300	0.071
HSW52	750	1000	1.300	0.085
HSW53	750	1000	0.650	0.064
HSW54	750	1000	0.650	0.038
HSW55	750	1000	0.325	0.083
HSW56	750	1000	0.325	0.094
HSW57	750	1500	0.325	0.123
HSW58	750	1500	0.325	0.091
HSW59	750	1500	0.650	0.114
HSW60	750	1500	0.650	0.065
HSW61	750	1500	1.300	0.050
HSW62	750	1500	1.300	0.050
HSW63	750	500	1.300	0.064
HSW64	750	500	1.300	0.032
HSW65	750	500	0.650	0.063
HSW66	750	500	0.650	0.057
HSW67	750	500	0.325	NA
HSW68	750	500	0.325	NA
HSW69	750	1000	1.300	NA
HSW70	750	1000	1.300	NA

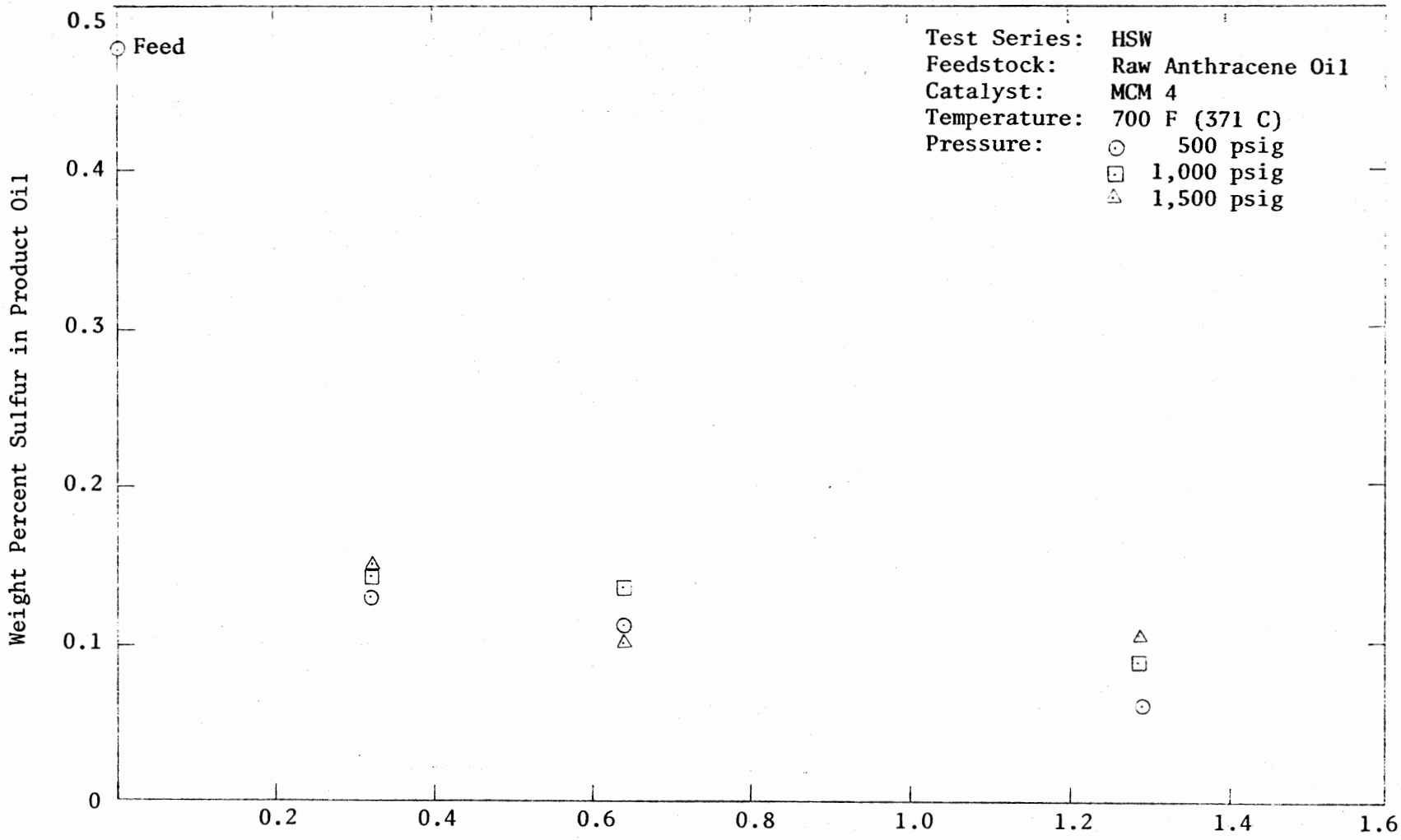

Figure 15. A Typical Pressure Effect on Sulfur Removal Efficiency

temperature effects were studied in Runs 1, 5, and 7. The reactor temperatures studied were any three of 600, 650, 700, and 750 F (314, 343, 371, and 399 C respectively) for a particular experimental run. The results of Runs 1 and 7 are presented in Tables XVIII and XIX respectively. The results of Run 5 were included earlier in the section on pressure effects. The effect of temperature between 600 F (314 C) and 700 F (371 C) was remarkable for MCM 1, MCM 4, and MCM 5 catalysts, whereas, at 750 F (399 C), the increase in sulfur removal ability of the catalyst was mostly undetectable due to the limitations of the analytical equipment. Figure 16 demonstrates a typical temperature effect on the extent of the sulfur removal from the product oil. A side effect of the reaction temperature is on catalyst deactivation. Certain samples collected to examine this effect are listed in Table XX. The results of these samples were then compared with the results of samples collected earlier at the same reactor conditions. A very moderate deactivation was apparent from the samples collected during the latter part of the experimental run.

Space Time Effects and Rate Equations

Almost all of the experimental reaction kinetic studies include the effects of space time on the rate of reaction and this study was no exception. The overall effect of space time was generally in the direction of higher conversion for higher space time. But the order and the rate of a chemical reaction are dependent on numerous process variables. The reaction rate could be unique for a particular set of catalyst and reaction conditions. Therefore, the kinetic data were generally represented in a form of correlation such that the research

TABLE XVIII

EXPERIMENTAL RUN 1, MCM 1 CATALYST

Sample Number	Nominal Temp., F	LVHST Hour	Wt % S in Product Oil
SP 1	600	2.500	0.133
SP 2	600	2.500	0.102
SP 3	600	2.500	0.072
SP 4	600	2.500	0.076
SP 5	600	2.500	0.067
SP 6	600	1.250	0.082
SP 7	600	1.250	0.103
SP 8	600	0.626	0.152
SP 9	600	0.626	0.177
SP10	600	2.500	0.116
SP11	600	2.500	0.110
SP12	650	2.500	0.062
SP13	650	2.500	0.067
SP14	650	1.250	0.084
SP15	650	1.250	0.100
SP16	650	0.626	0.128
SP17	650	0.626	0.128
SP18	650	2.500	0.080
SP19	650	2.500	0.055
SP20	750	2.500	0.014
SP21	750	2.500	0.013
SP22	750	1.250	0.012
SP23	750	1.250	0.007
SP24	750	0.626	0.047
SP25	750	0.626	0.044
SP26	750	2.500	0.016
SP27	750	2.500	0.017

Note: The nominal reactor pressure at all times was maintained at 1000 psig.

TABLE XIX

EXPERIMENTAL RUN 7, MCM 5 CATALYST

Sample Number	Nominal Temp., F	LVHST Hour	Wt % S in Product Oil
NAL 1	650	1.480	0.152
NAL 2	650	1.480	0.112
NAL 3	650	1.480	0.107
NAL 4	650	1.480	0.109
NAL 5	650	1.480	0.143
NAL 6	650	1.480	0.122
NAL 7	650	1.480	0.134
NAL 8	650	1.480	0.185
NAL 9	650	1.480	0.115
NAL10	650	1.480	0.088
NAL11	650	1.480	0.139
NAL12	650	1.480	0.108
NAL13	650	0.740	0.143
NAL14	650	0.740	0.163
NAL15	650	0.740	0.173
NAL16	650	0.370	0.175
NAL17	650	0.370	0.202
NAL18	650	0.370	0.215
NAL19	650	1.480	0.130
NAL20	650	1.480	0.108
NAL21	650	1.480	0.118
NAL22	700	1.480	0.069
NAL23	700	1.480	0.048
NAL24	700	1.480	0.092
NAL25	700	0.740	0.142
NAL26	700	0.740	0.066
NAL27	700	0.740	0.068
NAL28	700	0.370	0.105
NAL29	700	0.370	0.111
NAL30	700	0.370	0.102
NAL31	700	1.480	0.111
NAL32	700	1.480	0.041
NAL33	700	1.480	0.064
NAL34	750	1.480	0.042
NAL35	750	1.480	0.025
NAL36	750	1.480	0.040
NAL37	750	0.740	0.121
NAL38	750	0.740	0.044
NAL39	750	0.740	0.183
NAL40	750	0.493	0.108
NAL41	750	0.493	0.050
NAL42	750	0.493	0.039
NAL43	750	1.480	0.038

TABLE XIX (Continued)

Sample Number	Nominal Temp., F	LVHST Hour	Wt % S in Product Oil
NAL44	750	1.480	0.034
NAL45	750	1.480	0.062

Note: The nominal reactor pressure at all times was maintained at 1000 psig.

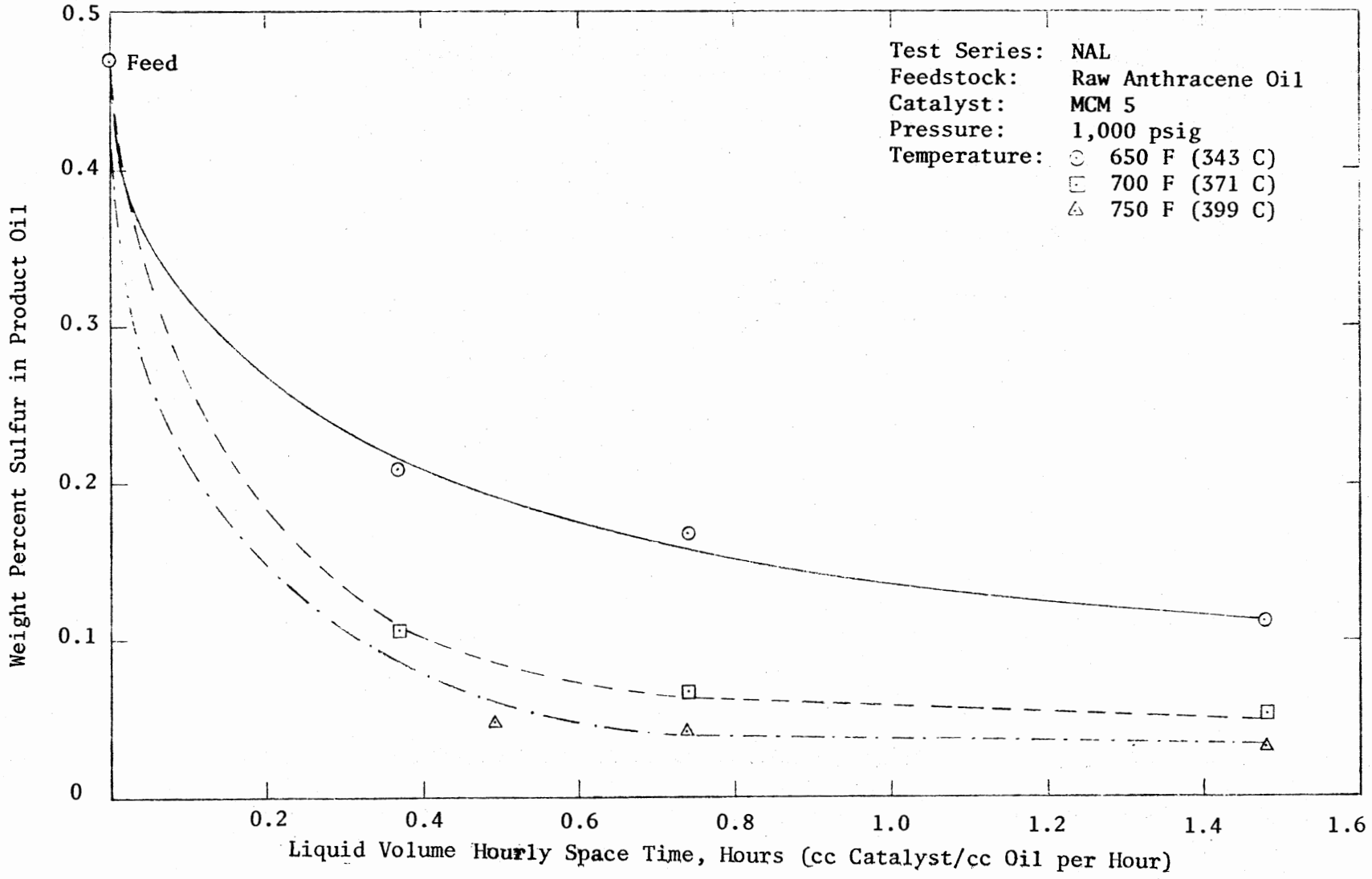

Figure 16. A Typical Temperature Effect on Sulfur Removal Efficiency

TABLE XX

LIST OF SAMPLES COLLECTED FOR CATALYST ACTIVITY TESTS

Sample[a] Number	Hours[b] on Oil	Avg % S in Product Oil	Sample[a] Number	Hours[b] on Oil	Avg % S in Product Oil
SP 4			SP10		
SP 5	18	0.071	SP11	31	0.113
SP12			SP18		
SP13	37	0.065	SP19	48	0.067
SP20			SP26		
SP21	55	0.014	SP27	67	0.017
HSW11			HSW29		
HSW12	50	0.109	HSW30	98	0.118
HSW31			HSW49		
HSW32	108	0.088	HSW50	168	0.068
HSW51			HSW69		
HSW52	177	0.078	HSW70	236	NA
NAL11			NAL20		
NAL12	48	0.124	NAL21	63	0.113
NAL23			NAL32		
NAL24	71	0.070	NAL33	86	0.053
NAL35			NAL44		
NAL36	94	0.033	NAL45	109	0.048

[a]Samples in these two columns were collected at the identical reactor conditions but at different time during the same experimental run.

[b]Total hours which the catalyst has been in contact with oil.

data could be used for future industrial designs. The general assumptions found in the literature (60), (61), (75), (76) are that an individual compound desulfurization follows a first order reaction rate, but the overall desulfurization follows a second order reaction. There are others who believe that the HDS follows a fractional order reaction. Therefore, five kinetic models with the orders of reaction of 1.0, 1.5, 2.0, 2.5, and 3.0 were assessed for fit of the experimental data. The kinetic model used did not incorporate any effects of liquid distribution or liquid backmixing. These will be considered in the next chapter. The kinetic model studied was a simple power order such as:

$$-\frac{dC_s}{dt} = k \cdot C_s^{\,n} \qquad (5.3)$$

where C_s = sulfur concentration in the product oil, t = space time, k = reaction rate constant, and n = order of reaction. Figure 17 illustrates the comparative fit of these power order models on a typical data set. The set of data for each isotherm from different pressures and various catalysts were tested for fit of each of the kinetic models using a computerized least square technique. The standard deviations for each of the model fit were also calculated. The sum of the standard deviations for each of the kinetic model gives an idea of the comparative suitability of the models tested. The results of all the kinetic model testing and the respective standard deviations are listed in Table XXI. For a perfect fit, the standard deviation would be zero. Hence, the lower the value the better the model representation.

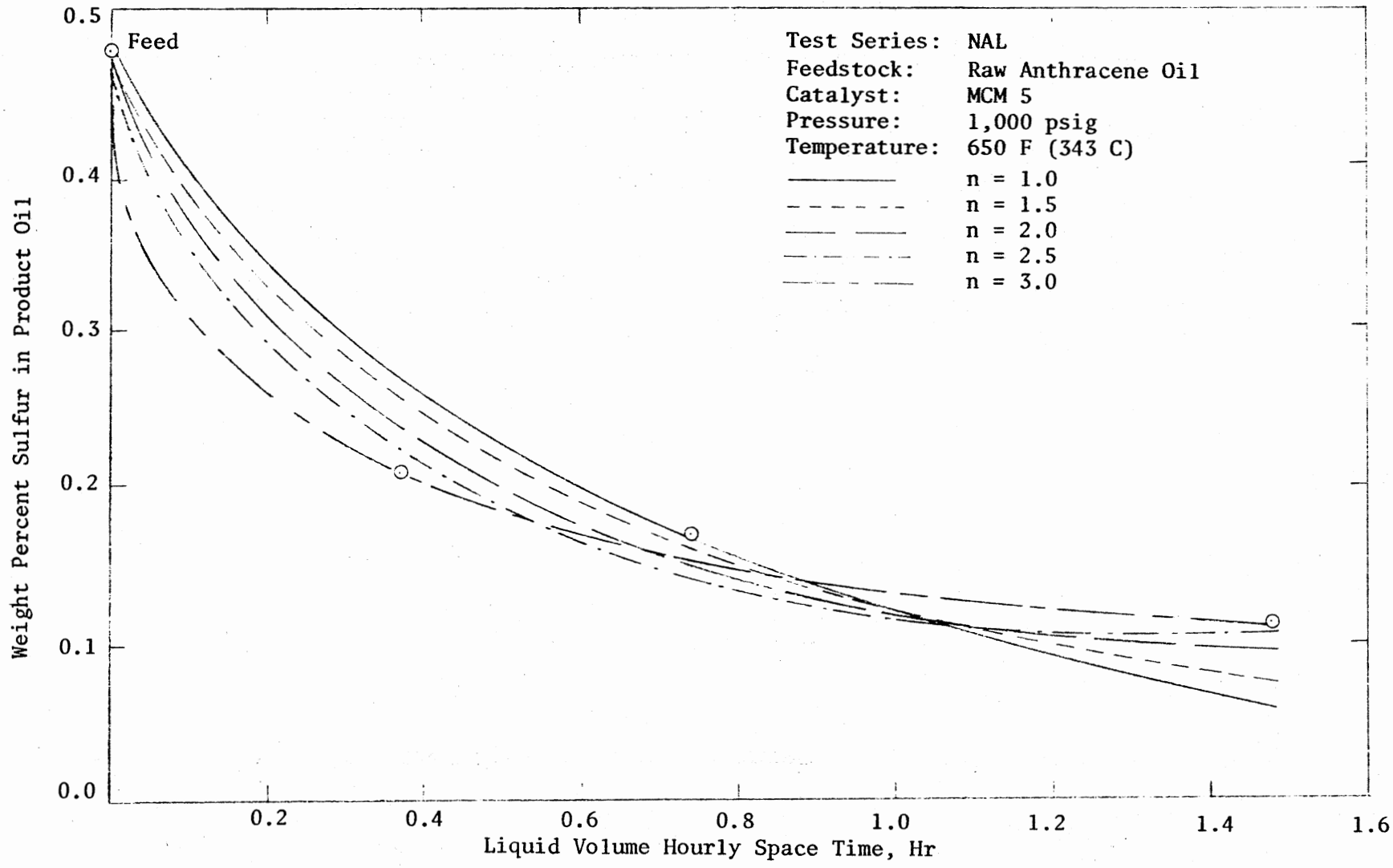

Figure 17. Comparative Fit of Various Reaction Models to a Typcial Data Set

TABLE XXI

RESULTS OF THE RELATIVE FITS OF FIVE KINETIC MODELS

Run	Order of Reaction	Catalyst Type	Nominal Temp., F	Nominal Press., psig	Standard Deviation
1	1.0	MCM 1	600	1000	0.03400
1	1.0	MCM 1	650	1000	0.03720
5	1.0	MCM 4	650	1000	0.04660
5	1.0	MCM 4	700	1000	0.04680
5	1.0	MCM 4	750	1000	0.04160
5	1.0	MCM 4	650	500	0.04850
5	1.0	MCM 4	700	500	0.03960
5	1.0	MCM 4	750	500	0.03170
5	1.0	MCM 4	650	1500	0.04850
5	1.0	MCM 4	700	1500	0.05070
5	1.0	MCM 4	750	1500	0.03690
7	1.0	MCM 5	650	1000	0.04180
7	1.0	MCM 5	700	1000	0.02990
7	1.0	MCM 5	750	1000	0.02550
			Sum of the Standard Deviations =		0.55930
1	1.5	MCM 1	600	1000	0.01940
1	1.5	MCM 1	650	1000	0.02250
5	1.5	MCM 4	650	1000	0.03160
5	1.5	MCM 4	700	1000	0.03100
5	1.5	MCM 4	750	1000	0.03130
5	1.5	MCM 4	650	500	0.03430
5	1.5	MCM 4	700	500	0.02470
5	1.5	MCM 4	750	500	0.02090
5	1.5	MCM 4	650	1500	0.03350
5	1.5	MCM 4	700	1500	0.03540
5	1.5	MCM 4	750	1500	0.02310
7	1.5	MCM 5	650	1000	0.02750
7	1.5	MCM 5	700	1000	NA
7	1.5	MCM 5	750	1000	NA
			Sum of the Standard Deviations =		0.33620
1	2.0	MCM 1	600	1000	0.01070
1	2.0	MCM 1	650	1000	0.01170
5	2.0	MCM 4	650	1000	0.02030
5	2.0	MCM 4	700	1000	0.01960
5	2.0	MCM 4	750	1000	0.02480
5	2.0	MCM 4	650	500	0.02310
5	2.0	MCM 4	700	500	0.01440
5	2.0	MCM 4	750	500	0.01240
5	2.0	MCM 4	650	1500	0.02210

TABLE XXI (continued)

Run	Order of Reaction	Catalyst Type	Nominal Temp., F	Nominal Press., psig	Standard Deviation
5	2.0	MCM 4	700	1500	0.02440
5	2.0	MCM 4	750	1500	0.01350
7	2.0	MCM 5	650	1000	0.01660
7	2.0	MCM 5	700	1000	0.00774
7	2.0	MCM 5	750	1000	0.01260
			Sum of the Standard Deviations =		0.23394
1	2.5	MCM 1	600	1000	0.00936
1	2.5	MCM 1	650	1000	0.00418
5	2.5	MCM 4	650	1000	0.01200
5	2.5	MCM 4	700	1000	0.01160
5	2.5	MCM 4	750	1000	0.02010
5	2.5	MCM 4	650	500	0.01450
5	2.5	MCM 4	700	500	0.00847
5	2.5	MCM 4	750	500	0.00668
5	2.5	MCM 4	650	1500	0.01360
5	2.5	MCM 4	700	1500	0.01680
5	2.5	MCM 4	750	1500	0.00783
7	2.5	MCM 5	650	1000	0.00888
7	2.5	MCM 5	700	1000	0.00209
7	2.5	MCM 5	750	1000	0.00857
			Sum of the Standard Deviations =		0.14466
1	3.0	MCM 1	600	1000	0.01220
1	3.0	MCM 1	650	1000	0.00159
5	3.0	MCM 4	650	1000	0.00663
5	3.0	MCM 4	700	1000	0.00659
5	3.0	MCM 4	750	1000	0.01730
5	3.0	MCM 4	650	500	0.00800
5	3.0	MCM 4	700	500	0.00714
5	3.0	MCM 4	750	500	0.00290
5	3.0	MCM 4	650	1500	0.00758
5	3.0	MCM 4	700	1500	0.01190
5	3.0	MCM 4	750	1500	0.00610
7	3.0	MCM 5	650	1000	0.00526
7	3.0	MCM 5	700	1000	0.00400
7	3.0	MCM 5	750	1000	NA
			Sum of the Standard Deviations =		0.09719

The sum of the standard deviations for any particular kinetic model demonstrates that the first order model was the worst, with suitability increaseing with complexity. This was probably an indication that the HDS reaction itself is very complex.

Effects of Catalyst Pore Size Distribution

One of the major catalyst properties studied to evaluate the relative performance of the catalyst was pore size distribution. The five catalysts investigated for activity decay provided a wide range of pore size distribution. This varied from a narrow range, low pore size catalyst to a broad range, higher pore size catalysts with two peaks in the pore size distribution. All the catalysts, save one have essentially the same chemical compositions, according to vendor specifications. All five activity test runs were conducted at the identical pre-run preparations and with the same reactor conditions during the run. The liquid weight hourly space time for each of the run was the same. The catalysts also had quite a range in their surface areas. All the available properties of these five catalysts are summarized in Table XXII. The pore size distributions of the catalysts were estimated from the results of the mercury penetration porosimetry performed by the American Instrument Company, Inc. The results of the experiments by the American Instrument Company, Inc. showed the amount of mercury that penetrated into the catalyst particle at a given pressure. The operating pressure on the catalyst particle corresponded to a certain pore diameter. The plots developed in Figures 18, 19, 20, 21 and 22 are the plots of $\Delta V/\Delta(\ln r)$ vs r. These figures provide a picture of the relative frequency at which

TABLE XXII

COMPARISON OF CATALYST CHEMICAL ANALYSES AND PHYSICAL PROPERTIES

Category	MCM 1	MCM 2	MCM 3	MCM 4	MCM 5
		Chemical Analyses			
MoO_3, wt %	12.50	12.50	12.50	15.00	12.50
CoO, wt %	3.50	3.50	3.50	3.00	3.50
Na_2O, wt %	0.08	0.08			
Fe_2O_3, wt %	0.03	0.03			
SiO_2, wt %	1.50	1.50			
Al_2O_3, wt %	82.39	82.39			
		Physical Properties			
Surface area, m^2/gm	270.00	270.00	297.70	220.00	240.00
Pore volume, cc/gm	0.65	0.51		0.50	
Packed density, gm/cc	0.48	0.73		0.73	

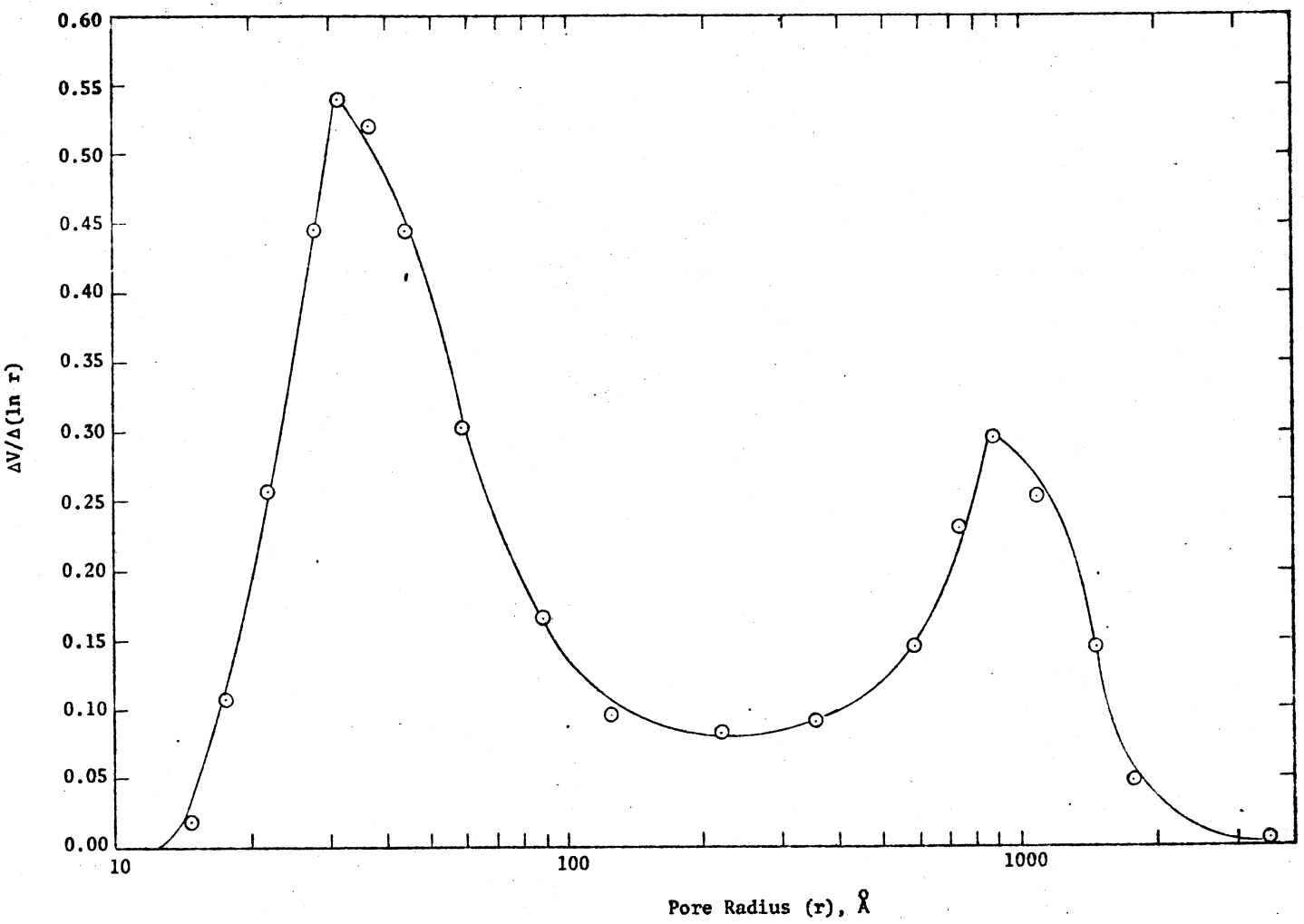

Figure 18. Pore Size Distribution of MCM 1 Catalyst

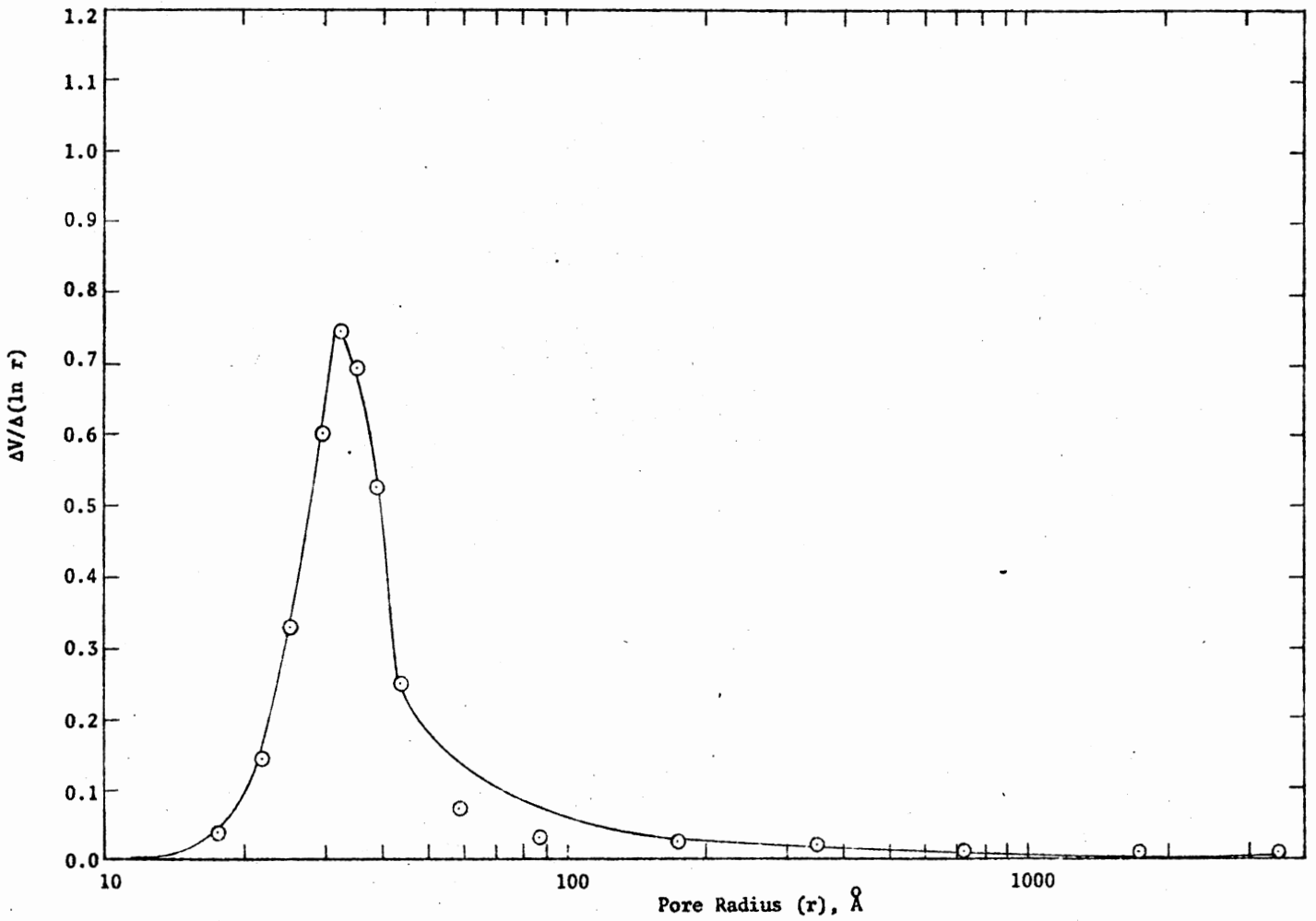

Figure 19. Pore Size Distribution of MCM 2 Catalyst

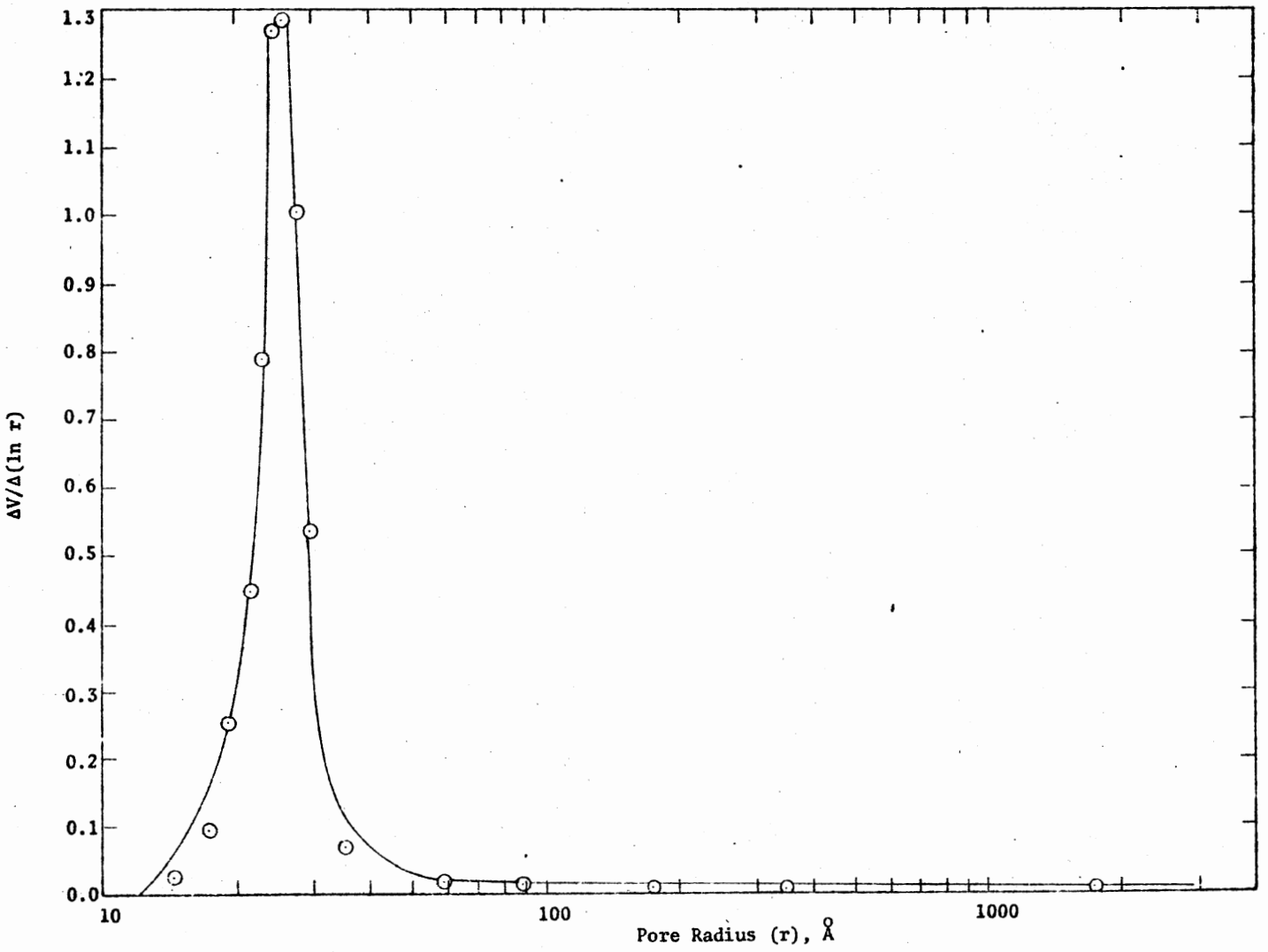

Figure 20. Pore Size Distribution of MCM 3 Catalyst

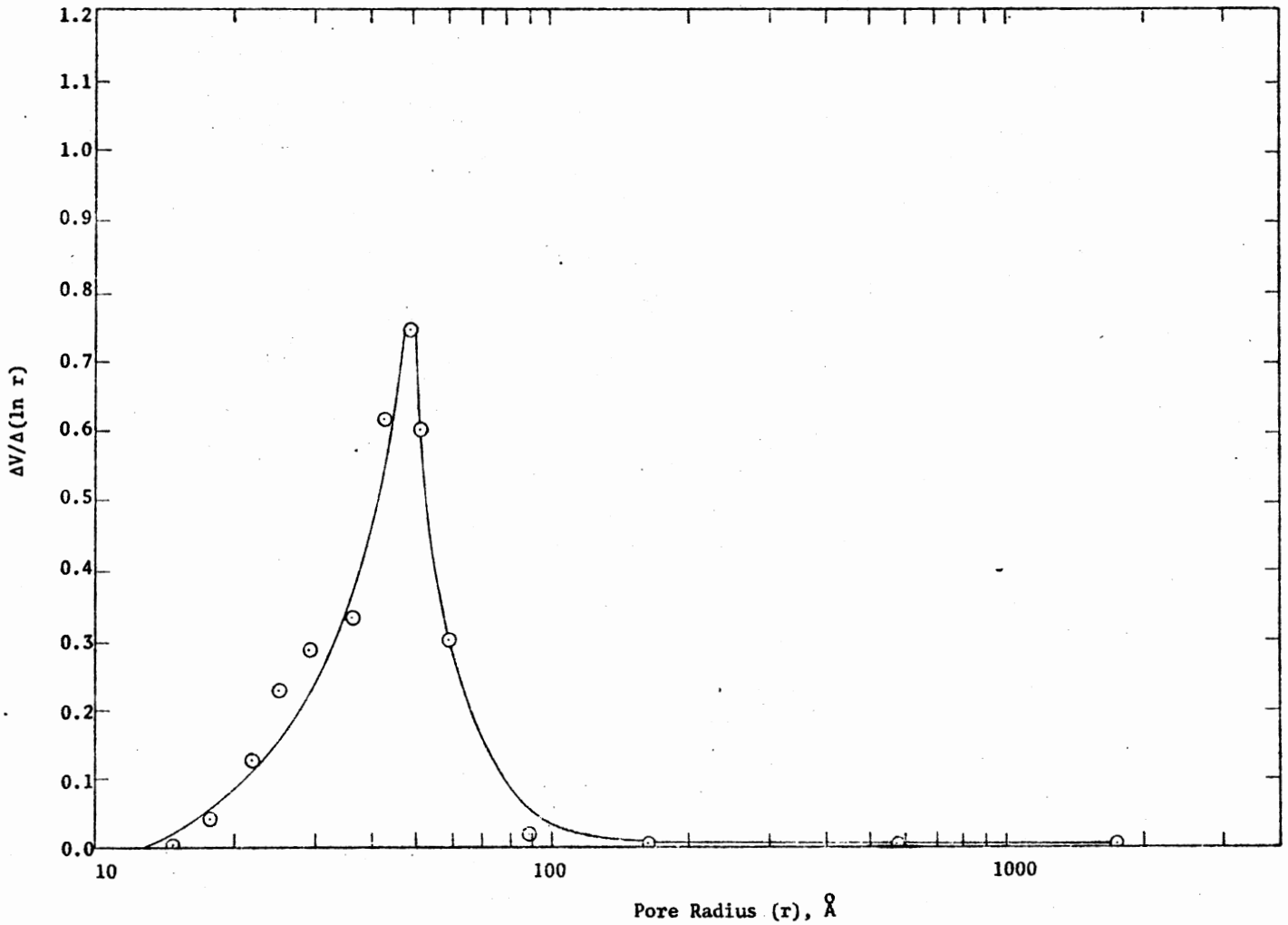

Figure 21. Pore Size Distribution of MCM 4 Catalyst

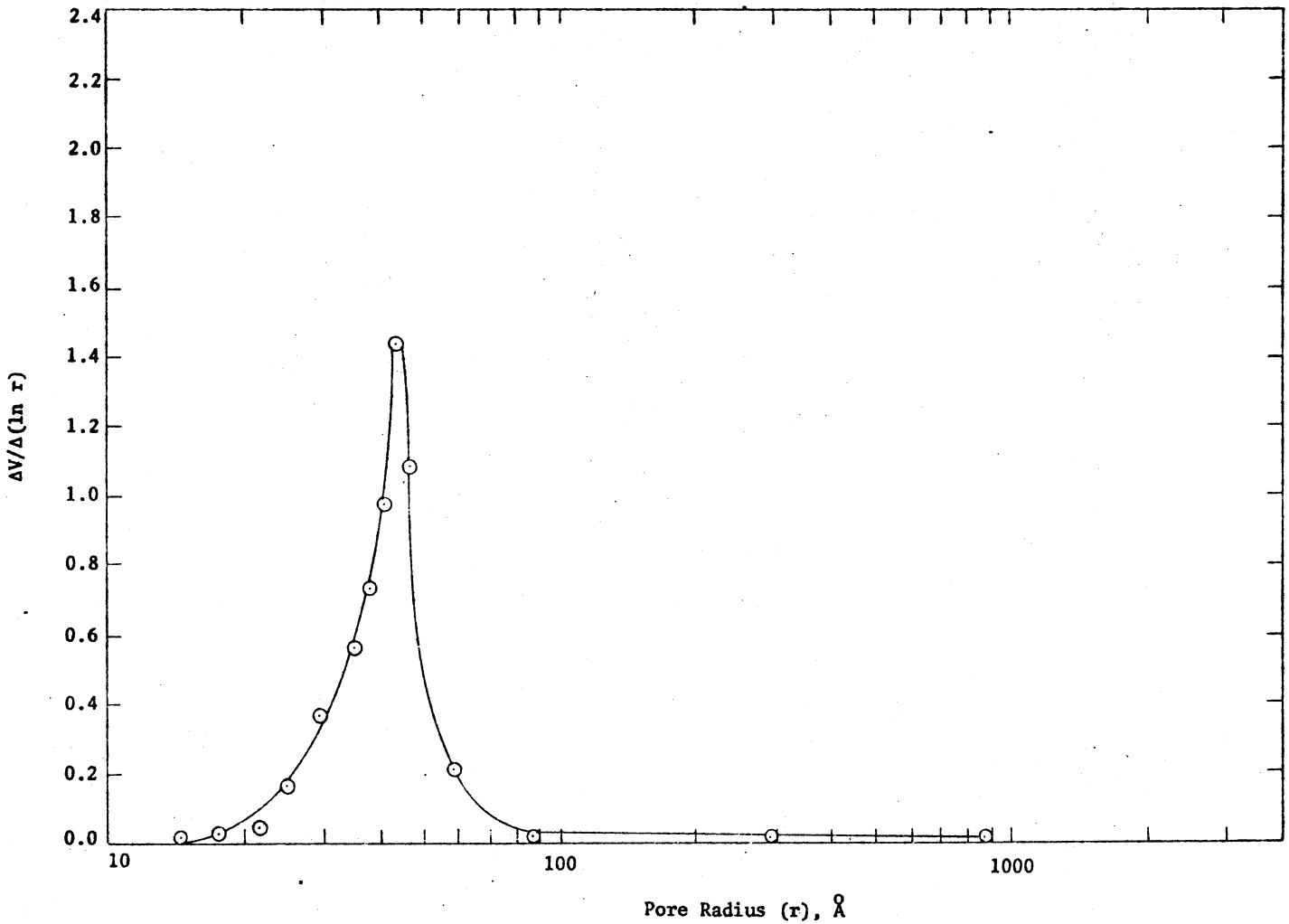

Figure 22. Pore Size Distribution of MCM 5 Catalyst

certain pore diameter was occurring in a particular catalyst. The term $\Delta V/\Delta$ (ln r) represents the differential change in the amount of the penetrating mercury by a change in the exerted pressure divided by the natural log of the pore radius corresponding to the exerted pressure. The raw mercury penetration data for all the catalysts and a method for calculating $\Delta V/\Delta$ (ln r) are presented in the Appendix C. The results of the activity runs are presented in Tables XII through XVI. The liquid weight hourly space time during each run was 0.44 hr, but depending upon respective catalyst densities, the LVHST would vary.

Physical Properties of Feed and Product Oils

One of the major aspects of any research study is the knowledge of the physical properties of the materials involved. Some portions of the physical properties data were provided by the supplier of the feed oil and others were generated by Sooter (61) at the earlier stages of this research project. The primary physical properties that are more frequently quoted for oil are chemical composition, normal boiling point data, and density, and kinematic viscosity of its distillation fractions. The feed oil properties and its normal boiling point data are listed in Table XXIII.

Table XXIV lists the kinematic viscosity of the distillation fractions of the feedstock at two different temperatures and also lists the density of each fraction at the room temperature.

One of the side effects of the desulfurization process is cracking of some of the higher boiling fractions. This is very well represented in comparing the distillation fractions of the feedstock and one of the typical product samples. The comparison of these boiling fractions is

shown in Table XXV.

TABLE XXIII

PHYSICAL PROPERTIES OF FEED OIL

Category	Composition
Carbon, wt %	90.65
Hydrogen	5.76
Nitrogen	0.91
Sulfur	0.47
Oxygen	2.21 (difference)
Ash	Nil
API gravity @ 60 F (16 C)	- 7.00
Distillation[a]	
380 F (193 C)	Initial
450 F (232 C)	10 vol %
570 F (300 C)	30 vol %
650 F (343 C)	50 vol %
700 F (371 C)	70 vol %
815 F (435 C)	90 vol %

[a]The estimate of the normal boiling point data was carried out from ASTM D1160 data taken at a pressure of 50 Hg absolute.

The results of the experimental and analytical work were presented with some explanation as to why the particular experiment was conducted. Analysis of the results is presented in the next chapter.

TABLE XXIV

DENSITY AND KINEMATIC VISCOSITY OF DISTILLATION FRACTIONS OF FEED

Fraction	Density @ 77 F (25 C) g/cc	Kinematic Viscosity, Centistokes @ 100 F (38 C)	@ 187.7 F (87 C)
1	0.959	1.71	0.813
2	1.020	3.48	1.293
3	1.060	6.22	1.833
4	1.075	10.57	2.370
5	1.092	18.04	3.060
6	1.107	31.10	4.025
7	1.122	65.93	5.480

TABLE XXV

COMPARISON OF WEIGHTS OF DISTILLATION FRACTIONS OF FEED AND PRODUCT SAMPLES

Fraction	Feed, wt %	Product, wt %	% Change
1	10.75	14.87	+ 38.40
2	11.58	17.28	+ 49.30
3	12.55	11.94	- 4.85
4	10.62	12.93	+ 21.70
5	18.05	15.24	- 15.60
6	8.39	7.35	- 12.40
7	13.21	9.40	- 29.00
8	14.85	10.99	- 26.00

CHAPTER VI

DISCUSSION

The results of the desulfurization experiments present an overall picture of the chemical and physical processes involved in the trickle bed reactor for the particular feedstock. However, further in-depth understanding of the reaction mechanism and kinetics is essential for future application and developments. The subjects discussed in this chapter are presented in the order of increasing influence on the rate and mechanism of the HDS reactions.

The analysis of the results begins with the test for the precision of the data to establish the reliability of the experiments. The precision tests are performed for both the process and the analytical equipment. The subjects discussed next are the liquid distribution and mass transfer characteristics of the fluid flow situations. These characteristics have inherent influences of the particle size, which are discussed jointly as well as separately. Next, the process parameters are analyzed in much detail because of their greater influence on the rate of reaction. The system pressure and hydrogen flow rate are presented first. The system temperature and the space time deserve close attention because of their dramatic effects on the rate of reaction. Several kinetic models are investigated to represent the results of the HDS experiments. The results from previous investigations are also tested on these models. The outcome of these tests is

then compared with established kinetic models. Finally, aging characteristics of several catalysts are examined and the influence of various experimental elements on the active life is discussed. Quite often the discussion of certain subjects might appear overlapping with the presentation in other sections, but that is only to emphasize the significance of any particular aspect of the process.

Consistency Test for Data

The consistent reproduction of the experimental data is a necessary and desirable condition to make any meaningful conclusions from an experiment. There are two different stages at which the precision of the results can be tested. The first and foremost is the precision of the equipment operation coupled with the experimental technique. This test can either be performed by conducting separate identical runs at identical reactor conditions as done by Sooter (61), or conducting separate experimental runs at partially overlapping reactor conditions. The results of the consistency test for equipment operation are presented in Table XXVI.

Runs 5 and 6 have certain common reactor conditions, as do Run 7 and 8. Runs 5 and 6 were both conducted on a Harshaw catalyst MCM 4, each with different experimental goals. The detailed reactor conditions for Runs 5 and 6 are presented in Tables XVII and XV respectively of the Experimental Results Chapter. Run 6 was conducted entirely at 700 F (371 C) temperature, 1,000 psig pressure, and 0.65 liquid volume hourly space time. Samples HSW 33 and 34 of Run 5 were collected at identical reactor conditions as in Run 6. Similarly, Runs 7 and 8 were both conducted on a Nalcomo catalyst MCM 5. The overall reactor

conditions, as well as the sulfur removal results for Runs 7 and 8, are presented in Tables XIX and XVI respectively of the Experimental Results Chapter. Run 8 was conducted entirely at 700 F (371 C) temperature, 1,000 psig, and 0.74 liquid volume hourly space time. The samples NAL 25 through NAL 27 of Run 7 were also collected at the identical reactor conditons used in Run 8. The results shown in Table XXVI indicate that the amount of sulfur remaining in the product samples collected at the overlapping reactor conditions of Runs 5 and 6 were within $\pm$ 7.2% of the average and those for Runs 7 and 8 were within $\pm$ 1.7% of the average. These reproducibilities of the experimental results from different runs demonstrate the precision of the experiment and the experimental technique.

TABLE XXVI

COMPARISON OF RESULTS FOR EQUIPMENT OPERATION CONSISTENCY TESTS

Run	Nominal Temp., F (C)	Nominal Press., psig	LVHST	Sample Numbers	%S, avg	Std Dev %S
5	700 (371)	1000	0.65	HSW 33 HSW 34	0.130	0.0095
6	700 (371)	1000	0.65	HRW 10 through HRW 40	0.150	0.0088
7	700 (371)	1000	0.74	NAL 25 through NAL 27	0.092	0.0037
8	700 (371)	1000	0.74	NAC 10 through NAC 40	0.095	0.0143

The second consistency test is for the precision of the analytical equipment. Each product sample was analyzed at least three times for sulfur content. The standard deviations of the total sulfur content of all samples are presented in Appendix B. The average standard deviations of the samples, grouped together according to their average total sulfur levels, are summarized in Table XI of Experimental Results Chapter. The degree of analytical precision attained in the present study is compared with the level of analytical precision achieved by Sooter (61) while using the same analytical equipment. The percent deviations presented in Table XI show that the degree of deviation or error in the determination of the total sulfur in the high sulfur samples is comparatively lower than those in the low sulfur samples. An extensive analytical technique, as outlined in the Experimental Procedure Chapter, was employed for the sulfur analysis. The sulfur content of other materials and chemicals used in the analysis, such as crucible, cover, MgO, iron chips, tin metal, etc., called "blank", was determined prior to each day's analytical work. Also a "reference" oil (anthracene oil) with known sulfur content was analyzed daily to establish the "furnace factor" which would compensate for any other factors affecting the sulfur analysis. The daily determinations of "blank" and "furnace factor" contributed significantly to the precision of the analytical measurements.

As mentioned earlier, the percent deviation for the samples having higher sulfur content was found to be relatively lower than those having low sulfur content. The high sulfur content samples were those collected at 600 F (314 C) and 650 F (343 C). As the reaction temperature rose, the extent of sulfur removal from the feedstock increased

to the point whereby the sulfur in the feedstock could no longer be analyzed with experimental precision by the LECO sulfur analyzer. The liquid volume hourly space time (LVHST) also has identical effects, although of varying degree of sensitivity, on the analytical precision as that of the reactor temperature. The higher LVHST led to improved sulfur removal and thus lower analytical precision. Table XI of the Experimental Results Chapter clearly showed that the average percent deviation in the estimation stayed around 7% for product samples having sulfur content as low as 0.06%. The percent deviation increased rather sharply for the product samples having lower sulfur content, such as about 11% for 0.05% sulfur samples and about 21% for 0.03% sulfur samples. These changes in the analytical precision present the uncertainties up to which the sulfur level in the product samples could be confidently analyzed.

Liquid Distribution and Backmixing

Adequate liquid distribution or lack of it is difficult, if not impossible, to examine visually for the HDS studies under actual experimental conditions. Therefore, the modes and effects of liquid distribution are generally analyzed using empirical models developed for other identical flow conditions. The effects of liquid distribution can principally be divided into two classes, intraparticle and interparticle.

The intraparticle effects are those of liquid distribution around an individual catalyst particle, termed catalyst wetting effects. These effects will be discussed in the next section of this chapter. The interparticle effects are those based on the liquid distribution

patterns among the various particles of the packed reactor bed. The formation of a third mode of liquid flow situation, wall channeling, was minimized with the use of fine screens at both ends of the reactor.

The two extremes of liquid flow patterns are plug flow and complete backmixing. The plug flow conditions provide the ideal and most desirable mode of flow pattern for the constant flow catalyst reactors. Any deviation from the plug flow condition means increased reactor volume to attain the same level of chemical reaction at identical process condition, and complete backmixing is the maximum nonideality from the plug flow. Therefore, the trickle bed reactors are designed to minimize the nonideality from the plug flow.

The amount of catalyst used in each of the experimental runs was identical (20 grams), but the length of the catalyst bed in the experiments of the present study differed because of variable catalyst packing densities. However, the length of the total packed bed of the reactor, including both catalysts and inerts, was the same during all the experimental runs.

There are several theoretical and empirical models used to determine the extent of the deviation from the plug flow situation in a trickle bed reactor. The theoretical models are called Dispersion model (Levenspiel), Modified Mixing-Cell model (Dean), Time Delay model (Hockman and Effron) (33). These models are based on a given set of reaction conditions and are suitable within their defined boundaries. Special experimental techniques are required, however, to gather data for determining the extent of deviation from plug flow situation. Mears (43) developed an empirical model which is applicable to any order of reaction and diverse conversion phenomena. For the reactor length

to be increased no more than 5% due to the axial dispersion effects over a minimum length required with plug flow, the criteria to be met is:

$$\frac{L}{d_p} > \frac{20\ n}{Pe_m} \ln \frac{C_i}{C_f} \qquad (2.1)$$

where L = length of the packed bed, d_p = particle diameter, n = order of reaction, Pe_m = Peclet number, C_i = initial concentration and C_f = final concentration.

Some desulfurization of anthracene oil over inerts had been demonstrated in two independent studies by Sooter (61) and Wells (114). At reactor operating conditions of 600 F (314 C), 1,000 psig and 0.375 LVHST, Sooter observed that about 50% of the sulfur in the feedstock was removed over the inert bed. Wells conducted his experiments on alumina bed using anthracene oil at reactor conditions of 750 F (399 C), 1,500 psig and LVHST up to 1.8 hour. Wells observed about 35% of the sulfur in the feedstock was removed over the alumina bed. Since some thermal desulfurization does occur over inert bed, the total bed length of the reactor including both inerts and catalysts is used to estimate the quantity L in the above equation. The quantity L for all the experimental runs was 31 inches (78.74 cms), where the length of the catalyst bed varied from 13.3 inches (33.78 cms) to 20.0 inches (50.80 cms), depending upon the catalyst packed bed density. The particle diameter, d_p, was 8-10 mesh (0.20 cm). The quantity L/d_p of the Equation (2.1) is thus calculated to be 393.7.

It is difficult to estimate the right hand side of the above equation. The order of the desulfurization reaction has been reported to be first to third, as discussed in the Literature Review Chapter.

And the more general consensus is that the HDS reaction is a pseudo-second order reaction. Therefore, the value chosen for the quantity n was two. The degree of sulfur removal in various experimental runs averaged between 75% and 85% at 700 F (371 C) and 1,000 psig, with an average sulfur removal of 81%.

The Peclet number for the experiments is estimated using the Hockman-Effron (40) model, which is applicable for the cocurrent flow in a trickle bed reactor. The detailed calculations for estimating Peclet number are shown in Appendix G. The Peclet number for most of the experimental conditions is estimated to be 0.1735. All the estimated values are fed into Equation (2.1). Using the value of 0.1735 for Pe_m and a value of two for the quantity n, with appropriate sulfur concentrations, the right hand side of Equation (2.1) is 382.9. By comparison, this value is less than the value for the left hand side (393.7). Within the errors of estimation, both of these values are essentially the same. Even then, by definition of Equation (2.1), the criteria for restricted (less than 5%) deviation from the plug flow condition is met. The process conditions used to estimate the Peclet number are the most frequently occurring reactor conditions and any deviations from those conditions would result in change in the extent of deviation from the plug flow conditions. However, the reactor conditions used for the test were considerably severe and compare closely with most sets of reactor conditions. Therefore, axial dispersion does not seem to effect any significant variation in the rate of the HDS reactions.

Catalyst Wetting and Mass Transfer Effects

The other class of liquid distribution is the intraparticle mass transfer. These effects are primarily caused by the resistance towards mass transfer encountered by the reactive molecules in the liquid and gas phases inside and around a catalyst pellet. There are several mass transfer steps necessary within and around a catalyst pellet in order for a heterogeneous chemical reaction to occur. These steps include diffusion of reactants in the gas and liquid bulk phases to the liquid film surrounding the catalyst pellet, diffusion of reactants through the liquid film, diffusion of reactants through the catalyst pores to the active sites, adsorption of reactants on the active sites, chemical reaction between the reactive molecules on the catalyst surface, desorption of products from the active sites, diffusion of the products through the catalyst pores, diffusion of products through the liquid film and, finally, the diffusion of products to the bulk gas and liquid phases. Any one or a combination of these steps could be the rate controlling step(s) for a specific reaction. The reactants in the present case are the sulfur containing compounds in anthracene oil and hydrogen, and the overall reaction is hydrodesulfurization. The catalytic phenomenon is characterized by the assumption that, in the gas-liquid-solid reaction, a fresh batch of anthracene oil almost completely surrounds each and every catalyst pellet, and the hydrogen and sulfur containing molecules have to diffuse through the liquid film for the reaction to occur.

The above indicates that any heterogeneous chemical reaction can hardly be modelled without incorporating catalyst wetting. The

phenomenon of an individual catalyst pellet being freshly wetted by the flowing liquid is defined as catalyst wetting (43). The major design variables affecting catalyst wetting are liquid flow rate, gas flow rate, interparticle liquid distribution, physical properties of liquid, shape and size of the catalyst pellets, reaction temperature, pressure and length of the packed bed. There are no simple models available in the literature to estimate catalyst wetting. A complex model requiring numerous operating conditions is discussed later in this chapter. Secondly, the visual counting of the freshly wetted catalyst pellets in a packed bed is impossible under actual experimental conditions. Mears (43) has developed a kinetic model incorporating catalyst wetting to represent the HDS reactions for coal liquids. Mears suggests that, besides other process parameters, the rate of chemical reaction is directly proportional to the catalyst external surface effectively wetted by the flowing liquid. However, Sylvester and Pitayagulasarn (51) claimed that for certain heterogeneous chemical reactions, the rate of chemical reaction is inversely proportional to the catalyst external surface effectively wetted by the flowing liquid. The results of their study demonstrated that for a non-volatile liquid phase, Mears' concept of direct proportionality holds true. However, for a volatile liquid phase, the gas phase to liquid phase diffusivity ratio of the reactants (benzothiophene and dibenzothiophene) determines the effects of catalyst wetting. Sylvester and Pitayagulasarn illustrated that, at higher gas phase to liquid phase diffusion ratio of the reactants, the reaction rate increased as catalyst wetting increases. And conversely, at lower gas phase to liquid phase diffusion ratio of the reactants, the reaction rate decreased as catalyst wetting

increased. Since the feedstock used in the present study was a non-volatile high molecular weight feedstock, the rate of the HDS reaction increases as the catalyst wetting increases, and vice versa.

The experiments by Paraskos, Frayer and Shah (115) also support the influence of catalyst wetting on the rate of HDS reaction. The effective catalyst wetting as correlated by Mears is shown in Equation (6.1):

$$A_{eff} = C\ (L)^{\gamma}\ (LHST)^{-\gamma} \qquad (6.1)$$

where, A_{eff} = correlation factor for the rate of HDS reaction, L = length of catalyst bed, C = proportionality constant, γ = Mears' constand and LHST = liquid hourly space time. The above mentioned arguments suggest that catalyst wetting would be a contributing factor in determining the rate of the HDS reaction. The effects of catalyst wetting will be estimated along with the effects of reactor temperature and space time later in this chapter. Equation (6.1) will be coupled with certain kinetic models and tested to represent the results of the experiments conducted during the present study and those conducted by Sooter (61).

Particle Size and Effectiveness Factor

There are two sets of physical properties of a catalyst particle - internal and external - that can contribute to the influence of a catalyst on the rate of the HDS reaction. The internal properties are based upon the catalyst pore size, and these will be evaluated in later sections. The external propoerties depend primarily on the size of a catalyst particle. Even though both types of properties relate to the same catalyst particle, either the internal or the external properties

of a catalyst can be altered to a certain degree by physical and chemical techniques without affecting the other.

The change in the size of a catalyst particle can have at least three different effects on the flow characteristics and thereby on the rate of the HDS reaction. The first among these is an effect on the interparticle liquid distribution. Referring to Equation (2.1) presented earlier in this chapter, with other quantities held constant, the catalyst particle size can be changed appropriately to minimize the occurrence of liquid backmixing in the trickle bed reactor. Plug flow is the ideal and most desirable mode of flow for the HDS studies. Therefore, reducing the catalyst particle size can minimize any prevailing backmixing effects and approach plug flow more closely.

The second effect of changing particle size is on the packed bed density. However, the experiments by many researchers (116) including Sooter (61) in studies directly related to the present work, have demonstrated conclusively that a reduction in the particle size does not noticeably increase the packed bed density. Therefore, the porosity of the packed bed remains almost identical for particles within a certain size range. However, a drop in the particle size does reduce the center-to-center distance between the adjoining particles, which results in a higher pressure drop across the packed bed at the same flow rates. On an industrial scale, this can mean an additional capital investment as well as increased operating costs. At times, these items do become significant enough to be decisive factors in the selection or rejection of a particular catalyst for a given process or a process for a given product.

A more direct effect of the catalyst particle size on the HDS reaction rate is presented by Satterfield (32), and other researchers before him, who derived the definition of an effectiveness factor (η). Even though the concentration of a reactant in the catalyst pore would vary, the average concentration is generally used in formulating the reaction rate models. The effectiveness factor is defined as the ratio of the average concentration of a reactant in the catalyst pore to the maximum possible concentration. The numerical value of η varies from near 0 to 1.0 for isothermal pellets. The effectiveness factor is estimated through another variable known as the Thiele modulus Φ. η and Φ are correlated as shown in Equation (6.2) for spherical particles:

$$\eta = \frac{1}{3\Phi^2}(3\Phi \coth 3\Phi - 1) \qquad (6.2)$$

and Φ is defined as in Equation (6.3):

$$\Phi = \frac{R}{3}\left(\frac{k \cdot C_s^{m-1}}{D_{eff}}\right)^{1/2} \qquad (6.3)$$

where, R is the radius of the catalyst particle (the ratio of catalyst volume to catalyst surface area replaces the term R/3 for non-spherical particles), k is the reaction rate constant per unit catalyst surface area, C_s is the concentration of the reactant (sulfur containing compounds), m is the order of reaction, and D_{eff} is the effective diffusion coefficient of the reactant (sulfur containing compounds). Figure 23 demonstrates the relationship between η and Φ, as in Equation (6.2). A lower value of Φ would mean a higher η, and vice versa. Equation (6.3) describes Φ in direct proportionality with the particle size. Therefore, with other quantities remaining constant in Equation (6.3),

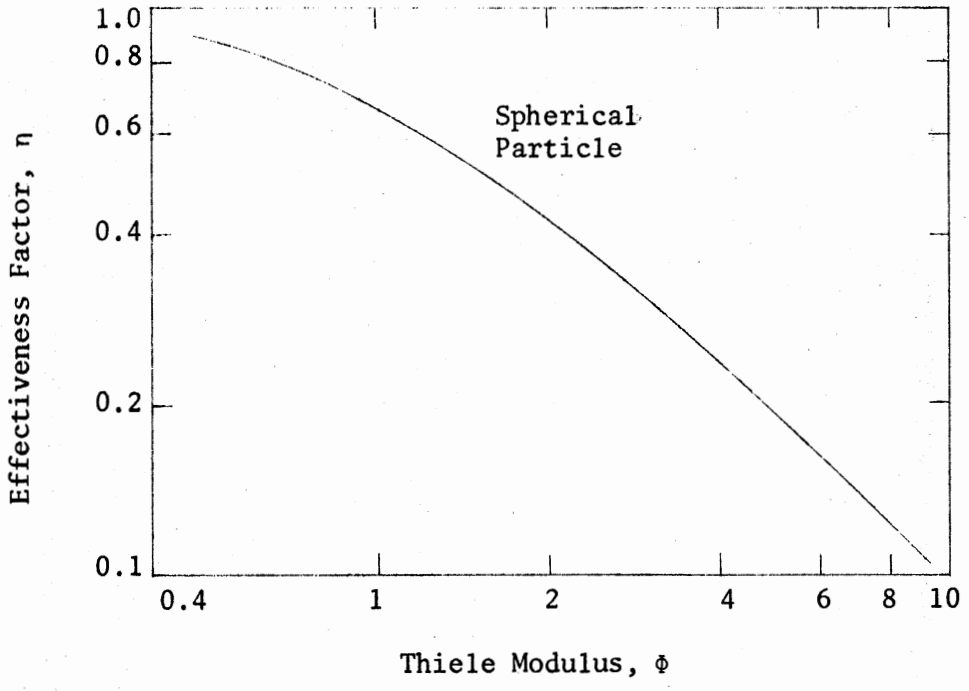

Figure 23. Thiele Modulus vs. Effectiveness Factor

the catalyst particle size can be adjusted sufficiently to increase the effectiveness factor. However, the sensitivity of changing particle size would depend largely upon the other properties included in Equation (6.3).

Calculations to estimate Φ and η are presented in Appendix I. The predicted values of the physical properties of hydrogen and sulfur containing compounds, or their equivalent (dibenzothiophene) are presented in Appendix H. These physical properties and the average of the second order reaction rate constant are used to estimate Φ and η. The Thiele modulus for the HDS reactions at 700 F (371 C) and 1,000 psig is computed to be 0.125 and the effectiveness factor is computed to be 0.99. The estimation of the effectiveness factor to be essentially unity suggests that the rates of diffusion of hydrogen and sulfur containing compounds through the catalyst pores have an insignificant effect in determining the overall rate of the HDS reactions for the process conditions and catalysts investigated during the present study. A similar conclusion was drawn by Sooter (61) in studies directly related to the present work.

The discussion so far has been focused on the mass transfer and fluid dynamics of the trickle bed reactor system and their effect on the HDS reaction rates. The discussion in the following sections is directed towards process parameters such as concentrations, pressure, temperature and the space time which are generally known to have a greater influence on the HDS reaction rate.

Hydrogen Rate

Hydrogen is one of the key reactants in the HDS reactions, and therefore, any variations in the hydrogen flow rate could have multiple effects on the reaction rate. Theoretically, there are primarily three effects that changes in the hydrogen flow rate can have on the overall reaction rate - (a) an effect on the rate of mass transfer of hydrogen from the bulk gas phase through the liquid film surrounding the catalyst pellet because of the hydrogen concentrations in the bulk gas phase; (b) an effect on the degree of wetted external catalyst surface because of the film disturbance caused by the mass transfer of hydrogen through the liquid film surrounding catalyst pellet; and (c) the simple effect of the law of mass action of hydrogen at the reaction site to complete the overall HDS reactions.

The diffusional mass transfer of hydrogen through the liquid film surrounding the catalyst pellet is one of the several major steps involved in achieving the HDS reactions. Among others, the major factor in determining diffusion rate is the difference in the hydrogen concentrations in the bulk gas phase and the liquid phase and also the differential hydrogen concentrations in the liquid phase and in the catalyst pores. The estimation of diffusion rate for individual pores is beyond the scope of the present study, but the calculations for an average diffusion rate are presented in Appendix H along with other physical property estimations of hydrogen and sulfur containing compounds. Increasing the hydrogen diffusion rate to liquid phase and to the catalyst pores would improve the HDS reaction rate only if the hydrogen transfer is a rate controlling step. The experiments by

Wan (52) and Sooter (61) demonstrated that bulk hydrogen flow rates as low as 1,500 scf per Bbl did not affect the sulfur removal capability of the catalyst tested for the same feedstock and with identical experimental conditions. Therefore, the bulk hydrogen flow rate in the present study was always maintained above 1,500 scf/Bbl.

The bulk hydrogen flow rate also has a bearing on the catalyst wetting characteristics. Higher bulk flow rate of hydrogen would tend to disturb the existing liquid film around the catalyst pellet, and thereby, improve the prospects of formation of fresh liquid film around catalyst pellet. Thus, an increase in the bulk hydrogen flow rate would tend to increase the catalyst wetting phenomenon for incompletely wetted catalysts. The contribution of the catalyst wetting phenomenon will be correlated later in this chapter to represent the rates of HDS reactions.

Foremost of all the concerns is that a sufficient quantity of hydrogen is supplied to the reaction zone. The gas flow rate in the present study was measured as the product gas exited from the reactor at the ambient conditions. The measured gas flow rate corresponded to the excess or unreacted hydrogen and the gases generated during the HDS reaction. Brunn, et al. (117) reported that, during their HDS studies on residual fuels via the Gulf process, the maximum quantity of the fuel gas vaporized was estimated to be 5%. Chem Systems (118) reported that during their coal liquefaction studies on a coal sample from the Pittsburg and Midway Coal Company (PAMCO) at reactor conditions up to 800 F (427 C) and 3,000 psig, the maximum coal extract vaporized in the cocurrent upflow packed bed reactor was not more than 5%. The molecular weight (MW) of the product vapor mixture exiting

the reactor was estimated to be approximately 28.6 by Chem Systems (118).

Based on the above observations, the gas produced in the reactor is estimated to be 238 scf/Bbl of oil fed. Detailed calculations are presented in Appendix D. Therefore, of a total effluent gas flow rate of 1,500 scf/Bbl, at least 1,262 scf/Bbl was hydrogen. From the calculations shown in Appendix E, about 431 scf/Bbl of hydrogen was consumed in the various heterogeneous reactions. Therefore, the hydrogen flow rate at the inlet to the reactor was approximately 1,693 scf/Bbl, an excess of 1,500 scf/Bbl. These calculations, coupled with the findings of Wan (52) and Sooter (61) regarding no noticeable increase in the sulfur removal capability with the bulk flow rate of hydrogen gas in excess of 1,500 scf/Bbl, indicate that sufficient quantity of hydrogen gas was provided to the system to minimize any variations in the sulfur removal capabilities of the catalyst because of the hydrogen supply situations.

Pressure Effects

The primary contribution of the total reactor pressure in the HDS reaction is its influence on the diffusional mass transfer of hydrogen gas through the liquid film surrounding the catalyst pellet to the catalyst pores. Changes in the total reactor pressure almost change proportionately the hydrogen partial pressure and the hydrogen molar concentration, which are needed to materilize the diffusion of hydrogen when the liquid film is not saturated with hydrogen molecules. The results of previous investigations by Wan (52) and Sooter (61) have shown that there is an increase in the rate of the HDS reaction with

increase in the total reactor pressure from 500 psig to 1,000 psig, but relatively little effect when changing the total reactor pressure from 1,000 psig to 1,500 psig.

One of the goals for conducting Run 5 (HSW series) of this study was to investigate the effect of change in the total reactor pressure on the overall HDS reaction rate along with the effects of reactor temperature and the liquid volume hourly space time. A Harshaw catalyst, MCM 4, was used during this experimental run. The results of Run 5 are presented in Table XVII of the previous chapter, and are shown in Figures 24, 25, and 26. Each of these figures illustrates the influence of the total reactor pressure at reactor temperatures of 650 F, 700 F, and 750 F (343 C, 371 C, and 399 C) respectively.

Figures 24, 25, and 26 do not show signs of any distinct trend in the extent of sulfur removal and consequently in the rate of HDS reaction, by changing reactor pressure from 500 to 1,000 to 1,500 psig. These figures indicate that, despite the increase in the total reactor pressure, the HDS reaction rate has not changed noticeably for this catalyst, because the liquid is saturated by the hydrogen molecules and/or all the reaction sites are occupied with the reactive molecules. The above results are in contrast to the study by Sooter (61) on an identical feedstock but different catalyst. However, the results of Run 5 have shown a remarkable consistency of this lack of pressure effect at the three temperature conditions.

The support material used for the Harshaw catalyst and the Nalco catalyst used in Sooter's study were similar with the four major differences. The Harshaw catalyst had the surface area of 220 m^2/gm, 15% of MoO_3, 3% of CoO, and the pore radius of 50 Å. Whereas, the

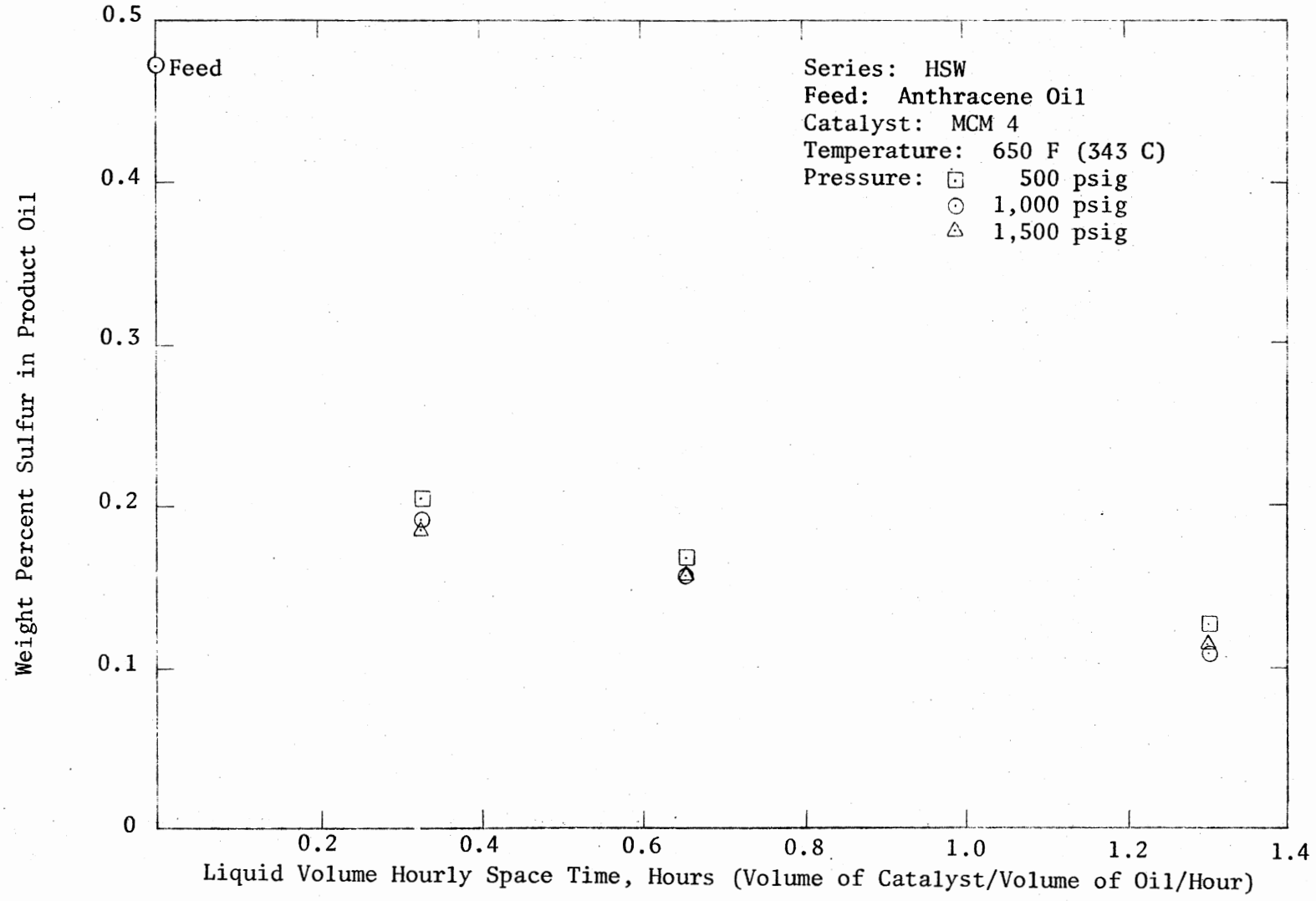

Figure 24. Effect of Pressure on Sulfur Removal at 650 F

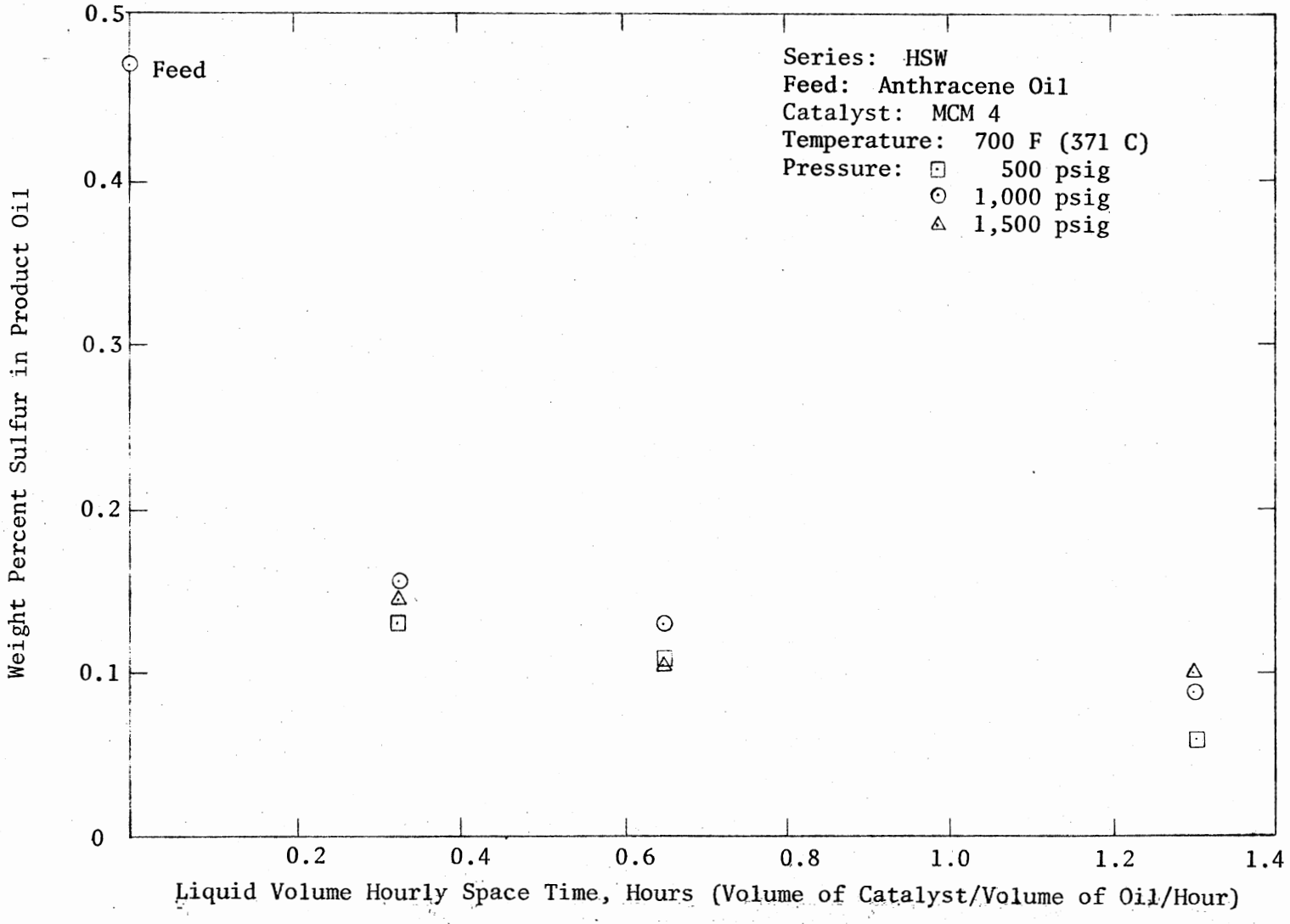

Figure 25. Effect of Pressure on Sulfur Removal at 700 F

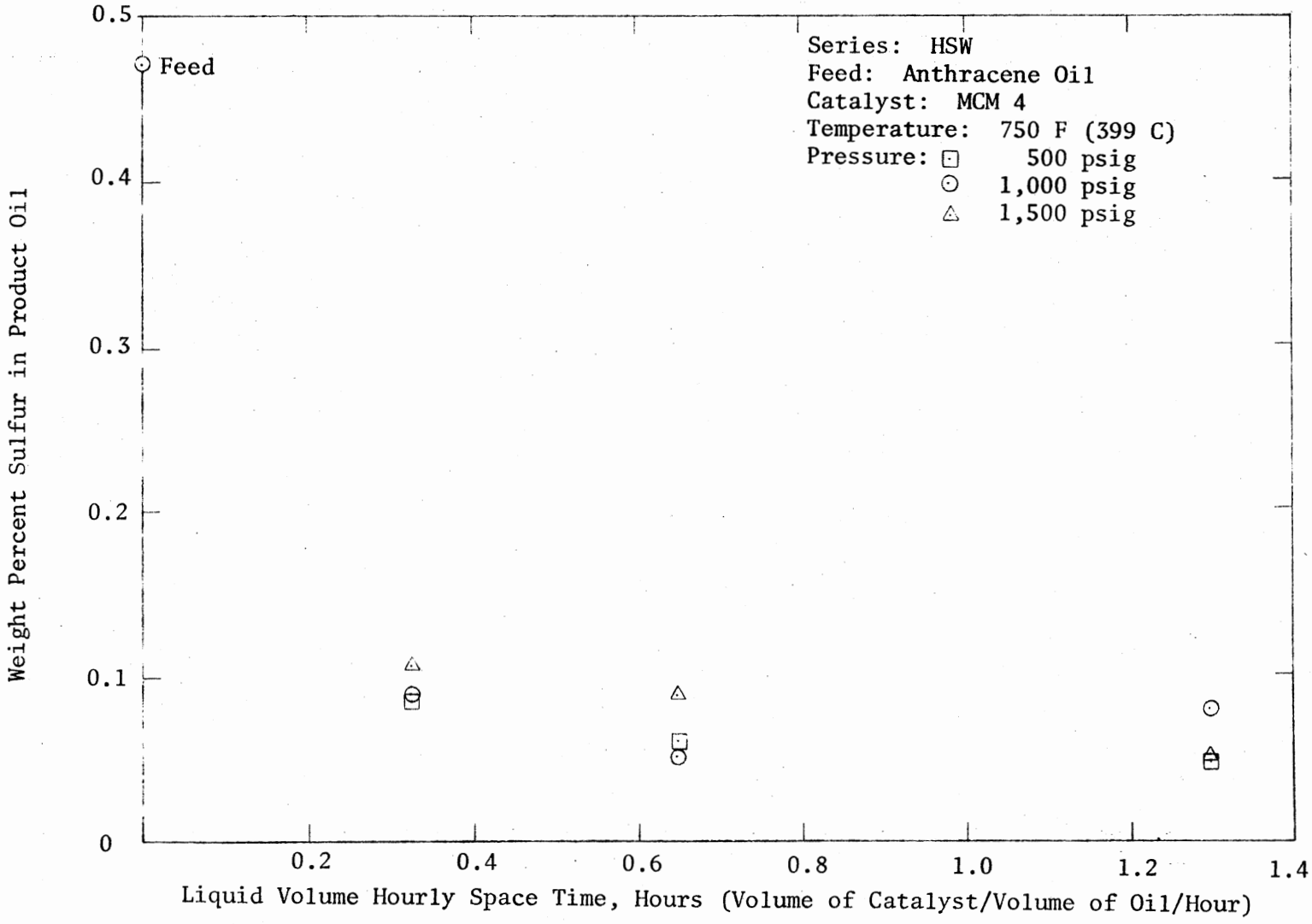

Figure 26. Effect of Pressure on Sulfur Removal at 750 F

Nalco catalyst had the surface area of 270 m^2/gm, 12.5% by weight MoO_3, 3.5% by weight CoO, and the pore radius of 33 Å. The greater pore radius reduces the resistance for the sulfur containing molecules to reach the reaction sites. The Harshaw catalyst had about 19% less surface area than the Nalco catalyst. Consequently, the reaction sites of the Harshaw catalyst could accommodate fewer reactants than the Nalco catalyst on a unit mass basis. Therefore, the inference from the above results is that the effects of the total reactor pressure depend largely upon the catalyst used for the study.

Temperature and Space Time Effects

The principal gaseous product of the feedstock desulfurization reaction is H_2S. The heat of formation of H_2S from its elemental components is exothermic (119). Two published studies (89), (90) have attempted to formulate the desulfurization reaction network by working with two of the most frequently occurring sulfur containing compounds in the feedstocks, thiophene and methyldihydro-benzothiophene. The pathways detected in these studies indicate that, even though one of intermediate steps during the overall desulfurization reaction is reversible, the H_2S forming reaction step is irreversible. A recent study by Ueda, et al. (120) estimated the heat of HDS reaction of heavy oil to be -51,700 Btu/mole (-28.7 Kcal/mole). Combining the observations of irreversibility and heat generation during H_2S formation, the overall HDS reaction appears to be exothermic and irreversible. Such reacting systems are difficult to study under isothermal conditions.

Because of the exothermic nature of the HDS reaction, the temperature control at the two ends of the catalyst zone in the packed bed was critical and most of the diversions from the desired isothermal conditions occurred in those regions. Otherwise, the temperature profiles along the axial direction of the catalyst bed were almost flat and isothermal (see Figure 13). The uniform heating of the reactor from all sides by the specially designed heaters significantly improved the isothermic condition in the catalyst bed. The thermocouple of the temperature programmer measured the wall temperature of the reactor. The thermocouple in the thermowell measured the temperature along the central axis of the reactor. The temperatures measured during the present study by these thermocouples showed a maximum radial deviation of 3 F (1.6 C). These radial temperature gradients are almost identical to those observed in the axial direction and amount to less than 0.5% of the desired temperature. Therefore, the reactor, and especially the catalyst zone, will always be isothermal.

The overall reactor isothermic condition also means negligible temperature gradient in the catalyst pores. The temperature gradient in the catalyst pores depends upon the physical and chemical properties of the reacting fluid and catalysts. The detailed calculations presented in Appendix J indicate that the maximum possible temperature gradient in the catalyst pores would not exceed 2.3 F (1.3 C). Since the temperature gradient in the catalyst pores was no more than the temperature gradient in other parts of the reactor, the overall temperature in the reactor could be assessed as isothermal.

The effects of the reactor temperature and space time on the rate of the overall desulfurization reaction are incorporated in the rate model. However, the temperature effects are generally incorporated indirectly in the determination of the reaction rate constant, k. The dependence of k on reaction temperture, T, is expressed by the Arrhenius law as shown in Equation (6.4).

$$k = A \cdot e^{-\Delta E/RT} \tag{6.4}$$

where, A = proportionality constant or frequency factor, ΔE = activation energy and R = universal gas constant. The estimated values of k will be presented later in this section and Equation (6.4) will be used to determine the activation energies of the various HDS reactions.

The general assumptions found in the literature (59), (60), (83), (86) state that an individual compound desulfurization follows a first order reaction, but the overall desulfurization reaction follows a second order reaction. There are others who believe that the HDS reaction follows a fractional order reaction (97). Therefore, a simple nth order reaction rate model as shown in Equation (5.3) was tested to determine the order of the overall HDS reaction.

$$-\frac{dC_s}{dt} = k \cdot C_s^{\,n} \tag{5.3}$$

where, C_s = sulfur concentration in the product oil

t = space time

k = reaction rate constant

and n = order of reaction

The simple power model shown in Equation (5.3) with varying values of n ranging from 1.0 to 3.0 at an interval of 0.5, was used to fit the data collected during the desulfurization experiments. The results

of the data fit are presented in Table XXI of the Experimental Results Chapter, and show that the degree of fit improves as the order of the reaction is increased. The third order reaction rate model provides the best fit. This continuing improvement in the data fit suggests that, if the order of the reation rate model is increased further, the degree of fit will improve. However, the information available in the literature overwhelmingly indicates that the order of the HDS reaction lies between one-half and three (59), (60), (75), (76), (77). This leads one to infer that the HDS reaction mechanism is not well represented by rate models as simple as Equation (5.3). The overall HDS reaction mechanism appears to be quite complex and one of the major factors affecting the HDS reaction could be the fluid flow characteristics of the trickle bed, such as liquid backmixing and catalyst wetting. In his study on the same feedstock, Sooter (61) developed a rate model consisting of two parallel first order reactions without incorporating any flow characteristics. However, the perfect fit offered by Sooter's model appears to be incomplete and unsupported by other experiments. The basis for these remarks is discussed later in this section.

The effects of various flow characteristics were discussed earlier in this chapter. The discussion demonstrated that the deviations from the plug flow situations were very negligible (less than 5%) and, consequently, would have no significant influence on the rate of the HDS reaction. The earlier discussion also showed that catalyst wetting could be playing a role in the rate of the overall HDS reaction. The influence of catalyst wetting is correlated into the fomulation of the reaction rate model using Mears' (42) model as shown in Equation (6.1).

Based on the literature survey, the Mears' model is often used to correlate catalyst wetting and liquid holdup. The Mears' constant, γ, represents the fraction of the external catalyst pellet surface not effectively wetted by the fresh batch of flowing liquid. Physically, γ represents the fraction of the average external catalyst surface, and thereby the fraction of the catalyst bed, which is not actively participating in the HDS reaction at one time or another.

Paraskos, Frayer and Shah (115) extensively used the Mears' model to represent various reactions, including desulfurization, denitrogenation, and demetallization of petroleum feeds. They applied the Mears' model to first and second order HDS reactions and the results of their study indicated that the value of $1 - \gamma$ varied from 0.532 to 0.922. Paraskos, et al. (115) reported that the value of γ which ranges from 0.078 to 0.468 decreased with an increase in the reaction temperature for most of the reactions, but the value of γ did decrease with an increase in the reaction temperature for a few of the reactions. This variable change indicates that the Mears' constant, γ, stays between 0.078 and 0.468 but ascends or descends with temperature depending upon the type of reaction. However, as suggested by Mears, γ stays more closely to and averages about 0.32 at reaction temperatures from 650 F to 800 F (343 C to 427 C) and pressures from 1,000 psig to 2,000 psig.

The most frequently occurring sulfur containing compounds found in anthracene oil are thiophene, benzothiophene and dibenzothiophene (94). The kinetics of HDS of one or more of these compounds from residual oils have been investigated by several researchers. Hargreaves, et al. (79) reported that the HDS of thiophene followed a first order reaction.

Bartsch and Tanielian (80) studied the HDS of benzothiophene (BT) and dibenzothiophene (DBT) and reported that both of these compounds follow a second order reaction rate model. Aboul-Gheit, et al. (77) investigated the HDS of thiophene in crude oil and found that thiophene followed a pseudo-first order reaction. Lee and Butt (78), while studying the HDS of thiophene, observed that the HDS reaction was first order with respect to thiophene and hydrogen each, and the overall reaction rate was a second order. The desulfurization experiments by Yergey, et al. (86) on ten different coal samples showed that the organic sulfur containing compounds in these coal samples followed different orders of reactions ranging from one-half to two. The experiments by Cecil, et al. (74) also showed that, in the HDS studies, the sulfur containing compounds in coal samples followed variable orders of reactions ranging from one to two. From all the above observations, the HDS reactions for the coal derived liquids would also follow one-half to second order of reactions.

The Mears' effective catalyst wetting model can be incorporated with any of the simple order reaction rate models. Because of the above mentioned findings of variable orders of reactions being followed by the sulfur containing compounds during the desulfurization experiments, the results of this study are correlated into first and second order reaction rate models. The most appropriate reaction rate model is then selected based upon the best of the two fits and the estimated value of Mears' constant. The first and second order reaction rate models correlating γ are shown in Equations (6.5) and (6.6). No catalyst wetting problems exist at $\gamma = 0$ if the real reactions are first or second order.

First order rate model:

$$C_o/C_i = \exp\left(-k_1 \cdot \tau^{(1-\gamma)}\right) \quad (6.5)$$

Second order rate model:

$$\frac{1}{C_o} - \frac{1}{C_i} = k_2 \cdot \tau^{(1-\gamma)} \quad (6.6)$$

where, C_o = sulfur concentration at the reactor outlet

C_i = sulfur concentration at the reactor inlet

k_1 & k_2 = modified reaction rate constants

τ = liquid hourly space time

γ = Mears' constant

The Equations (6.5) and (6.6) each have two unknowns, k_1 and γ or k_2 and γ, respectively. The results of the HDS experiments presented in the previous chapter are used to estimate these unknowns with the help of the non-linear regression analysis (121). The value of C_i was constant at all times because the same feedstock was used during all of the experimental runs of this study. The values of C_o were determined at the preselected values of τ for various catalysts. The sets of data used for the regression analysis are listed in Table XXVII. More than two sets of data points are required to avoid getting unique values for k_1 and γ or k_2 and γ in the Equations (6.5) and (6.6), respectively. Therefore, the minimum required three sets of data points encompassing a wide range of values for C_o and τ were collected at various reactor conditions to correlate in Equations (6.5) and (6.6). The results of non-linear regression analyses are presented in Tables XXVIII and XXIX. Some of Sooter's (61) data on the same feedstock using different catalysts were also tested to fit both of the above mentioned models. The results of their fit are also included in

TABLE XXVII

SETS OF DATA USED FOR THE NON-LINEAR REGRESSION ANALYSIS

Run	Nominal Temp., F	Nominal Press., psig	C_1	τ_1	C_2	τ_2	C_3	τ_3
1	600	1000	0.165	0.626	0.090	1.250	0.075	2.500
1	650	1000	0.130	0.626	0.090	1.250	0.065	2.500
5	650	1000	0.190	0.325	0.157	0.650	0.109	1.300
5	700	1000	0.156	0.325	0.130	0.650	0.088	1.300
5	750	1000	0.089	0.325	0.051	0.650	0.078	1.300
5	650	500	0.205	0.325	0.167	0.650	0.128	1.300
5	700	500	0.130	0.325	0.107	0.650	0.060	1.300
5	750	500	0.082	0.325	0.060	0.650	0.048	1.300
5	650	1500	0.188	0.325	0.156	0.650	0.113	1.300
5	700	1500	0.144	0.325	0.102	0.650	0.100	1.300
5	750	1500	0.107	0.325	0.089	0.650	0.050	1.300
7	650	1000	0.209	0.370	0.168	0.740	0.112	1.480
7	700	1000	0.106	0.370	0.067	0.740	0.048	1.480
7	750	1000	0.045	0.370	0.044	0.740	0.033	1.480
			Sooter's Data (61)					
2	650	1000	0.100	0.375	0.077	0.750	0.049	1.500
2	600	1000	0.182	0.375	0.131	0.750	0.091	1.500
3	700	500	0.085	0.375	0.043	0.750	0.027	1.500
3	650	1000	0.093	0.375	0.078	0.750	0.042	1.500
3	650	1500	0.104	0.375	0.052	0.750	0.040	1.500
3	650	500	0.134	0.375	0.095	0.750	0.062	1.500
3	600	1000	0.166	0.375	0.114	0.750	0.082	1.500
10	600	1000	0.089	0.375	0.142	0.750	0.091	1.500
10	650	1000	0.109	0.375	0.083	0.750	0.051	1.500

TABLE XXVIII

RESULTS OF THE NON-LINEAR REGRESSION ANALYSIS
OF FIRST ORDER REACTION MODEL

Run	Catalyst	Nominal Temp., F (C)	Nominal Press., psig	k_1	γ	Standard Deviation
Present Study						
1	MCM 1	600 (314)	1000	1.341	0.569	0.01265
1	MCM 1	650 (343)	1000	1.505	0.684	0.00252
5	MCM 4	650 (343)	1000	1.311	0.657	0.00384
5	MCM 4	700 (371)	1000	1.515	0.702	0.00433
5	MCM 4	750 (399)	1000	1.919	0.370	0.01530
5	MCM 4	650 (343)	500	1.193	0.676	0.00032
5	MCM 4	700 (371)	500	1.808	0.674	0.00673
5	MCM 4	750 (399)	500	2.196	0.803	0.00180
5	MCM 4	650 (343)	1500	1.294	0.682	0.00285
5	MCM 4	700 (371)	1500	1.536	0.800	0.00913
5	MCM 4	750 (399)	1500	1.991	0.715	0.00596
7	MCM 5	650 (343)	1000	1.200	0.589	0.00375
7	MCM 5	700 (371)	1000	2.070	0.682	0.00339
7	MCM 5	750 (399)	1000	2.515	0.915	0.00248
			Average γ = 0.680		Sub total =	0.06605
Sooter's Study (61)						
2*	MCM 2	650 (343)	1000	1.996	0.732	0.00212
2*	MCM 2	600 (314)	1000	1.411	0.603	0.00181
3*	MCM 2	700 (371)	500	2.561	0.601	0.00375
3*	MCM 2	650 (343)	1000	2.062	0.730	0.00597
3*	MCM 2	650 (343)	1500	2.269	0.610	0.00736
3*	MCM 2	650 (343)	500	1.763	0.654	0.00020
3*	MCM 2	600 (314)	1000	1.530	0.622	0.00374
10*	MCM 2	600 (314)	1000	1.371	0.577	0.00169
10*	MCM 2	650 (343)	1000	1.934	0.704	0.00250
			Average γ = 0.648		Sub total =	0.02914
			Overall Average γ = 0.668		Grand total =	0.09519

* The Run numbers are same as in reference (61).

TABLE XXIX

RESULTS OF THE NON-LINEAR REGRESSION ANALYSIS
OF SECOND ORDER REACTION MODEL

Run	Catalyst	Nominal Temp., F (C)	Nominal Press., psig	k_2	γ	Standard Deviation
Present Study						
1	MCM 1	600 (314)	1000	6.163	0.153	0.01083
1	MCM 1	650 (343)	1000	7.572	0.361	0.00153
5	MCM 4	650 (343)	1000	5.787	0.431	0.00488
5	MCM 4	700 (371)	1000	7.563	0.468	0.00517
5	MCM 4	750 (399)	1000	12.430	0.853	0.01523
5	MCM 4	650 (343)	500	4.908	0.479	0.00120
5	MCM 4	700 (371)	500	10.830	0.368	0.00776
5	MCM 4	750 (399)	500	17.078	0.540	0.00143
5	MCM 4	650 (343)	1500	5.651	0.473	0.00374
5	MCM 4	700 (371)	1500	7.812	0.618	0.00873
5	MCM 4	750 (399)	1500	13.422	0.410	0.00674
7	MCM 5	650 (343)	1000	4.991	0.338	0.00516
7	MCM 5	700 (371)	1000	14.986	0.292	0.00241
7	MCM 5	750 (399)	1000	24.187	0.775	0.00254
		Average γ = 0.468			Sub total =	0.07735
Sooter's Study (61)						
2*	MCM 2	650 (343)	1000	13.640	0.420	0.00282
2*	MCM 2	600 (314)	1000	6.700	0.300	0.00035
3*	MCM 2	700 (371)	500	26.010	0.000	0.00247
3*	MCM 2	650 (343)	1000	14.670	0.411	0.00666
3*	MCM 2	650 (343)	1500	19.060	0.080	0.00598
3*	MCM 2	650 (343)	500	10.420	0.312	0.00097
3*	MCM 2	600 (314)	1000	7.829	0.301	0.00236
10*	MCM 2	600 (314)	1000	6.344	0.273	0.00331
10*	MCM 2	650 (343)	1000	12.704	0.378	0.00335
		Average γ = 0.275			Sub total =	0.02827
		Overall Average γ = 0.392			Grand total =	0.10562

* The Run numbers are same as in reference (61).

Tables XXVIII and XXIX.

The Mears' constant is an indicator of the fraction of the external catalyst surface not surrounded by a fresh batch of flowing liquid, and consequently, not actively participating in the HDS reaction. The average values of γ are 0.668 by the first order reaction rate model and 0.392 by the second order reaction rate model. This indicates that about 39% or 67% of the reactor bed was not actively involved in the HDS reaction at any given time. The experiments by Mears have found the value of γ to be averaging 0.32. These results are later used in this section to determine the appropriate reaction rate model most suitable for the HDS reaction.

There are four primary conclusions that can be derived from the results of the regression analysis. The first of these conclusions is regarding the comparative fit of the reaction rate models presented in Table XXX and the relative fit of a typical and representative data set to the reaction rate models is illustrated in Figure 27. Comparing the overall standard deviations shown in Table XXX, the data fit of both the models incorporating the effective catalyst wetting are significantly better than all the simple nth order reaction rate models. The inclusion of effective catalyst wetting improves the data fit by 20% to 30% compared to the previous best of the third order rate model. Despite the fact that a model with two adjustable parameters is likely to have a better data fit than a one parameter model, the improvement in the data fit also demonstrates that the HDS reaction is more complex than just a simple nth order reaction. Therefore, the results reflect that the effective catalyst wetting is very likely a significant factor in the HDS reaction rate. A clear cut choice

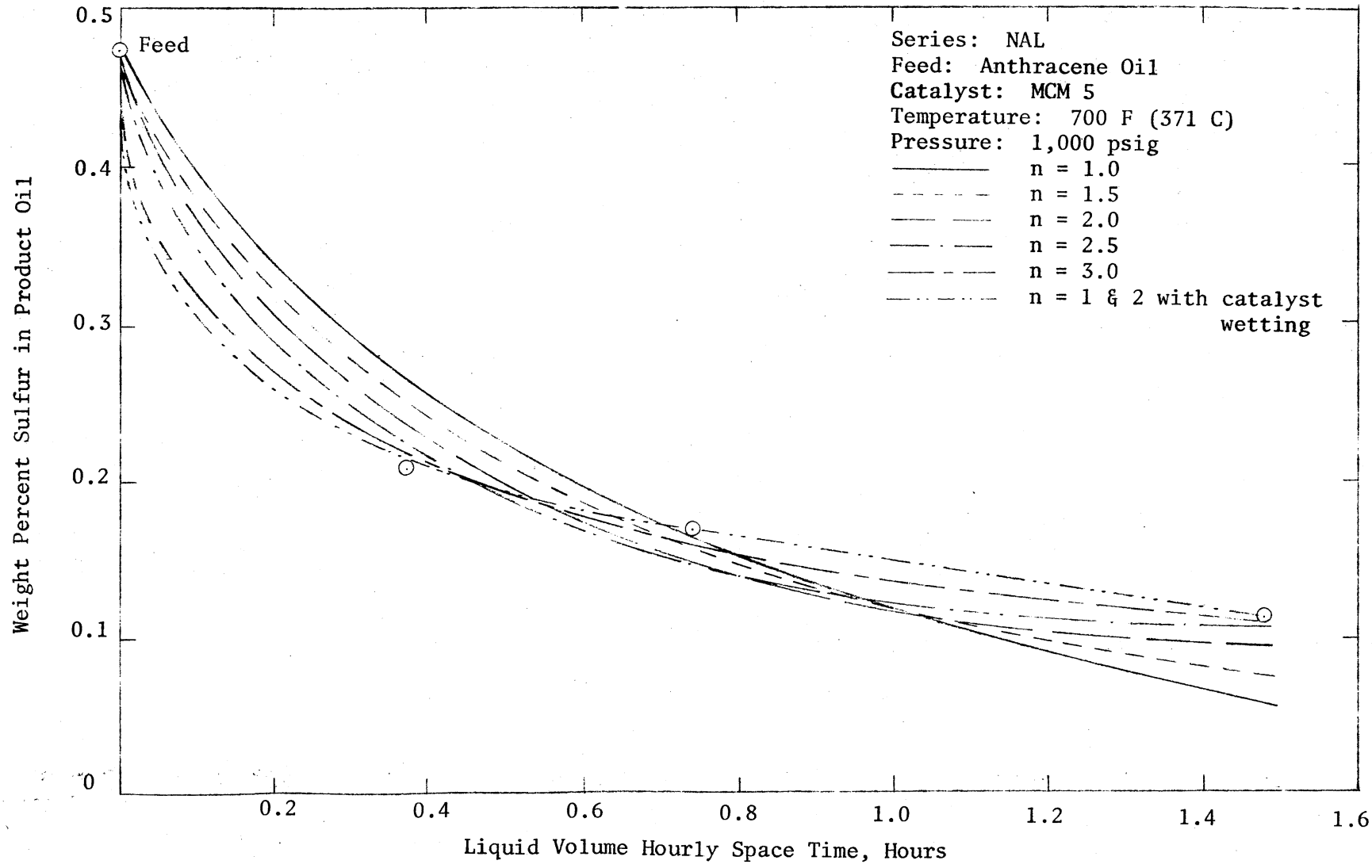

Figure 27. Comparative Fit of Various Reaction Rate Models

between either of the Equations (6.5) or (6.6) can not be made because of the relatively close fit of both of the models.

TABLE XXX

COMPARATIVE FIT OF VARIOUS REACTION RATE MODELS

Data Source	Reaction Rate Model	Overall Std. Dev.
This study	Simple 1.0 order	0.55930
This study	Simple 1.5 order	0.33620
This study	Simple 2.0 order	0.23394
This study	Simple 2.5 order	0.14466
This study	Simple 3.0 order	0.09719
This study	1.0 order - cat. wetting	0.06605
This study	2.0 order - cat. wetting	0.07735
Sooter's study	1.0 order - cat. wetting	0.02914
Sooter's study	2.0 order - cat. wetting	0.02827

The first order model provides an overall data fit about 10% better than that of the second order model. Inversely, the second order model provides a better fit than the first order model for the data from Sooter's study. These variations are close enough to be attributed to the complexity of the three-phase HDS reaction. The reaction rate model most appropriately representing the HDS reaction is selected on the basis of the estimated values of the Mears' constant, γ. The average value of γ is estimated to be 0.32 by Mears (42) from his studies. The range of γ values was estimated to be from 0.078 to 0.468 by Paraskos, et al. (115) from their experiments on different feedstocks

(varying fractions of Kuwait crude). The results presented in Table XXVIII show that the estimated values of γ from the first order rate model are out of this range for all but one data set and γ averages 0.668. However, the results for the second order rate model presented in Table XXIX show that the γ values stay within the above mentioned range in three of the four sets of experiments and γ averages 0.392. Therefore, based on these comparisons, the second order reaction rate model, i. e. Equation (6.6), is suggested to represent the overall HDS reaction over other models tested for the feedstock and conditions studied.

The k values for all of the catalysts increase with the increase in the reactor temperature as in the Arrhenius law, but these do not show any trend with changing reactor pressure. The estimated values of k, are related to the nominal reactor temperature according to the Arrhenius law in Equation (6.4). The activation energy according to Arrhenius law generally does not change with temperature but has been found to be influenced by the type of catalyst and the reactor pressure (116). Therefore, activation energies for the overall HDS reaction are estimated using Equation (6.4) and the values of k_2 for each of the catalysts at various reactor pressures. The results of the calculations presented in Appendix K are listed in Table XXXI. As can be seen, the activation energy values range from 9,627 to 46,807 Btu/mole (5,348 to 26,000 cal/gm mole) depending upon the catalyst and the reactor pressure. These values are in the range of those found in the literature (56), (61), (67), (69). The results also demonstrate a distinct effect of pressure on the activation energy.

TABLE XXXI

ACTIVATION ENERGIES

Run	Catalyst	Nominal Temp. Range, F (C)	Nominal Press., psig	Activation Energy Btu/mole
1	MCM 1	600-650 (314-343)	1000	9,627
5	MCM 4	650-750 (343-399)	500	33,385
5	MCM 4	650-750 (343-399)	1000	20,302
5	MCM 4	650-750 (343-399)	1500	22,989
7	MCM 5	650-750 (343-399)	1000	42,329
2*	MCM 2	600-650 (314-343)	1000	33,240
3*	MCM 2	650-700 (343-371)	500	46,807
3*	MCM 2	600-650 (314-343)	1000	29,363
10*	MCM 2	600-650 (314-343)	1000	32,469

*These Run numbers are same as in reference (61).

The next conclusion concerns the effects of process conditions on the value of γ. Puranik and Vogelpohl (50) have developed a correlation to estimate incomplete contacing in absorbers loaded with varying packing size and shape. The packing size in their tests ranged from 0.8 cm to 3.5 cm. Puranik and Vogelpohl further claim that their correlation can estimate the wetted suface area within a maximum error of $\pm$ 20 percent. An examination of their plot comparing predicted versus experimental data indicates that the deviation from the experimental value for particle sizes of 0.8 cm is close to 20 percent. The particle sizes used in the present study (0.2 cm) were much smaller than the particle size of 0.8 cm. The correlation by Puranik and Vogelpohl is as shown in Equation (6.7).

$$\frac{a_w}{a_t} = 1.05\ (Re)^{0.047}\ (We)^{0.135}\ (\sigma_c/\sigma)^{-0.206} \qquad (6.7)$$

where Re is the particle Reynold's number, We is the particle Weber number, and σ_c/σ relates to the surface tension properties. Equation (6.7) could not be used to estimate the wetting surface area because the data gathered during this study was not sufficient to estimate all the complex items in the equation. No distinct trend was observed in the value of γ when reactor temperature and pressure were varied.

Sooter (61) conducted certain HDS studies on the same feedstock as in this study, but using different catalysts. His study also included some experimental runs using the inert materials in place of the catalyst. The results obtained in Sooter's study coincide with the results observed by Wells (114) regarding the occurrances of some desulfurization of the same feedstock on the bed of inerts. Based on the results of his experiments with inerts only, Sooter concluded that a fraction of the sulfur containing compounds in the oil reacted almost instantaneously. This observation, coupled with the results of the other runs using different catalysts, led him to conclude that the HDS reaction was a combination of two first order parallel reactions. Sooter concluded that a fraction of the sulfur containing compounds in the feedstock followed a first order reaction and reacted almost instantaneously, whereas the remaining fraction of the sulfur containing compounds in the feedstock followed another first order reaction which was relatively slower. Sooter's rate model is shown in Equation (6.8).

$$C_o/C_i = x \cdot \exp(-k_3 \cdot \tau) + (1 - x) \cdot \exp(-k_4 \cdot \tau) \qquad (6.8)$$

where, C_o = sulfur concentration at the reactor outlet

C_i = sulfur concentration at the reactor inlet

x = fraction of sulfur following the fast reaction

k_3 = reaction rate constant for the fast reaction

k_4 = reaction rate constant for the slow reaction

τ = liquid volume hourly space time

In Equation (6.8), C_i is a known quantity, and C_o and τ are the experimental data points and x, k_3 and k_4 are the three parameters to be determined. Sooter tested Equation (6.8) using his sets of data and found a perfect fit. That means the standard deviations of all the sets of data were estimated to be 0.00000. The concept of the perfect model is most desirable but rather difficult to achieve from the three phase heterogeneous catalytic reaction.

There are two important points concerning Sooter's rate model that suggest that Equation (6.8) probably does not completely represent the overall HDS reaction. Three independent sets of data of τ and C_o were collected at a given set of process conditions. Since C_i is treated as a known quantity in the above model, the initial condition of $C_o = C_i$ at $\tau = 0$ is not considered as another independent set of data. The first and foremost point is that there are three unknowns in Equation (6.8) and only three independent sets of data used in the regression analysis to estimate these unknowns. Therefore, in all probability, a perfect fit is inevitable. The results of the present study, which coincidently have three independent sets of data at any reaction conditions, were tested to fit Sooter's model, i. e. Equation (6.8). The overall standard deviation from the non-linear regression analysis was again 0.00000. Therefore, it is concluded that more than three independent sets of data are required to test the reaction rate model shown in Equation (6.8).

The second point concerns the relative values of k_3 and k_4. The right hand side (r.h.s.) of Equation (6.8) is a sum of two first order reactions, i. e. the sum of two exponential terms. Therefore, the sensitivity of the regression analysis of these two r.h.s. terms depends upon their relative magnitudes. The relative magnitudes of these two terms depend largely upon the values of k_3 and k_4. Because of the composition of Equation (6.8), the relative magnitude of the first and second terms on the r.h.s. are practically equal to the exponent of the difference of k_3 and k_4, $e^{(k_3-k_4)}$. Sooter's study shows that the difference of k_3 and k_4 varies from 5.5 to 226 to 3,109 at the reactor temperatures ranging from 600 F (314 C) to 650 F (343 C) to 700 F (371 C), respectively. Consequently, the relative magnitudes of the first and second term of the r.h.s. vary at least by a factor of $e^{5.5}$, or about 245. Such a large factor in the values of the terms of any equation such as Equation (6.8) certainly reduces the sensitivity of the regression analysis.

These two points lead one to conclude that Equation (6.8) although completely representative of the overall HDS reaction, is not really a good model. Additional sets of data (more than three) are requied to study the applicability of Equation (6.8) The reaction rate model proposed in this study, Equation (6.6), is free from both of these limitations and the estimated values of the unknowns are within the range of those found in previous studies (42), (115).

Effect of Catalyst Pore Size

There are, in general, three diverse factors that have substantive influence on the phenomena of the HDS reaction. These influences may

not, however, be entirely independent of each other. The first factor consists of the fluid flow characteristics in the trickle bed reactor, such as axial dispersion and effective catalyst wetting. The second factor includes the reactor operating conditions, such as reactor bed temperature, total pressure, hydrogen partial pressure, hydrogen flow rate, and liquid volume hourly space time. The last factor covers the characteristics of the basic substances involved in the HDS reaction, e. g. catalyst and sulfur containing compounds. The first two factors have already been discussed in the previous sections of this chapter.

The characteristics of the several catalysts tested during the present study that can contribute to the reaction rate are the most frequently occurring pore size (sometimes referred to as the average pore size), d_f, active surface area, active life of the catalyst, catalyst support material and active metals in the catalyst, among others. The effect of the catalyst active life will be discussed in the next section. The average pore size, the surface area, catalyst support material and the metal content are generally interlinked and are therefore treated collectively.

Figure 28 displays the typical most frequently occurring pore size distributions. The pore size is plotted against the frequency at which the pore size occurs in the catalyst, as estimated by the mercury porosimeter. The figures show either one or two peaks in the pore size frequency. Figure 28a shows a very narrow peak meaning that only a very short range of sizes is occurring at a high frequency. Figure 28a obviously has a very narrow pore distribution. Figure 28b has a sharp peak but the smaller pore sizes are also occurring at a measurable frequency. This has widened the pore distribution and skewed the

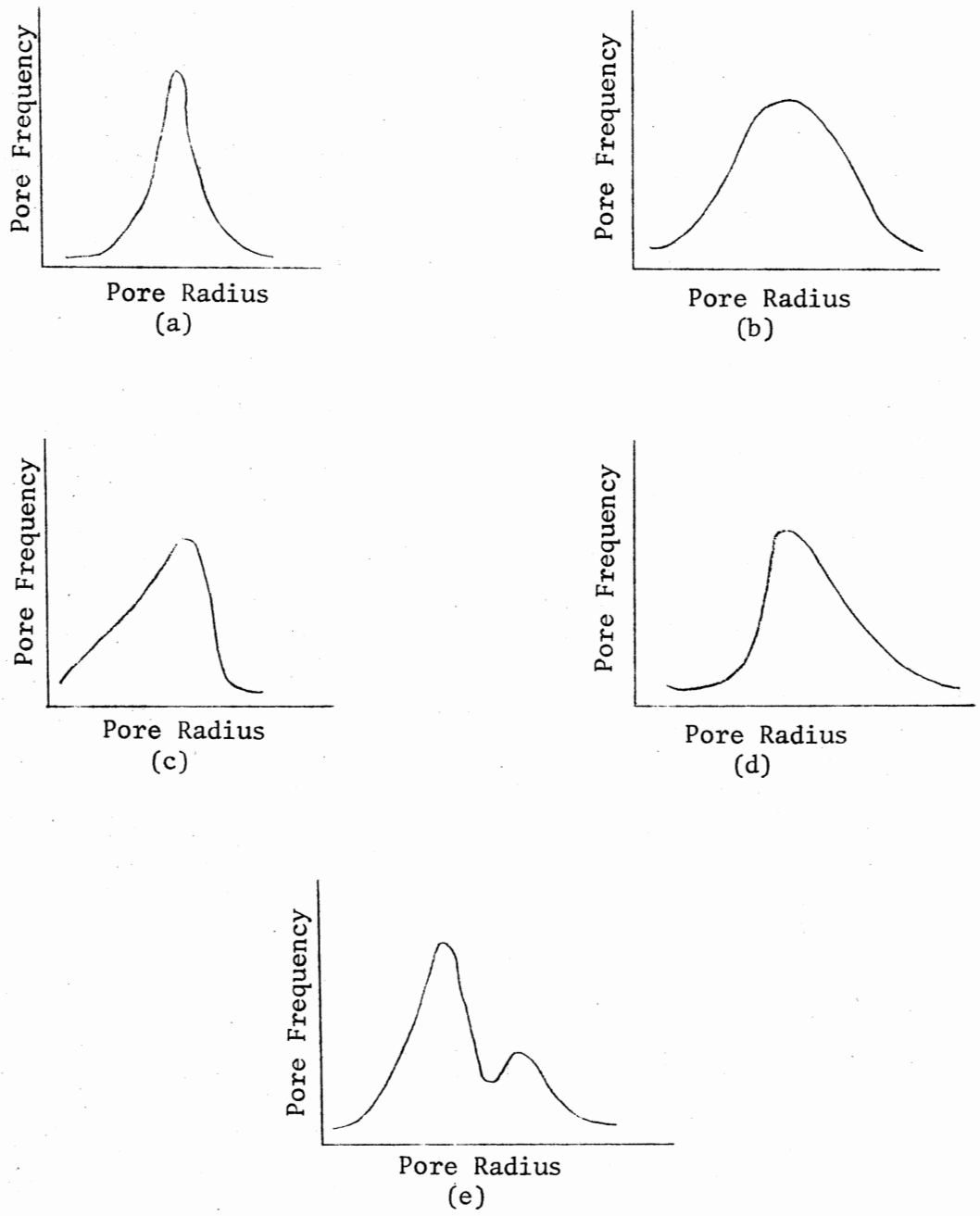

Figure 28. Typical Pore Size Distributions (61)

frequency curve to the small pore size side. Figure 28c shows a sharp peak and a wide pore distribution with the curve skewed to the large pore size side. The sulfur containing compounds found in various feedstocks are very complex and thus would come in a wide range of molecular size. Therefore, the wider pore distribution increases the range of the molecular size of the reactant that can be accommodated by the catalyst, other things being equal. Figure 28d illustrates a shallow peak and a very wide pore distribution. This type of catalyst can accommodate a very wide range of molecules for a chemical reaction. Figure 28e shows that the catalyst has two peaks (bidispensed) and that probably increases the chances of the high rate of reaction.

As mentioned above, the effectiveness of a catalyst in removing sulfur is also dependent upon the size of the sulfur containing molecules. Empirical methods were used to estimate the molecular diameters of the sulfur containing compounds. Sivasubramanian (122) outlined a simplified procedure to estimate the molecular diameter which essentially calculates the same value as estimated by a model available in the literature. The method involves the assumption that all the atoms in a molecule are planar in configuration and the molecular distances between the atoms can be added to estimate the size of a molecule. The distance between two carbon atoms connected by a single bond is 1.54 Å and the same for a double bond is 1.34 Å. Since there are three alternating single and double bonds each in a benzene ring, the average distance between the carbon atoms in a benzene ring is assumed to be 1.44 Å. Based on this, the longest distance or the molecular diameter of a benzene ring is 2.88 Å.

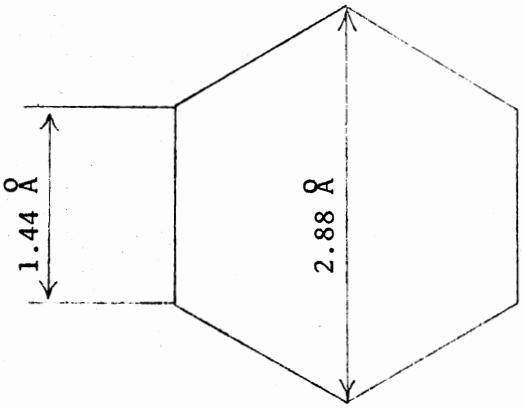

The same concept is then used to calculate the molecular diameters of some of the sulfur containing compounds found in anthracene oil.

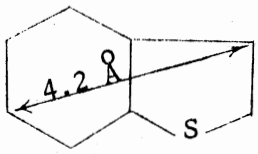

Benzothiophene

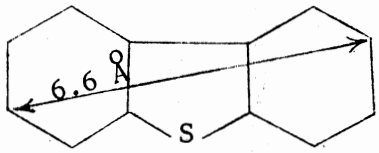

Dibenzothiophene

The molecular sieves used for the selective adsorption separate molecules on the basis of another molecular dimension called critical diameter. The critical diameter of benzene is 6.7 Å. Comparing the critical diameter of benzene with its molecular diameter calculated earlier, the critical diameters of benzothiophene and dibenzothiophene would be 9.8 Å and 15.3 Å respectively. The pore radius of the five catalysts tested ranged from 26 Å to 800 Å. Obviously, the larger pore sizes would reduce the resistance for diffusion of larger size sulfur containing molecules to the active sites and smaller pore sizes would mean greater resistance for the diffusion of larger size sulfur containing molecules. The effect of pore size on the HDS reaction rate would be significant if pore diffusion is the rate controlling step, or offers a substantial part of the overall resistance.

In spite of all these classifications of catalysts, one must recognize that the pore size distribution depends upon the method of manufacturing the catalyst support material and preparation of the catalyst. But manufacturing catalysts with consistent pore size distributions is a significantly difficult task. Another observation is that the larger pore size, d_f, tends to reduce the catalyst surface area. Thus one can see mixed effects of pore sizes. On one hand, the larger pores would reduce the resistance for diffusion of the reactive molecules to the active sites. But, on the other hand, the larger pore sizes reduce the catalyst surface area available for reaction. Therefore, differentiation between the effects of pore sizes and catalyst surface area is difficult. The reaction rate constants were calculated based on the unit surface area to see the effects of catalyst surface area on the rate of the HDS reaction. The reaction rate constant based on unit surface area was calculated using the relationship shown in Equation (6.9)

$$k_s = k_2 \times V/S \qquad (6.9)$$

where, k_s = reaction rate constant based on unit surface area

k_2 = reaction rate constant per unit volume, from Table XXIX

V = volume of the catalyst bed

S = total catalyst surface area

The results in table XXXII indicate that the catalyst surface area could be influencing the rate of reaction at reactor temperature of 650 F (343 C), but no such conclusion can be derived for the reactor temperatures of 700 and 750 F (371 and 399 C respectively).

TABLE XXXII

REACTION RATE CONSTANT PER UNIT CATALYST SURFACE AREA

Run	Catalyst	Nominal Press., psig	k_2	k_sx100
@ 650 F (343 C)				
1	MCM 1	1000	7.572	5.834
5	MCM 4	1000	5.787	3.858
5	MCM 4	500	4.900	3.272
5	MCM 4	1500	5.651	3.767
7	MCM 5	1000	4.991	3.461
@ 700 F (371 C)				
5	MCM 4	1000	7.563	5.042
5	MCM 4	500	10.830	7.220
5	MCM 4	1500	7.812	5.208
7	MCM 5	1000	14.986	10.393
@ 750 F (399 C)				
5	MCM 4	1000	12.430	8.287
5	MCM 4	500	17.078	11.385
5	MCM 4	1500	13.422	8.948
7	MCM 5	1000	24.187	16.773

Catalyst Aging Characteristics

The active life of a set of catalysts is another major characteristic investigated in the present study. The active life of a catalyst is the time a fresh batch of catalyst can be continuously used to participate in a chemical reaction without a significant loss of reactivity. The literature review indicated that the most widely tested factors for the aging of catalyst for the HDS and hydrocracking of the Middle Eastern and Venezualan crudes are the deposition of the reaction

products, metal sulfides, and coke on the catalyst during the reactions (104). A study by Aoshima and Wise (123) observed that catalyst deactivation was also possible because of the severity of the reactor conditions which can effect the catalyst surface area and the pore structure. Aoshima and Wise found that very high reactor temperatures tend to disintegrate the catalyst pores and thereby reduce the active catalyst surface area.

There are several experimental parameters that have direct effect on the catalyst aging. The experiments by Gavalas, et al. (105) and Newson (103) have illustrated and theoretically demonstrated that, for the HDS of various crude oils, the reactor temperature, liquid hourly space velocity (LHSV), pressure, and the metallic contents of the reactants have direct bearing on the catalyst aging. From the experimental data and his model, Newson (103) showed that the active life of a catalyst for the desulfurization of crude oils jumped almost threefold when the extent of sulfur removal was reduced from 75% to 63%. This reduction in sulfur removal could be achieved by adjustment of three process variables of reactor temperature, pressure, and LHSV. The rise in reactor pressure from 800 psig to 1500 psig increased the catalyst life from 400 hours to 800 hours. Apparently, high temperature and low pressure promote the tendency for coking. Newson's model presented a dramatic change in the catalyst life from 400 hours to 1,200 hours by merely increasing the LHSV from 0.5 per hour to 0.7 per hour and maintaining constant outlet sulfur content by reducing the catalyst bed height. Since one of the reasons for the deactivation is the deposition of the metallic sulfides in the pores, it is inferred that larger catalyst pore size should improve the catalyst life.

Newson illustrated that the rise in the pore radius from 20 Å to 32.5 Å improved the catalyst active life from 400 hours to 1,200 hours. The other qualitative conclusions from Newson's work include the effect of active metal content and reactor temperature. Higher reactor temperature would enhance coking and thereby would reduce catalyst life. Similarly, higher metallic content in the feedstock would promote deposition of more sulfides and thus lower the catalyst active life. Johnson and coworkers (84) found that the active life of the catalyst used in the HDS of residual oils could be increased from 700 hours to 1,600 hours by reducing the metallic content of petroleum residuum from 200 ppm to 40 ppm.

The present study was partially devoted to the determination of the aging characteristics of different catalysts for the desulfurization reaction. About 20 grams of each catalyst were packed in the reactor during five separate experiments. A constant weight of catalyst provided a constant LWHST, but because of the differing densities, the LVHST varied. Other process conditions were set constant during all five experiments. The nominal reactor temperature was maintained at 700 F (371 C) and the nominal reactor pressure was maintained at 1,000 psig. The liquid flow rate was set at 40 cc/hr and the hydrogen flow rate was set at 1,500 scf/Bbl of oil. Each of the five experiments was conducted for a continuous 200 hours at the above mentioned conditions before a planned shutdown. The results of the experiments were tabulated in Tables XII, XIII, XIV, XV, and XVI in the Experimental Results Chapter. Those results are plotted here in Figures 29-33.

One can see from these figures that the system stabilized after about 50 hours of the initial operation. However, it appears difficult

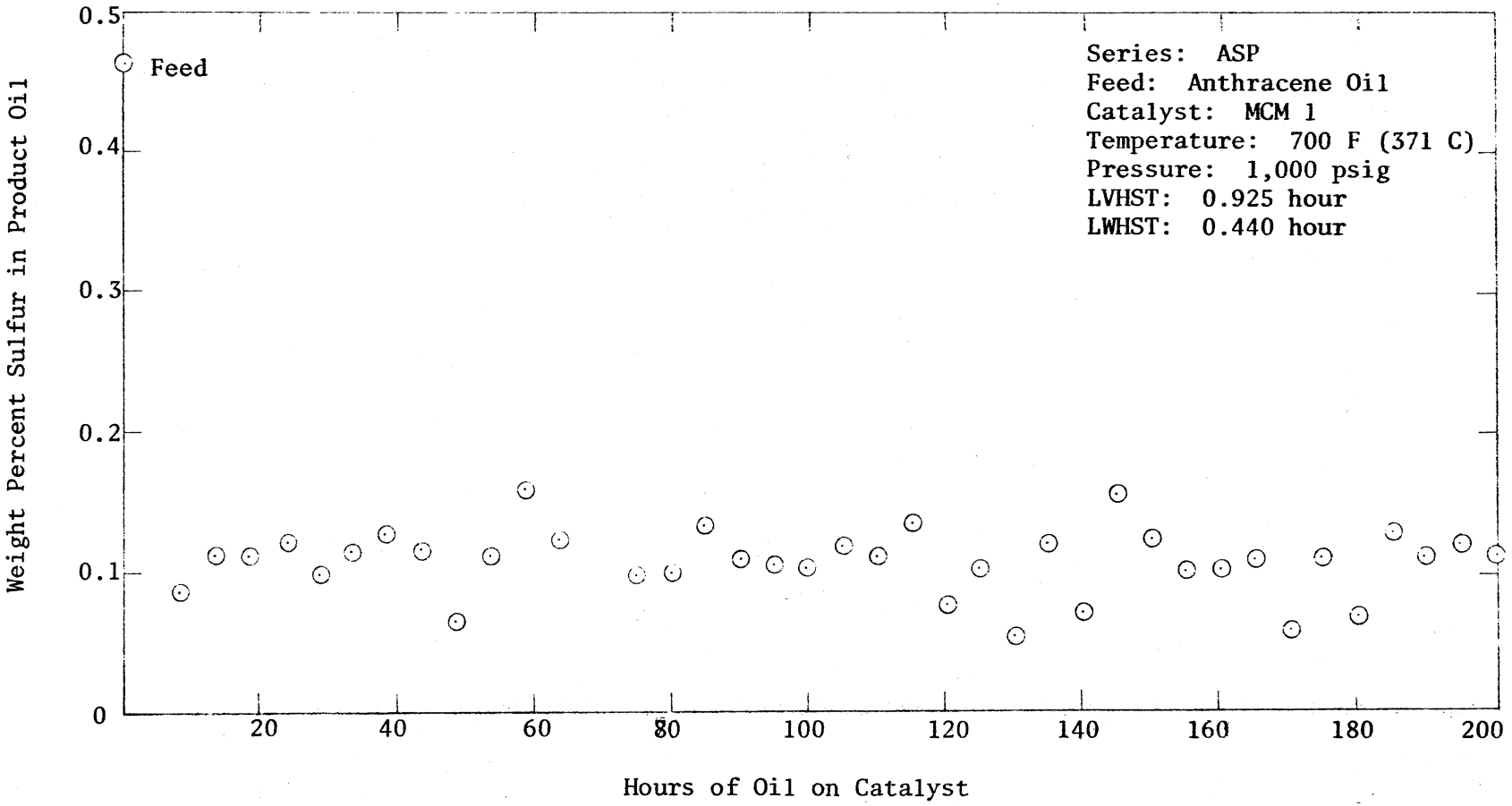

Figure 29. Results of Catalyst Aging Test Run for MCM 1 Catalyst

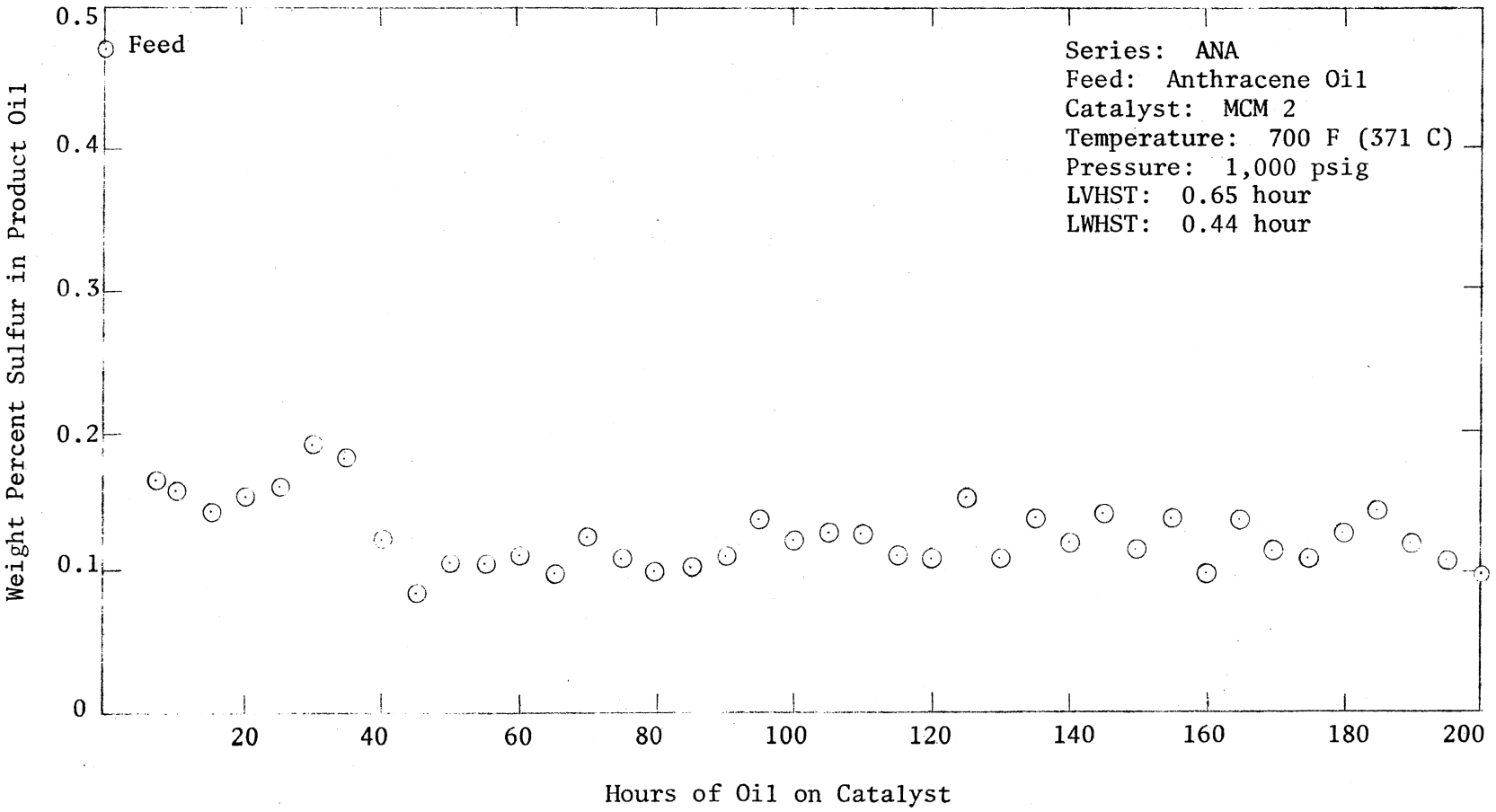

Figure 30. Results of Catalyst Aging Test Run for MCM 2 Catalyst

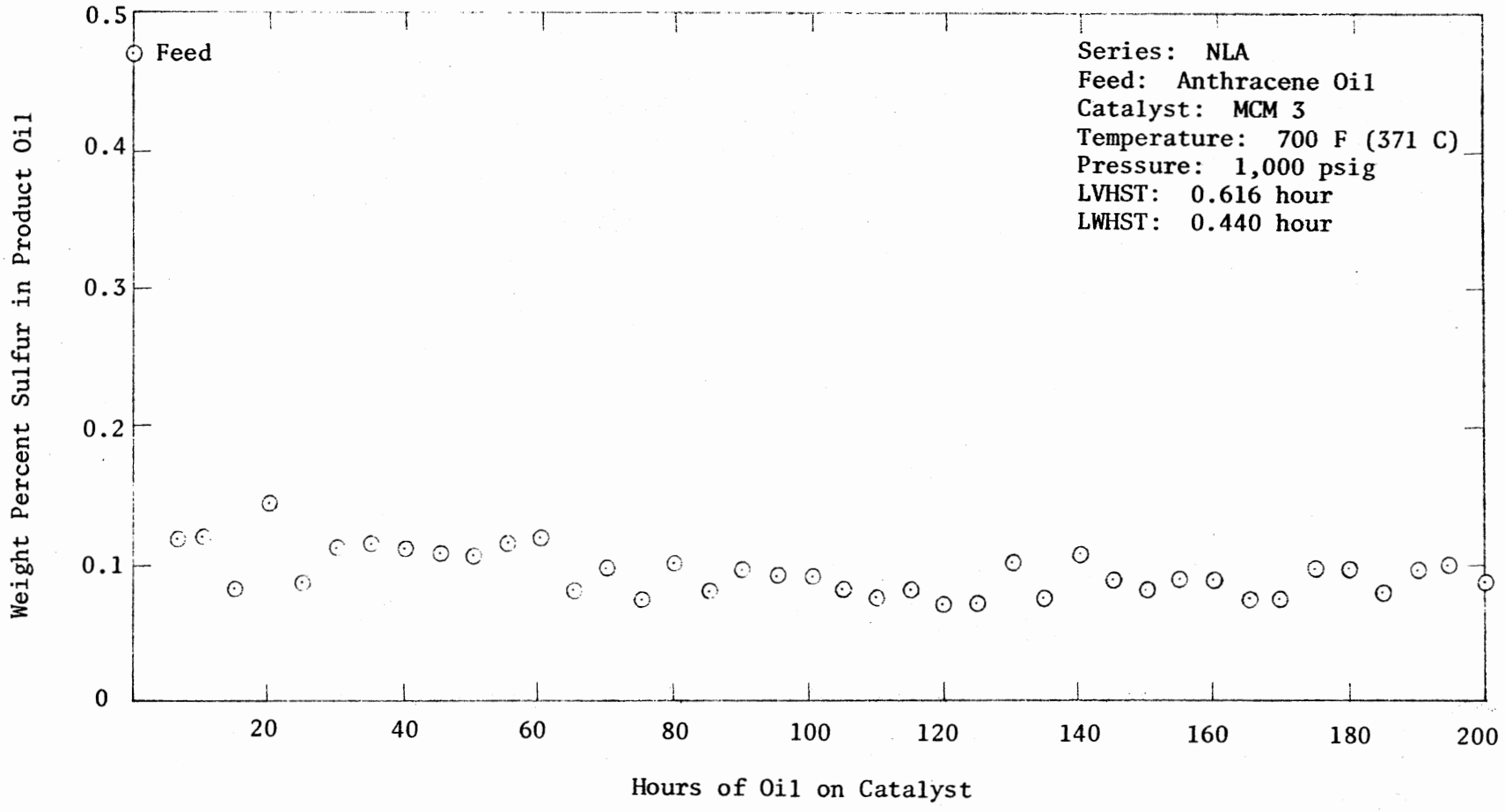

Figure 31. Results of Catalyst Aging Test Run for MCM 3 Catalyst

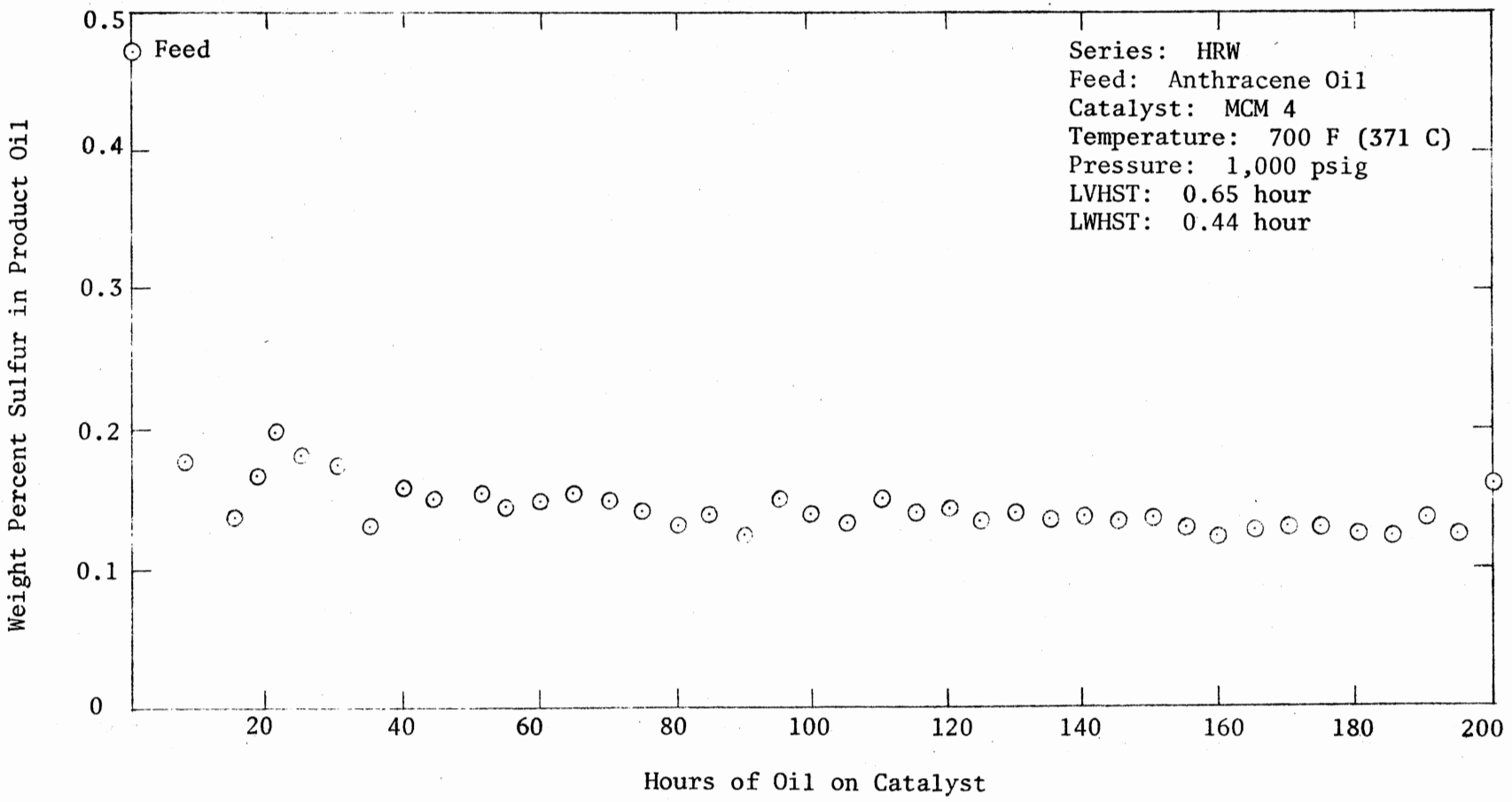

Figure 32. Results of Catalyst Aging Test Run for MCM 4 Catalyst

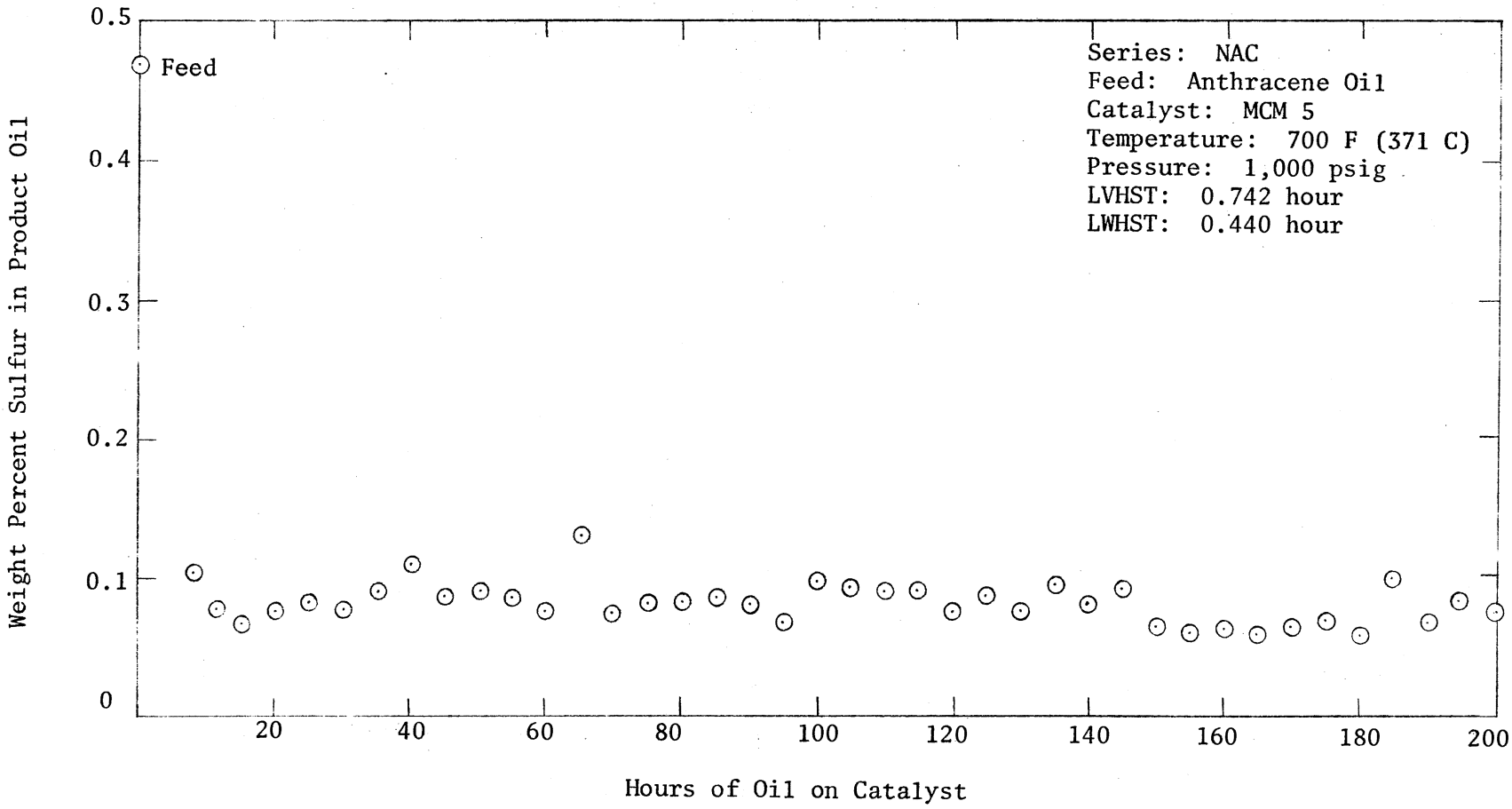

Figure 33. Results of Catalyst Aging Test Run for MCM 5 Catalyst

to judge whether there is any loss of catalyst activity. Therefore, the results of each experiment after the initial 50 hours of stabilization period are anlyzed using a linear regression technique. The results of the regression analysis are presented in Table XXXIII.

TABLE XXXIII

RESULTS OF THE AGING TESTS

Run	Catalyst	Intercept Avg. %S	Std. Dev. %S	Slope %S/hour
2	MCM 1	0.125	0.0241	-0.0001297
3	MCM 2	0.111	0.0148	0.0000524
4	MCM 3	0.098	0.0129	-0.0000851
6	MCM 4	0.150	0.0088	-0.0001059
8	MCM 5	0.095	0.0143	-0.0001518

The results in Table XXXIII show very little noticeable change in the average sulfur content of the product samples in a given run. This indicates that there is no loss of catalyst activity during the 200 hours of the continuous operation. One of the reasons for the absence of deactivation could be the absence of the metallic or other inorganic species in the feedstock. The other possible reason is the apparent short duration of the continuous operation. The test runs for determining the catalyst performances at varying reactor pressure, temperature, and space time were conducted continuously for about 200 hours. Therefore, the catalyst aging test runs were also conducted for

200 hours to see whether catalyst deactivation was an added variable in the performance tests. The results in Table XXXIII conclusively show that the catalyst activity had not changed noticeably to add any extra variables.

As shown in Table XXXIII, various catalysts used in this study show varying levels of sulfur removal during the aging tests. The differences in the degree of sulfur removal at constant process conditions must be caused by the catalyst physical and chemical properties. Catalyst MCM 4 had the lowest surface area and Co-Mo atom ratio of 0.24 as compared to 0.34 for other catalysts tested. These lower values may have caused the lowest sulfur removal by the MCM 4 catalyst. During their studies on the HDS of residual oils, Kushiyama, et al. (99). They observed that the removal of sulfur containing compounds from Khafji residual oil increased as the Co-Mo atom ratio increased at constant Mo concentration and the removal was maximum at the Co-Mo atom ratio of o.5-0.6 : 1, regardless of Mo concentration. All the other four catalysts had different pore sizes and surface areas but the same concentration of Co. However, only three of these, i. e. MCM 2, MCM 3 and MCM 5, have nearly identical levels of sulfur removal. The intermediate level of sulfur removal by catalyst MCM 1 is rather confusing. Theoretically, the negative slopes mean that the catalyst activities were actually improving with time, but the relative magnitudes of these slopes are too small to be conclusive.

In summary, one can see that the experimental and analytical techniques employed in the present study have been thorough enough to generate consistent results. The analysis also demonstrated that the liquid backmixing does not contribute significantly to the rate of

desulfurization reaction, but the effective catalyst wetting does play a role in the rate of desulfurization reaction. The effective catalyst wetting is incorporated into a second order reaction rate model, which appears to better represent the desulfurization reaction than any model tested or developed previously. In the catalyst aging tests, the results indicate no noticeable loss of catalyst activity during the 200 hours of the continuous operation. The conclusions of this study and the recommendations for future investigations based on those conclusions are presented in the next chapter.

CHAPTER VII

CONCLUSIONS AND RECOMMENDATIONS

Conclusions

A trickle bed reactor bed was selected to study the HDS of raw anthracene oil, a coal derived liquid, over various commercially available Co-Mo-Alumina catalysts. The experimental equipment was designed for operating conditions ranging from ambient to 850 F (455 C) and 1,800 psig. The HDS studies were conducted at reactor temperatures of 600, 650, 700, and 750 F (314, 343, 371, and 399 C respectively), at reactor pressures of 500, 1,000, and 1,500 psig and at liquid volume hourly space times ranging from 0.325 to 1.480 hours. The hydrotreating catalysts were also studied for their aging characteristics. The following conclusions are presented:

1. The trickle bed reactor was an excellent tool for studying HDS of the coal derived liquid. With the choice of the specially designed heaters, the reactor temperature was very close to isothermal conditions, and the pressure could be maintained steady at all times. The liquid distribution was adequate and backmixing effects were held to a minimum by appropriately selecting the reactor dimensions.
2. The effective catalyst wetting was an influencing factor in the rate of HDS of raw anthracene oil.

3. The results of the HDS of raw anthracene oil were satisfactorily correlated to fit a second order model incorporating partial catalyst wetting. The results demonstrate a better fit as the order of the simple reaction rate model increases.
4. The fraction of the external catalyst surface not surrounded by a fresh batch of flowing liquid (or Mears' constant Y) was found to vary from 0.153 to 0.853 and averaging 0.392. A definite correlation could not be established between the value of the Mears' constant and the reactor operating conditions.
5. The catalysts used in the HDS of raw anthracene oil did not indicate any loss of activity during the 200 hours of continuous reactor operation.
6. The total available catalyst surface area showed a limited influence on the rates of the overall HDS reaction.
7. The rates of the overall HDS reaction were not influenced by the changing catalyst pore radius within the range of 30 to 50 Å. The bidispersed catalyst also did not demonstrate any noticeable improvement in the sulfur removal capability over the other monodispersed catalysts.
8. The results suggest a moderate influence of Co-Mo atom ratio in the the cataklyst on the rates of the overall HDS reaction. 5#3 the higher Co-Mo atom ratio indicated an increase in sulfur removal.
9. The results of this study indicate that the reactor pressure does not influence the rate of the overall HDS reaction

in the range from 500 to 1,500 psig.

10. The reproduction of the experimental and analytical results were consistent, considering the three phase flow situation in the HDS reactions.

Recommendations

The use of coal as an energy supply is increasing. The greater emphasis on the use of coal in the future has made coal conversion technology of greater importance. With pollution control regulations becoming more and more stringent, the hydrotreating of coal derived liquids will have to be more thoroughly understood. The following test programs are recommended based on the results collected and the experiences encountered during the present study.

1. Catalyst deactivation studies of longer test run time should be conducted. The longer run time demonstrating deactivation would provide a more definite time period for continuing catalyst activity at a steady level.
2. Varying concentrations of metal content in the feedstock should be tested to evaluate the tolerance level of each of the catalysts. The results of such a study will help decide whether a demetallization process is necessary for a particular feedstock prior to the hydrotreating step.
3. Since coking of feedstock is one of the influencing characteristics of catalyst deactivation, a particular catalyst should be tested against feedstock with varying coking characteristics. Such an information would help in selecting a catalyst for hydrotreating the corresponding feedstock.

4. With confusion and, at times, conflicting observations regarding the order of the overall HDS reaction, an attempt should be made to study the HDS of individual sulfur containing compounds and preselected varying combinations of the sulfur containing compounds. Such a study would provide more insight into this complex reaction.
5. A greater variation of the physical characteristics of the catalysts, such as surface area, pore size distribution and support materials should be tested. The results of such a study would help in the selection of a catalyst for the hydrotreating of a feedstock.
6. The presence of certain chemicals, specifically Co and Mo, in a catalyst were found to have a degree of influence on the extent of the overall HDS. A wider variety of experiments should be conducted to evaluate the effects of each of these components. Furthermore, an additional chemical component in the catalyst should also be tested to estimate its effects.

In conclusion, the method used to study the HDS in a trickle bed reactor is excellent and future studies should be continued in a similar reactor.

A SELECTED BIBLIOGRAPHY

1. "Coal's Share of Nation's Energy Rose Slightly," Coal Age, Vol. 80, No. 5, (May 1975), p. 21.

2. Hydrocarbon Processing, Vol. 56, April 1977, p. 15.

3. Bridges, Jack H., "Understanding the National Energy Dilemma," Prepared for the Joint Committee on Atomic Energy, March 1973.

4. "World Shaken by Arab Oil-Export Cuts, Price Hikes," The Oil & Gas J., Vol. 71, Oct. 29, 1973, pp. 49-52.

5. Time Magazine, Vol. 104, Nov. 10, 1974.

6. "The Energy Crisis: Whys and Hows," Mining Engineering, Vol. 27, May 1975, pp. 10-11.

7. Culbertson, LeRoy, "Energy in Engineering," Presented at the Twenty-Fifth Annual Trisectional Meeting of AIChE, Oklahoma State University, Stillwater, Oklahoma, April 23, 1971.

8. American Gas Association, The Oil & Gas J., Vol. 75, Feb. 28, 1977, p. 170.

9. "Project Independence: A Critical Look," Chemical Engineering, Vol. 82, Jan. 6, 1975, pp. 92-105.

10. Hydrocarbon Processing, Vol. 55, Feb. 1976, p. 17.

11. "Newsbreak," Gas, Vol. 47, No. 7, 1971, p. 6.

12. "Rush for Riches on the Great Pipeline," Time Magazine, Vol. 105, No. 23, June 2, 1975, pp. 12-20.

13. Wilson, Howard M., "Alyeska Maps Complex System Start-up," The Oil & Gas J., Vol. 75, March 14, 1977, pp. 36-37.

14. Gardner, F. J., "World's Offshore Oil Potential Keeps Growing," The Oil & Gas J., Vol. 73, May 5, 1975, pp. 175-181.

15. Welt, Ted, "Coal: Future source of oil and gas," The Oil & Gas J., Vol 75, No. 35, August 1977, pp. 517-522.

16. "Energy Sources: Coal, Oil and Gas," Power, Vol. 121, No. 9, September, 1977, pp. 46-52.

17. Bituminous Coal Research, Inc., Gas Generator Research and Development - Survey and Evaluation, Phase One, Volumes One and Two, OCR Contract No. 14-01-0001-324, BCR Report No. L-156, Oct. 1965.

18. Mehta, D. C., M. S. Thesis, Oklahoma State University, Stillwater, Oklahoma, July 1972.

19. Sapre, Ashok, R., Ph. D. Dissertation, Oklahoma State University, Stillwater, Oklahoma, July 1974.

20. Coal Age, Vol. 80, No. 5, May 1975, p. 20.

21. U. S. Bureau of Mines, News Release, Department of the Interior, Oct. 10, 1974.

22. Balzhiser, Richard E., "Energy Options to the Year 2000," Chemical Engineering, Vol. 84, Jan. 3, 1977, pp. 73-90.

23. Satterfield, Charles N., "Trickle-Bed Reactors," AIChE J., Vol. 21, No. 2, Mar. 1975, pp. 209-228.

24. Baral, William J. and Huffman, Hal C., "Advances in Hydrocracking of Distillates," Eighth World Petroleum Congress - Proceedings, Vol. 4, Applied Science Publishers Ltd., London, 1971, pp. 119-127.

25. Partington, J. and Parker, F., J. S. C. I., 75, (1919).

26. Scott, A. H., Trans. Inst. Chem. Engr., Vol. 13, p. 211, (1935).

27. Baker, T., Chilton, T. H. and Vernon, H. C., Trans. Am. Inst. Chem. Engr., Vol. 31, p. 296, (1935).

28. Schwartz, C. E. and Smith, J. M., "Flow Distribution in Packed Beds," I & EC, Vol. 45, No. 6, 1953, pp. 1209-1218.

29. Schiesser, W. E. and Lapidus, Leon, "Further Studies of Fluid Flow and Mass Transfer in Trickle Beds," AIChE J., Vol. 7, No. 1, 1961, pp. 163-171.

30. Glaser, M. B. and Lichtenstein, Ira, "Interrelation of Packing and Mixed Phase Flow Parameters with Liquid Residence Time Distribution," AIChE J., Vol. 9, 1963, pp. 30-34.

31. Wilhelm, R. H., "Progress Towards the a Priori Design of Chemical Reactors," Pure and Applied Chemistry, Vol. 5, 1962, pp. 403-421.

32. Satterfield, C. N., "Mass Transfer in Heterogeneous Catalysis," M. I. T. Press, Cambridge, Mass., 1970.

33. Schwartz, John G. and Roberts, George W., "An Evaluation of Models for Liquid Backmixing in Trickle Bed Reactors," I & EC Process Design and Development, Vol. 12, 1973, pp. 262-271.

34. Levenspiel, Octave and Smith, W. K., "Notes on the Diffusion-Type Model for the Longitudinal Mixing of Fluids in Flow," Chemical Engineering Science, Vol. 6, 1957, pp. 227-233.

35. Dean, H. A., "A Mathematical Model for the Dispersion in the Direction of Flow in Porous Media," Society of Petroleum Engineers Journal, Vol. 3, 1963, pp. 49-52.

36. Hoogendoorn, C. J. and Lips, J., "Axial Mixing of Liquid in Gas-Liquid Flow Through Packed Beds," The Canadian Journal of Chemical Engineering, Vol. 43, 1965, pp. 125-131.

37. Buffham, B. A., Gibilaro, H. G. and Rather, M. N., "A Probabilistic Time Delay Description of Flow in Packed Beds," AIChE J., Vol. 16, 1970, pp. 218-223.

38. Van Swaaij, W. P. M., Charpentier, J. C. and Villermaux, J., "Residence Time Distribution in the Liquid Phase of Trickle Flow in Packed Columns," Chemical Engineering Science, Vol. 24, 1969, pp. 1083-1095.

39. Furzer, I. A. and Mitchell, R. W., "Liquid Phase Dispersion in Packed Beds with Two-Phase Flow," AIChE J., Vol. 16, No. 3, 1970, pp. 380-385.

40. Hockman, Jack M. and Effron, Edward, "Two-Phase Cocurrent Downflow in Packed Beds," I & EC Fundamentals, Vol. 8, No 1, 1969, pp. 63-71.

41. Sater, V. E. and Levenspiel, Octave, "Two-Phase Flow in Packed Beds," I & EC Fundamentals, Vol. 5, No. 1, 1969, pp. 86-92.

42. Mears, D. E., "The Role of Axial Dispersion in Trickle-Flow Laboratory Reactors," Chemical Engineering Science, Vol. 26, 1971, p. 1361.

43. Mears, D. E., "The Role of Liquid Holdup and Effective Wetting in the Performance of Trickle-Bed Reactors," Advances in Chemistry Series, No. 133, 1974, pp. 218-227.

44. Ma, Y. H., Satterfield, C. N. and Sherwood, T. K., "The Effectiveness Factor in a Liquid-Filled Porous Catalyst," Inst. Chem. Engr. Symp. Ser. No. 28, Inst. Chem. Engrs., London, 1968, p. 22.

45. Van Deemter, J. J., "Trickle Hydrodesulfurization - A Case History," Third Equropean Symposium on Chemical Reaction Engineering, 1964, p. 215.

46. Adlington, D. and Thompson, E., "Desulfurization in Fixed and Fluidized Bed Catalyst Systems," Third European Symposium on Chemical Reaction Engineering, 1964, p. 203.

47. Van Zoonen, D. and Douwes, C., "Effect of Pellet Pore Structure on Catalyst Performance in Hydrodesulfurization of Straight-Run Gas Oil," J. Inst. Petroleum, Vol. 49, 1963, p. 383.

48. Henry, H. C. and Gilbert, J. B., "Scale Up of Pilot Plant Data for Catalytic Hydroprocessing," I & EC Process Design and Development, Vol. 12, 1973, p. 328.

49. Sedriks, W. and Kenney, C. N., "Partial Wetting in Trickle Bed Reactors - The Reduction of Cronoaldehyde Over a Palladium Catalyst," Chemical Engineering Science, Vol. 28, 1973, pp. 559-568.

50. Puranik, S. S. and Vogelpohl, A., "Effective Interfacial Area in Irrigated Packed Columns," Chemical Engineering Science, Vol. 29, 1974, p. 501.

51. Sylvester, N. D. and Pitayagulsarn, Punya, "Effect of Catalyst Wetting on Conversion in a Trickle Bed Reactor," The Canadian Journal of Chemical Engineering, Vol. 52, 1974, p. 539.

52. Wan, K. T., M. S. Thesis, Oklahoma State University, Stillwater, Oklahoma, May 1972.

53. Jones, J. and Friedman, "Char Oil Energy Development - Final Report," R&D Report No. 56, U. S. Department of the Interior, Office of Coal Research, 1972.

54. Byrns, A. C., Bradley, W. E. and Lee, M. W., "Catalytic Desulfurization of Gasolines by Cobalt Molybdate Process," I & EC, Vol. 35, No. 11, 1953, pp. 1160-1167.

55. Gwin, G. T., Heinrich, R. L., Hoffmann, E. J., Manne, R. S., Meyer, M. W. H., Miller, J. R. and Thorpe, C. L., "Hydrogenation of Asphalt for Fuel Products," I & EC, Vol. 49, No. 4, 1957, pp. 668-672.

56. Berg, C., Bradley, W. E., Stirton, R. I., Fairfield, R. G., Leflert, C. B. and Ballard, J. H., Trans, Am. Inst. Chem. Engr., Vol. 43, 1972, p. 1.

57. Stevenson, D. H. and Heinemann, Heinz, "Residuum Hydrocracking," I & EC, Vol. 49, No. 4, 1957, pp. 664-667.

58. Frost, C. M. and Cottingham, P. L., U. S. Bureau of Mines, Report of Investigation, 7464, (1971).

59. Gregoli, A. A. and Hartos, G. R., "Hydrodesulfurization of Residuals," Advances in Chemistry Series, No. 127, 1973, pp. 98-104.

60. Schmid, B. K. and Beuther, H., Sixth World Petroleum Congress, Section VII, 1963, p. 233.

61. Sooter, M. C., Ph. D. Dissertation, Oklahoma State University, Stillwater, Oklahoma, May 1974.

62. Hoog, H., Klinkert, H. G. and Schaafsma, A., "New Shell Hydrodesulfurization Process Shows," Petroleum Refiner, Vol. 32, No. 5, 1953, pp. 137-141.

63. Qader, S. A. and Hill, G. R., "Catalytic Hydrocracking -- Hydrocracking of a low Temperature Coal Tar," I & EC Process Design and Development, Vol. 8, No. 4, 1969, pp. 450-455.

64. Qader, S. A. and Hill, G. R., "Catalytic Hdrocracking -- Mechanism of Hydrocracking of Low Temperature Coal Tar," I & EC Process Design and Development, Vol. 8, No. 4, 1969, pp. 456-461.

65. Qader, S. A. and Hill, G. R., "Production of Low Sulfur Fuel Oils from Utah Coals," Advances in Chemistry Series, No. 127, 1973, pp. 91-97.

66. U. S. Patent No. 3,686,095.

67. Wilson, W. A., Voreck, W. E. and Malo, R. V., I & EC, Vol. 49, 1957, p. 657.

68. Frost, C. M. and Cottingham, P. L., U. S. Bureau of Mines, Report of Investigations, 7418, (1970).

69. Frye, C. G. and Mosby, J. F., "Kinetics of Hydrodesulfurization," Chemical Engineering Progress, Vol. 63, No. 9, 1967, pp. 66-70.

70. Bridge, A. G., Scott, J. W. and Reed, E. M., "Resid Hydroprocessing Options Multiply with New Technology," The Oil & Gas J., Vol. 73, May 19, 1975, pp. 94-100.

71. Reed, E. M., Tamm, P. W. and Goldstein, R. F., "HDS Goes Deeper into Barrel Bottoms," The Oil & Gas J., Vol. 70, July 17, 1972, pp. 103-108.

72. Karanth, N. G. and Hughes, R., "Temperature and Concentration Gradients in a Catalyst Packed Bed Reactor," Advances in Chemistry Series, No. 133, 1974, pp. 449-462.

73. McGreavy, C. and Soliman, M. A., "Stability of a Catalyst Particle Under Periodic Variations in Temperature and Concentration," The Chemical Engineering Journal, Vol. 6, 1973, pp. 99-106.

74. Cecil, R. R., Mayer, F. X. and Cart, E. N., "Fuel Oil Hydrodesulfurization Studies in Pilot Plant Reactors," Paper Presented at AIChE Meeting, Los Angeles, 1968.

75. Yitzhaki, Dan and Aharoni, Chain, "Hydrodesulfurization of Gas Oil, Reaction Rates in Narrow Boiling Range Fractions," AIChE J., Vol. 23, No. 3, 1977, pp. 342-346.

76. Qader, S. A., Wiser, W. H. and Hill, G. R., "Kinetics of Hydroremoval of Sulfur, Oxygen, and Nitrogen from a Low Temperature Coal Tar," I & EC Process Design and Development, Vol. 7, No. 3, 1968, pp. 390-397.

77. Aboul-Gheit, Ahmed K. and Abdou, Ismail K., "Catalytic HDS of Petroleum Distillate Fractions Under Hydrotreating Conditions," Egypt J. of Chemistry, Vol. 18, 1975, pp. 87-97.

78. Lee, H. C. and Butt, J. B., "Kinetics of Desulfurization of Thiophene: Reactions of Thiophene and Butene," J. of Catalysis, Vol. 49, Sept. 1977, pp. 320-331.

79. Hargreaves, Anthony E. and Ross, Julian R. H., "An Investigation of the Mechanism of the Hydrodesulphurization of Thiophene Over Sulphided Co-Mo-Al_2O_3 Catalysts. Part I. The Activation of the Catalysts and the Effect of Co-Mo Ratio on the Activity and Selectivity," Proceedings of the Sixth International Congress on Catalysis, Vol. 2, 1976, pp. 937-950.

80. Bartsch, R. and Tanielian, C., "Hydrodesulfurization II. Hydrogenolysis of Benzothiophene and Dibenzothiophene Over Prereduced Fe_2O_3-Al_2O_3 Catalysts," J. of Catalysis, Vol. 50, Oct. 1977, pp. 35-42.

81. Bruijn, Arie De, "Testing of HDS Catalysts in Small Trickle Phase Reactors," Proceedings of the Sixth International Congress on Catalysis, Vol. 2, 1976, pp. 951-964.

82. Morooka, S. and Hamrin, Charles E., Jr., "Desulfurization of Model Coal Sulfur Compounds by Coal Mineral Matter and a Cobalt Molybdate Catalyst - Thiophene," Chemical Engineering Science, Vol. 32, 1977, pp. 125-133.

83. Phillipson, J. J., "Kinetics of Hydrodesulfurization of Light and Middle Distillates," Paper Presented at AIChE Meeting, Houston, 1971.

84. Johnson, A. R., Wolk, R. H., Hippeli, R. F. and Nongbri, G., "H-Oil Desulfurization of Heavy Fuels," Advances in Chemistry Series, No. 127, 1973, pp. 105-120.

85. Hisamitsu, T., Shite, Y., Maruyama, F., Yamane, M., Satomi, Y. and Ozaki, H., "Studies on Hydrodesulfurization of Heavy Distillates - Hydrogen Consumption and Reaction Kinetics," Bulletin of Japan Petroleum Institute, Vol. 18, 1976, pp. 146-152.

86. Yergey, Alfred L., et al., "Nonisothermal Kinetics Studies of the Hydrodesulfurization of Coal," I & EC Process Design and Development, Vol. 13, No. 3, 1974, pp. 233-240.

87. Hoog, H., J. Inst. Petrol., Vol. 36, p. 738 (1950).

88. Massagutov, R. M., Berg, G. A., Kulinich, G. M. and Kirillov, T. S., Proceedings of Seventh World Petroleum Congress, Vol. 4, 1976, p. 177.

89. Owens, P. J. and Amberg, C. H., "Thiophene Desulfurization by a Microreactor Technique," Advances in Chemistry Series, No. 33, 1961, p. 182.

90. Satterfield, C. N. and Roberts, G. W., "Kinetics of Thiophene Hydrogenolysis on a Cobalt Molybdate Catalyst," AIChE J., Vol. 14, 1968, p. 159.

91. Givens, E. N. and Venuto, P. B., "Hydrogenolysis of Benzo(b)thiophene and Related Intermediates over Cobalt Molybdena Catalyst," ACS, Div. of Petrol. Chem. Preprints, Vol. 15, No. 4, 1970, p. A183.

92. Rall, H. T., Thompson, C. J., Coleman, H. J. and Hopkins, R. L., U. S. Bureau of Mines, Separation and Identification Section, RP48A, 1970.

93. Akhtar, S., Sharkey, A. G., Jr., Shultz, J. L. and Yavorsky, P. M., "Organic Sulfur Compounds in Coal Hydrogenation Products," ACS, Div. of Fuel Chemistry Preprints, Vol. 19, No. 1, 1974, pp. 207-214.

94. Greenwood, Gil Jay, Ph. D. Dissertation, Oklahoma State University, Stillwater, Oklahoma, 1977.

95. Jewell, D. M., Ruberto, R. G. and Swansiger, J. T., "Sulfur Compounds in Petroleum: Isolation and Characteristics," ACS, Div. of Petroleum Chemistry Preprints, Vol. 20, No. 1, 1975, pp. 19-29.

96. Hammer, C. G. Bertil, "Selective Hydrogenation of Sulphur Compounds from Highly Unsaturated Cracked Gasoline," Third World Petroleum Congress - Proceedings, Section IV, 1951, p. 295.

97. Sinfelt, J. H., "Catalystic Specificity," AIChE J., Vol. 19, No. 4, 1973, pp. 673-683.

98. Kawa, W., Friedman, S., Wu, W. R., Frank, L. V. and Yavorsky, P. M., "Evaluation of Catalysts for Hydrodesulfurization and Liquefaction of Coal," ACS, Div. of Fuel Chemistry, Vol. 19, No. 1, 1974, pp. 192-208.

99. Kushiyama, S., Koinuma, Y., Aizawa, R., Kobayashi, S., Nishikata, H., Inoue, K., Simizu, Y. and Egi, K., "HDS of Residual Oil. The Effect of Chemical Composition of Catalyst on Removal of Sulfur, Vanadium, Nickle and Nitrogen," Sekiyu Gakkai Shi, Vol. 19, No. 12, 1976, pp. 1016-1021.

100. Parsons, Basil I. and Ternan, Marten, "The Hydrodesulphurization and Hydrocracking Activity of Some Supported Binary Metal Oxide Catalysts," Proceedings of the Sixth International Congress on Catalysts, Vol. 2, 1976, pp. 965-977.

101. Allessandrini, G., Cairati, L., Forzatti, P., Villa, P. C. and Trifiro, F., "Chemical, Structural and Catalytic Modifications of Pure and Doped Iron (III) Molybdate," J. of Less Common Metals, Vol. 54, No. 2, Aug. 1977, pp. 373-386.

102. U. S. Patent 2,890,162.

103. Newson, Esmond, "Catalyst Deactivation Due to Pore-Plugging by Reaction Products," I & EC Process Design and Development, Vol. 14, No. 1, 1975, pp. 27-33.

104. Richardson, James T., "Experimental Determination of Catalyst Fouling Parameters," I & EC Process Design and Development, Vol. 11, No. 1, 1972, pp. 8-14.

105. Gavalas, G. R., Hsu, G. C. and Sinfeld, J. H., "Estimation of Catalyst Deactivation Parameters from Operating Reactor Data," Chemical Engineering J., Vol. 4, 1972, pp. 77-84.

106. Fowler, Carl, "How Gulfining Works for Daikyo," Hydrocarbon Processing, Vol. 52, Sept. 1973, pp. 131-133.

107. Weekman, Vern W., Jr., "Laboratory Reactors and Their Limitations," AIChE J., Vol. 20, No. 5, Sept. 1974, pp. 833-840.

108. Instruction Manual for Model 240 Temperature Programmer, Hewlett Packard F & M Scientific Division, Avondale, Pennsylvania, 1971.

109. Instruction Manual for Model 900 Numeric Display, Leeds & Northrup Corp., North Wales, Pennsylvania, 1971.

110. LECO Automatic Sulfur Determinator Instruction Manual, Laboratory Equipment Corp., St. Joseph, Michigan, 1970.

111. Mitchell, P. C. H. and Trifiro, F., "The Effect of Sulfiding on the Structure of a Cobalt-Molybdenum-Alumina Hydrodesulfurization Catalyst," Journal of Catalysis, Vol. 33, 1974, pp. 350-354.

112. Pressure Control - Grove Mity Mite Regulator, Grove Valve & Regulator Co., Bulletin No. G-60, Oakland, California, 1970.

113. Ruska Proportioning Instruction Manual, Ruska Instrument Corp., Houston, Texas, 1971.

114. Wells, J. W., M. S. Thesis, Oklahoma State University, Stillwater, Oklahoma, May 1977.

115. Paraskos, J. A. , Frayer, J. A. and Shah, Y. T., "Effect of Holdup, Incomplete Catalyst Wetting and Backmixing During Hydroprocessing in Trickle Bed Reactors," I & EC Process Design and Development, Vol. 14, No. 3, 1975, pp. 315-322.

116. Perry, Robert H. and Chilton, Cecil H., "Chemical Engineers' Handbook," Fifth Edition, McGraw-Hill Book Company, Inc., New York, 1973.

117. Brunn, L. W., Montagna, A. A. and Paraskos, J. A., "Clean Residual Fuels from the Gulf HDS Process," Vol. 21, No. 1, 1976, pp. 173-197.

118. Office of Coal Research, "Development of a Process for Producing an Ashless, Low Sulfur Fuel from Coal," Interim Report No. 3, R & D Report No. 53, U. S. Department of the Interior, 1971.

119. Smith, J. M. and Van Ness, H. C., "Introduction to Chemical Engineering Thermodynamics," McGraw-Hill Book Company, Inc., New York, 1959.

120. Ueda, S., Shinichi, Y., Tadao, I., Kazuo, M. and Gen, T., "The Heat of Hydrodesulfurization Reaction of Heavy Oil," I & EC Process Design and Development, Vol. 14, No. 4, 1975, pp. 493-499.

121. Erbar, John H., Personal Communications, Aug.-Sept. 1975.

122. Sivasubramanian, R., Ph. D. Dissertation, Oklahoma State University, Stillwater, Oklahoma, May 1977.

123. Aoshima, A. and Wise, H., Journal of Catalyst, Vol. 34, 1974, pp. 145-151

124. Wilke, C. R., Chemical Engineering Progress, Vol. 35, 1949, pp. 218-224.

APPENDIX A

ANALYSIS OF FEED OIL FOR SULFUR CONTENT

The standard deviation of analysis was estimated according to the relationship shown below. The feed oil was analyzed eight times for sulfur concentration.

$$S = \sqrt{\frac{\sum_{n=1}^{k} (\delta x_n)^2}{(k-1)}}$$

where, S = standard deviation

k = number of data points

δx = deviation of estimated sulfur concentration value from the predetermined value by Sooter (61)

The results of the analytical work are presented below.

Predetermined %S in feed oil = 0.470

	%S, determined	δx, deviation	% deviation	$(\delta x)^2$
(i)	0.474	+ 0.004	+ 0.85	0.000016
(ii)	0.460	- 0.010	- 2.06	0.000100
(iii)	0.483	+ 0.013	+ 2.71	0.000169
(iv)	0.473	+ 0.003	+ 0.64	0.000009
(v)	0.467	- 0.003	- 0.64	0.000009
(vi)	0.476	+ 0.006	+ 1.28	0.000036
(vii)	0.464	- 0.006	- 1.28	0.000036
(viii)	0.456	- 0.014	- 2.98	0.000196
				$\Sigma = 0.000571$

$$S = \sqrt{\frac{0.000571}{(8-1)}} = \pm 0.00903$$

Therefore, standard deviation = 0.00903

and %S, average = 0.469

APPENDIX B

ANALYTICAL DATA

The product samples collected during the experimental runs were analyzed at least three times for sulfur content. The repeated analysis of each of the samples was performed to minimize the possibility of measurement errors. The data gathered during the analyses are presented in Table XXXIV with their averages and the standard deviations of measurement of each sample. The standard deviation of each sample was calculated based on the following formula.

$$S = \sqrt{\frac{\sum_{i=1}^{n} x_i^2 - n \cdot \bar{x}^2}{n - 1}}$$

where, S = standard deviation of measurement

x_i = determined sulfur value

n = number of data points

$\bar{x}$ = average sulfur content of the sample estimated as,

$$\bar{x} = \frac{\sum_{i=n}^{n} x_i}{n}$$

A typical calculation is shown on the following page.

Sample Number	x_i	x_i^2
ASP11	0.163	0.026569
	0.167	0.027889
	0.150	0.022500

$x_i = 0.480$ $x_i^2 = 0.076958$

$\overline{x} = 0.480/3 = 0.160$

$$S = \sqrt{\frac{0.076958 - 3 \cdot (0.160)^2}{2}}$$

$S = 0.00889$

TABLE XXXIV

ANALYTICAL DATA

Sample Number	Weight Percent Sulfur			Average	Standard Deviation
	(i)	(ii)	(iii)		
SP 1	0.130	0.136	0.133	0.133	0.00269
SP 2	0.100	0.102	0.104	0.102	0.00217
SP 3	0.072	0.071	0.073	0.072	0.00068
SP 4	0.073	0.078	0.077	0.076	0.00269
SP 5	0.068	0.064	0.071	0.067	0.00381
SP 6	0.082	0.084	0.080	0.082	0.00196
SP 7	0.076	0.113	0.120	0.103	0.02376
SP 8	0.147	0.166	0.144	0.152	0.01178
SP 9	0.179	0.180	0.171	0.177	0.00454
SP10	0.123	0.099	0.127	0.116	0.01482
SP11	0.108	0.109	0.114	0.110	0.00328
SP12	0.056	0.071	0.060	0.062	0.00802
SP13	0.062	0.073	0.067	0.067	0.00564
SP14	0.083	0.084	0.086	0.084	0.00134
SP15	0.106	0.101	0.093	0.100	0.00675
SP16	0.127	0.137	0.119	0.128	0.00883
SP17	0.132	0.134	0.118	0.128	0.00860
SP18	0.074	0.088	0.077	0.080	0.00743
SP19	0.056	0.056	0.055	0.055	0.00017
SP20	0.011	0.017	0.013	0.014	0.00301
SP21	0.008	0.015	0.017	0.013	0.00456
SP22	0.016	0.011	0.008	0.012	0.00411
SP23	0.009	0.005	0.008	0.007	0.00166
SP24	0.047	0.042	0.051	0.047	0.00453
SP25	0.049	0.039	0.044	0.044	0.00502
SP26	0.019	0.017	0.011	0.016	0.00418
SP27	0.018	0.019	0.015	0.017	0.00238
ASP 1	0.086	0.091	0.082	0.086	0.00451
ASP 2	0.123	0.095	0.117	0.112	0.01474
ASP 3	0.115	0.115	0.116	0.115	0.00058
ASP 4	0.115	0.121	0.124	0.120	0.00458
ASP 5	0.102	0.089	0.106	0.099	0.00889
ASP 6	0.121	0.119	0.106	0.115	0.00814
ASP 7	0.150*	0.130	0.124	0.127	0.01361
ASP 8	0.126	0.109	0.114	0.116	0.00874
ASP 9	0.072	0.055	0.064	0.064	0.00850
ASP10	0.099	0.122	0.115	0.112	0.01179
ASP11	0.163	0.167	0.150	0.160	0.00889
ASP12	0.122	0.123	0.127	0.124	0.00265
ASP13				NA	
ASP14	0.101	0.082	0.112	0.098	0.01518

TABLE XXXIV (continued)

Sample Number	Weight Percent Sulfur			Average	Standard Deviation
	(i)	(ii)	(iii)		
ASP15	0.100	0.097	0.072	0.099	0.01537
ASP16	0.121	0.143	0.138	0.134	0.01153
ASP17	0.108	0.110	0.106	0.108	0.00200
ASP18	0.111	0.094	0.107	0.104	0.00889
ASP19	0.102	0.103	0.105	0.103	0.00153
ASP20	0.147*	0.122	0.113	0.118	0.01762
ASP21	0.120	0.094	0.115	0.110	0.01380
ASP22	0.155	0.133	0.118	0.135	0.01861
ASP23	0.068	0.082	0.081	0.077	0.00781
ASP24	0.105	0.105	0.099	0.103	0.00346
ASP25	0.055	0.058	0.048	0.054	0.00513
ASP26	0.123	0.119	0.120	0.121	0.00208
ASP27	0.078	0.064	0.073	0.072	0.00709
ASP28	0.154	0.154	0.164	0.157	0.00577
ASP29	0.131	0.122	0.119	0.124	0.00624
ASP30	0.104	0.094	0.106	0.101	0.00643
ASP31	0.106	0.105	0.099	0.104	0.00379
ASP32	0.104	0.107	0.114	0.108	0.00513
ASP33	0.053	0.068	0.055	0.059	0.00814
ASP34	0.107	0.106	0.118	0.110	0.00666
ASP35	0.072	0.072	0.062	0.069	0.00577
ASP36	0.161*	0.125	0.136	0.130	0.01845
ASP37	0.122	0.098	0.115	0.112	0.01234
ASP38	0.125	0.123	0.112	0.120	0.00700
ASP39	0.116	0.105	0.117	0.113	0.00666
ASP40	0.082	0.087	0.092	0.087	0.00500
NLA 1	0.115	0.117	0.121	0.118	0.00306
NLA 2	0.128	0.119	0.111	0.119	0.00850
NLA 3	0.075	0.084	0.083	0.081	0.00493
NLA 4	0.147	0.146	0.135	0.143	0.00666
NLA 5	0.085	0.083	0.085	0.084	0.00115
NLA 6	0.107	0.121	0.101	0.110	0.01026
NLA 7	0.111	0.125	0.109	0.115	0.00872
NLA 8	0.114	0.107	0.111	0.111	0.00351
NLA 9	0.108	0.108	0.105	0.107	0.00681
NLA10	0.119	0.094	0.109	0.107	0.01258
NLA11	0.116	0.116	0.114	0.115	0.00115
NLA12	0.122	0.110	0.118	0.117	0.00611
NLA13	0.080	0.082	0.077	0.080	0.00252
NLA14	0.093	0.098	0.102	0.098	0.00451
NLA15	0.074	0.077	0.073	0.075	0.00208
NLA16	0.100	0.103	0.096	0.100	0.00351
NLA17	0.077	0.090	0.075	0.081	0.00814

TABLE XXXIV (continued)

Sample Number	Weight Percent Sulfur			Average	Standard Deviation
	(i)	(ii)	(iii)		
NLA18	0.103	0.089	0.095	0.096	0.00702
NLA19	0.092	0.096	0.092	0.093	0.00321
NLA20	0.085	0.094	0.089	0.089	0.00451
NLA21	0.077	0.086	0.077	0.080	0.00520
NLA22	0.076	0.085	0.062	0.074	0.01159
NLA23	0.087	0.075	0.081	0.081	0.00600
NLA24	0.067	0.074	0.069	0.070	0.00361
NLA25	0.076	0.072	0.067	0.072	0.00451
NLA26	0.101	0.098	0.105	0.101	0.00351
NLA27	0.075	0.073	0.076	0.075	0.00153
NLA28	0.110	0.113	0.099	0.107	0.00737
NLA29	0.091	0.087	0.083	0.087	0.00400
NLA30	0.081	0.083	0.080	0.081	0.00153
NLA31	0.082	0.089	0.093	0.088	0.00557
NLA32	0.094	0.083	0.088	0.088	0.00551
NLA33	0.075	0.075	0.072	0.074	0.00173
NLA34	0.073	0.081	0.075	0.076	0.00416
NLA35	0.098	0.100	0.099	0.099	0.00100
NLA36	0.098	0.090	0.098	0.095	0.00462
NLA37	0.082	0.077	0.076	0.078	0.00321
NLA38	0.098	0.092	0.098	0.096	0.00346
NLA39	0.094	0.103	0.098	0.098	0.00451
NLA40	0.088	0.086	0.085	0.086	0.00153
NLA41	0.062	0.058	0.058	0.059	0.00231
ANA 1	0.179	0.163	0.152	0.165	0.01358
ANA 2	0.158	0.155	0.156	0.156	0.00153
ANA 3	0.148	0.139	0.138	0.142	0.00551
ANA 4	0.159	0.153	0.154	0.155	0.00321
ANA 5	0.181	0.163	0.142	0.163	0.01952
ANA 6	0.184	0.186	0.198	0.189	0.00757
ANA 7	0.178	0.174	0.189	0.180	0.00777
ANA 8	0.124	0.120	0.124	0.123	0.00231
ANA 9	0.090	0.075	0.084	0.083	0.00755
ANA10	0.113	0.106	0.091	0.103	0.01124
ANA11	0.105	0.102	0.108	0.105	0.00300
ANA12	0.114	0.108	0.113	0.112	0.00321
ANA13	0.103	0.094	0.092	0.096	0.00586
ANA14	0.167*	0.122	0.130	0.126	0.02401
ANA15	0.120	0.110	0.101	0.110	0.00950
ANA16	0.111	0.095	0.097	0.101	0.00872
ANA17	0.107	0.097	0.102	0.102	0.00500
ANA18	0.149	0.105	0.076	0.110	0.03676
ANA19	0.141	0.137	0.133	0.137	0.00400

TABLE XXXIV (continued)

Sample Number	Weight Percent Sulfur			Average	Standard Deviation
	(i)	(ii)	(iii)		
ANA20	0.133	0.114	0.118	0.122	0.01002
ANA21	0.132	0.125	0.126	0.128	0.00379
ANA22	0.120	0.130	0.126	0.125	0.00503
ANA23	0.115	0.113	0.106	0.111	0.00473
ANA24	0.112	0.103	0.111	0.109	0.00493
ANA25	0.161	0.158	0.135	0.151	0.01422
ANA26	0.126	0.110	0.092	0.109	0.01701
ANA27	0.139	0.138	0.135	0.137	0.00208
ANA28	0.123	0.118	0.117	0.120	0.00321
ANA29	0.149	0.140	0.129	0.139	0.01002
ANA30	0.114	0.123	0.109	0.115	0.00709
ANA31	0.136	0.148	0.123	0.136	0.01250
ANA32	0.090	0.096	0.100	0.095	0.00503
ANA33	0.138	0.139	0.129	0.135	0.00551
ANA34	0.112	0.111	0.122	0.115	0.00608
ANA35	0.099	0.113	0.110	0.107	0.00737
ANA36	0.123	0.119	0.133	0.125	0.00721
ANA37	0.158	0.145	0.121	0.141	0.01877
ANA38	0.115	0.118	0.117	0.117	0.00153
ANA39	0.117	0.100	0.100	0.106	0.00981
ANA40	0.095	0.095	0.101	0.097	0.00346
HSW 1	0.153	0.155	0.149	0.152	0.00306
HSW 2	0.155	0.153	0.155	0.154	0.00115
HSW 3	0.129	0.130	0.126	0.128	0.00208
HSW 4	0.134	0.138	0.134	0.135	0.00231
HSW 5	0.105*	0.170	0.177	0.174	0.03970
HSW 6	0.150	0.167	0.163	0.160	0.00889
HSW 7	0.155	0.124	0.127	0.122	0.00624
HSW 8	0.141	0.151	0.156	0.149	0.00764
HSW 9	0.115	0.111	0.105	0.110	0.00503
HSW10	0.132	0.123	0.127	0.127	0.00451
HSW11	0.108	0.121	0.114	0.114	0.00651
HSW12	0.109	0.106	0.098	0.104	0.00569
HSW13	0.195	0.197	0.191	0.194	0.00306
HSW14	0.144	0.158	0.168	0.157	0.01206
HSW15	0.201	0.195	0.198	0.198	0.00300
HSW16	0.187	0.175	0.185	0.182	0.00643
HSW17	0.205	0.203	0.207	0.205	0.00200
HSW18	0.193	0.159	0.157	0.170	0.02023
HSW19	0.220	0.214	0.229	0.221	0.00755
HSW20	0.160	0.154	0.155	0.156	0.00321
HSW21	0.125	0.119	0.119	0.121	0.00346
HSW22	0.108	0.102	0.103	0.104	0.00321

TABLE XXXIV (continued)

Sample Number	Weight Percent Sulfur			Average	Standard Deviation
	(i)	(ii)	(iii)		
HSW23	0.142	0.139	0.143	0.141	0.00208
HSW24	0.119	0.111	0.111	0.114	0.00462
HSW25	0.117	0.180	0.167	0.175	0.00681
HSW26	0.151	0.161	0.165	0.159	0.00721
HSW27	0.209	0.222	0.219	0.217	0.00681
HSW28	0.168	0.207	0.201	0.192	0.02100
HSW29	0.134	0.133	0.132	0.133	0.00100
HSW30	0.099	0.096	0.110	0.102	0.00737
HSW31	0.093	0.091	0.082	0.089	0.00586
HSW32	0.070	0.096	0.092	0.086	0.01400
HSW33	0.133	0.148	0.140	0.140	0.00751
HSW34	0.107	0.130	0.119	0.119	0.01150
HSW35	0.155	0.162	0.152	0.156	0.00513
HSW36	0.136	0.117	0.120	0.124	0.01021
HSW37	0.180	0.170	0.174	0.175	0.00503
HSW38	0.101	0.118	0.117	0.112	0.00954
HSW39	0.116	0.113	0.118	0.116	0.00252
HSW40	0.095	0.084	0.084	0.088	0.00635
HSW41	0.159	0.161	0.159	0.160	0.00115
HSW42	0.044	0.047	0.057	0.049	0.00681
HSW43	0.052	0.066	0.059	0.059	0.00700
HSW44	0.054	0.060	0.067	0.060	0.00651
HSW45	0.082	0.085	0.095	0.087	0.00681
HSW46	0.133	0.116	0.130	0.126	0.00907
HSW47	0.112	0.113	0.122	0.116	0.00551
HSW48	0.143	0.143	0.144	0.143	0.00058
HSW49	0.089	0.091	0.093	0.091	0.00200
HSW50	0.048	0.062	0.024	0.045	0.01922
HSW51	0.079	0.075	0.060	0.071	0.01002
HSW52	0.083	0.085	0.088	0.085	0.00252
HSW53	0.072	0.063	0.057	0.064	0.00755
HSW54	0.038	0.046	0.031	0.038	0.00751
HSW55	0.092	0.085	0.082	0.083	0.00513
HSW56	0.085	0.087	0.109	0.094	0.01332
HSW57	0.131	0.119	0.119	0.123	0.00693
HSW58	0.092	0.088	0.095	0.091	0.00351
HSW59	0.110	0.107	0.126	0.114	0.01021
HSW60	0.064	0.065	0.066	0.065	0.00100
HSW61	0.043	0.052	0.054	0.050	0.00586
HSW62	0.054	0.043	0.054	0.050	0.00635
HSW63	0.069	0.066	0.057	0.064	0.00624
HSW64	0.036	0.027	0.033	0.032	0.00458
HSW65	0.069	0.058	0.063	0.063	0.00551

TABLE XXXIV (continued)

Sample Number	Weight Percent Sulfur			Average	Standard Deviation
	(i)	(ii)	(iii)		
HSW66	0.059	0.053	0.054	0.057	0.00321
HRW 1	0.188	0.171	0.172	0.177	0.00954
HRW 2	0.137	0.137	0.134	0.136	0.00173
HRW 3	0.175	0.154	0.167	0.165	0.01060
HRW 4	0.201	0.192	0.198	0.197	0.00458
HRW 5	0.187	0.181	0.178	0.182	0.00458
HRW 6	0.167	0.175	0.176	0.173	0.00493
HRW 7	0.124	0.153	0.159	0.131	0.00889
HRW 8	0.156	0.153	0.159	0.156	0.00300
HRW 9	0.148	0.147	0.159	0.151	0.00666
HRW10	0.163	0.145	0.156	0.155	0.00907
HRW11	0.142	0.147	0.146	0.145	0.00265
HRW12	0.159	0.130	0.158	0.149	0.01646
HRW13	0.156	0.150	0.152	0.153	0.00306
HRW14	0.159	0.149	0.135	0.148	0.01206
HRW15	0.135	0.142	0.145	0.142	0.00513
HRW16	0.133	0.132	0.134	0.133	0.00100
HRW17	0.139	0.138	0.137	0.138	0.00100
HRW18	0.119	0.123	0.127	0.123	0.00400
HRW19	0.157	0.133	0.156	0.149	0.01358
HRW20	0.145	0.125	0.126	0.140	0.00500
HRW21	0.143	0.125	0.126	0.131	0.01012
HRW22	0.145	0.145	0.159	0.150	0.00808
HRW23	0.144	0.147	0.132	0.141	0.00794
HRW24	0.139	0.151	0.136	0.142	0.00794
HRW25	0.144	0.130	0.126	0.133	0.00945
HRW26	0.134	0.131	0.154	0.140	0.01250
HRW27	0.135	0.137	0.134	0.135	0.00153
HRW28	0.141	0.125	0.141	0.135	0.00924
HRW29	0.126	0.145	0.128	0.133	0.01044
HRW30	0.150	0.122	0.132	0.135	0.01419
HRW31	0.127	0.136	0.121	0.128	0.00755
HRW32	0.110	0.133	0.121	0.121	0.01150
HRW33	0.128	0.126	0.126	0.127	0.00115
HRW34	0.128	0.127	0.129	0.128	0.00100
HRW35	0.123	0.132	0.122	0.128	0.00551
HRW36	0.118	0.117	0.136	0.123	0.01069
HRW37	0.123	0.123	0.124	0.123	0.00058
HRW38	0.143	0.143	0.124	0.137	0.01097
HRW39	0.135	0.132	0.108	0.125	0.01480
HRW40	0.151	0.167	0.159	0.159	0.00800
NAL 1	0.147	0.155	0.155	0.152	0.00462
NAL 2	0.102	0.117	0.118	0.112	0.00896

TABLE XXXIV (continued)

Sample Number	Weight Percent Sulfur			Average	Standard Deviation
	(i)	(ii)	(iii)		
NAL 3	0.114	0.100	0.106	0.107	0.00702
NAL 4	0.113	0.108	0.107	0.109	0.00321
NAL 5	0.153	0.128	0.149	0.143	0.01343
NAL 6	0.120	0.117	0.129	0.122	0.00625
NAL 7	0.150	0.123	0.130	0.134	0.01401
NAL 8	0.188	0.193	0.173	0.185	0.01041
NAL 9	0.117	0.111	0.118	0.115	0.00379
NAL10	0.083	0.090	0.092	0.088	0.00473
NAL11	0.142	0.135	0.139	0.139	0.00351
NAL12	0.099	0.113	0.113	0.108	0.00808
NAL13	0.134	0.145	0.149	0.143	0.00777
NAL14	0.155	0.168	0.165	0.163	0.00681
NAL15	0.174	0.171	0.173	0.173	0.00153
NAL16	0.170	0.182	0.172	0.175	0.00643
NAL17	0.203	0.193	0.210	0.202	0.00854
NAL18	0.215	0.220	0.211	0.215	0.00451
NAL19	0.124	0.133	0.134	0.130	0.00551
NAL20	0.112	0.100	0.112	0.108	0.00693
NAL21	0.112	0.119	0.124	0.118	0.00603
NAL22	0.074	0.068	0.065	0.069	0.00458
NAL23	0.044	0.057	0.042	0.048	0.00814
NAL24	0.085	0.095	0.097	0.092	0.00643
NAL25	0.138	0.143	0.145	0.142	0.00361
NAL26	0.066	0.065	0.066	0.066	0.00058
NAL27	0.071	0.060	0.073	0.068	0.00700
NAL28	0.105	0.101	0.108	0.105	0.00351
NAL29	0.105	0.119	0.110	0.111	0.00709
NAL30	0.099	0.097	0.109	0.102	0.00643
NAL31	0.094	0.091	0.104	0.096	0.00681
NAL32	0.041	0.042	0.039	0.041	0.00153
NAL33	0.060	0.067	0.066	0.064	0.00379
NAL34	0.041	0.044	0.041	0.042	0.00173
NAL35	0.029	0.023	0.022	0.025	0.00379
NAL36	0.037	0.040	0.042	0.040	0.00252
NAL37	0.128	0.113	0.122	0.121	0.00755
NAL38	0.046	0.047	0.040	0.044	0.00379
NAL39	0.180	0.194	0.174	0.183	0.01026
NAL40	0.106	0.106	0.111	0.108	0.00289
NAL41	0.056	0.047	0.047	0.050	0.00520
NAL42	0.040	0.046	0.032	0.039	0.00702
NAL43	0.033	0.037	0.045	0.038	0.00611
NAL44	0.046	0.021	0.035	0.034	0.01253
NAL45	0.068	0.055	0.062	0.062	0.00651

TABLE XXXIV (continued)

Sample Number	Weight Percent Sulfur			Average	Standard Deviation
	(i)	(ii)	(iii)		
NAC 1	0.114	0.087	0.100	0.100	0.01350
NAC 2	0.078	0.077	0.076	0.077	0.00100
NAC 3	0.064	0.062	0.065	0.064	0.00153
NAC 4	0.067	0.077	0.068	0.071	0.00551
NAC 5	0.078	0.072	0.081	0.077	0.00458
NAC 6	0.074	0.063	0.082	0.073	0.00954
NAC 7	0.084	0.081	0.092	0.086	0.00569
NAC 8	0.110	0.147*	0.106	0.108	0.02261
NAC 9	0.083	0.086	0.080	0.083	0.00300
NAC10	0.087	0.096	0.074	0.086	0.01106
NAC11	0.087	0.073	0.084	0.081	0.00737
NAC12	0.071	0.077	0.069	0.072	0.00416
NAC13	0.219*	0.126	0.130	0.128	0.00283
NAC14	0.077	0.073	0.068	0.073	0.00451
NAC15	0.078	0.078	0.078	0.078	0.00000
NAC16	0.088	0.077	0.068	0.078	0.01002
NAC17	0.086	0.091	0.072	0.083	0.00985
NAC18	0.067	0.082	0.080	0.076	0.00814
NAC19	0.062	0.065	0.069	0.065	0.00351
NAC20	0.101	0.078	0.102	0.094	0.01358
NAC21	0.086	0.094	0.087	0.089	0.00436
NAC22	0.092	0.083	0.084	0.086	0.00493
NAC23	0.092	0.085	0.081	0.086	0.00557
NAC24	0.069	0.063	0.079	0.070	0.00808
NAC25	0.081	0.084	0.084	0.083	0.00173
NAC26	0.078	0.069	0.064	0.070	0.00709
NAC27	0.078	0.100	0.093	0.090	0.01124
NAC28	0.078	0.075	0.072	0.075	0.00300
NAC29	0.093	0.086	0.089	0.089	0.00351
NAC30	0.051	0.059	0.068	0.059	0.00850
NAC31	0.055	0.051	0.052	0.053	0.00208
NAC32	0.055	0.066	0.057	0.059	0.00586
NAC33	0.050	0.051	0.058	0.053	0.00436
NAC34	0.063	0.061	0.057	0.060	0.00306
NAC35	0.069	0.063	0.062	0.065	0.00379
NAC36	0.051	0.052	0.058	0.054	0.00379
NAC37	0.105	0.097	0.087	0.096	0.00902
NAC38	0.061	0.065	0.062	0.063	0.00208
NAC39	0.085	0.069	0.083	0.079	0.00872
NAC40	0.072	0.072	0.075	0.073	0.00173

*not included for averaging

APPENDIX C

CALCULATIONS FOR PORE SIZE DISTRIBUTION CURVES

Mercury penetration tests were conducted on each of the five catalysts used in the HDS studies to estimate pore size distribution. The mercury penetration tests were performed by American Instrument Company. The results of their tests are presented in terms of intrusion versus the exerted pressure as shown in Table XXXV.

The mercury penetration data from Table XXXV were used to calculate the pore size distribution of the respective catalysts. The pressure is inversely proportional to the pore radius, and the frequency of occurrance of a pore size is directly proportional to the change in cummulative volume. The cummulative volume at a given pressure for a catalyst is the difference between the maximum intrusion for the catalyst and the intrusion at the desired pressure. The sample calculation steps for pore size distribution are shown in Table XXXVI. The frequency of pores of a given size ($\Delta V/\Delta \ln r$) was then plotted against log of pore radius ($\ln r$) for each catalyst to generate Figures 18-22.

TABLE XXXV

MERCURY PENETRATION DATA

MCM 1 Catalyst		MCM 2 Catalyst		MCM 3 Catalyst		MCM 4 Catalyst		MCM 5 Catalyst	
Absolute Pressure psia	Intrusion cc/gm	Absolute Pressure psia	Intrusion cc/gm	Absolute Pressure psia	Intrusion cc/gm	Absolute Pressure psia	Intrusion cc/gm	Absolute Pressure psia	Intrusion cc/gm
1.8	0.000	1.8	0.000	1.8	0.000	1.8	0.000	1.8	0.000
9.9	0.000	9.9	0.000	9.9	0.005	9.9	0.006	9.9	0.004
250	0.003	49.9	0.004	49.9	0.009	500	0.006	1000	0.004
500	0.007	250	0.011	159.9	0.019	1500	0.011	3000	0.007
600	0.023	500	0.019	500	0.028	5000	0.011	10000	0.011
800	0.081	1200	0.022	2500	0.033	10000	0.011	15000	0.021
1000	0.143	2500	0.030	5000	0.038	15000	0.023	19000	0.113
1200	0.196	5000	0.049	10000	0.038	17000	0.074	20000	0.201
1500	0.238	10000	0.060	15000	0.047	18000	0.130	21000	0.257
2500	0.290	15000	0.078	25000	0.052	20000	0.216	23000	0.331
4000	0.326	20000	0.105	30000	0.075	24000	0.284	25000	0.381
7000	0.371	23000	0.161	32000	0.141	30000	0.346	30000	0.469
10000	0.411	25000	0.213	34000	0.216	35000	0.391	35000	0.511
15000	0.502	27000	0.272	36000	0.291	40000	0.414	40000	0.518
20000	0.609	30000	0.347	38000	0.343	50000	0.431	50000	0.525
24000	0.701	35000	0.418	40000	0.375	60000	0.431	60000	0.525
28000	0.785	40000	0.448	45000	0.418				
32000	0.857	50000	0.463	50000	0.432				
40000	0.935	60000	0.463	60000	0.441				
50000	0.974								
60000	0.981								

TABLE XXXVI

CALCULATIONS FOR PORE SIZE DISTRIBUTION CURVE
MCM 5 CATALYST

V Cumulative	ΔV	r	ln r	Δ ln r	$\frac{\Delta V}{\Delta \ln r}$
0.525		486000	13.09		
	0.004			1.70	0.0024
0.521		88400	11.39		
	0.000			4.60	0.0000
0.521		875	6.79		
	0.003			1.10	0.0027
0.518		292	5.69		
	0.004			1.22	0.0033
0.514		87.5	4.47		
	0.010			0.41	0.0244
0.504		58.3	4.06		
	0.092			0.23	0.4000
0.412		46.1	3.83		
	0.088			0.05	1.7600
0.324		43.7	3.78		
	0.056			0.05	1.1200
0.268		41.7	3.73		
	0.074			0.09	0.8222
0.194		38.0	3.64		
	0.050			0.08	0.6250
0.144		35.0	3.56		
	0.088			0.18	0.4889
0.056		29.2	3.38		
	0.042			0.16	0.2625
0.014		25.0	3.22		
	0.007			0.14	0.0500
0.007		21.9	3.08		
	0.007			0.22	0.0318
0.000		17.5	2.86		
	0.000			0.18	0.0000
0.000		14.6	2.68		

APPENDIX D

ESTIMATION OF THE GAS PRODUCED IN THE REACTOR

In this experimental study, the rate of gas going out of the reactor was measured on a wet test meter. The hydrogen flow rate at the entrance of the reactor was not measured because of the high pressure conditions. Therefore, the amount of gas produced from the gasified oil and the amount of hydrogen consumed in the various heterogeneous reactions calculated in Appendix E are necessary to estimate hydrogen entering the reactor. The literature (118) indicates that the assumption of 5% of the feedstock vaporized is reasonable, and thus, it is used below to estimate the amount of gas produced.

The maximum oil flow rate employed = 80 cc/hr

Oil flow rate = 80 cc/hr/(1.595 x 10^5 cc/Bbl) = 5.02 x 10^{-4} Bbl/hr

Amount of oil vaporized = 80 cc/hr x 1.13 gm/cc x 0.05 = 4.5 gms/hr

Assuming* the molecular weight of oil to be 28.6

Amount of vapor produced = 4.5 gm/hr/(28.6 gm/mole) = 0.152 gm-mole/hr

= 3.32 x 10^{-4} lb-mole/hr = 0.120 scf/hr

= 0.120 scf/hr/(5.02 x 10^{-4} Bbl/hr)

= <u>238 scf/Bbl</u>

*Gas produced and its molecular weight, from literature (118)

Component	Production Rate, tpd	Contribution to Average Molecular Weight (MW)
CO_2	259	2.47
H_2S	913	6.73
C_1	1903	6.60
C_2	830	5.39
C_3	483	4.60
C_4	224	2.80
	4612	Average = 28.59

APPENDIX E

ESTIMATION OF HYDROGEN CONSUMPTION FROM KNOWN HETEROGENEOUS REACTIONS

There are primarily five reactions during HDS in which the hydrogen gas is consumed, viz. sulfur removal, nitrogen removal, oxygen removal, vaporization, and hydrocracking. The hydrogen consumption in each of these reactions is estimated separately and added together to obtain the total hydrogen consumption.

(i) Sulfur Removal:

Initial concentration in feed oil = 0.47% by weight

Final concentration in product oil = 0.09% by weight

Sulfur removal = 0.38% by weight

= 0.0038 gm S/gm oil

= 0.000119 gm-mole S/gm oil

= 0.0428 lb-mole S/Bbl oil

H_2 consumption rate @ 1 mole H_2/mole S removed

= 0.0428 lb-mole/Bbl oil

= 16.2 scf/Bbl

(ii) Nitrogen Removal:

Nitrogen removal = 0.50% = 0.0050 gm N_2/gm oil

= 0.000179 gm-mole N_2/gm oil

= 0.0644 lb-mole N_2/Bbl oil

H_2 consumption rate @ 3 mole H_2/mole N_2 removed

= 0.193 lb-mole/Bbl oil

= 73.1 scf/Bbl

(iii) Oxygen Removal:

Oxygen removal (assume 2%) = 0.02 gm O_2/gm oil

= 0.000625 gm-mole O_2/gm oil

= 0.225 lb-mole O_2/Bbl oil

H_2 consumption rate @ 1/2 mole H_2/mole O_2 removed

= 0.1125 lb-mole/Bbl

= 42.6 scf/Bbl

(iv) Gas Production:

Gas produced = 238 scf/Bbl (from Appendix D)

H_2 consumption rate @ 1 mole H_2/mole gas produced

= 238 scf/Bbl

(v) Hydrocracking:

The experiments by Wan (52) on similar feedstock showed that about 8 volume % of the 650+ boilers were involved in hydrocracking.

Amount of oil hydrocracked = 0.08 Bbl/Bbl oil

= 28.8 lbs/Bbl oil

= 0.160 lb-mole/Bbl oil

(@ MW = 180)

H_2 consumption rate @ 1 mole H_2/mole hydrocracked

= 0.160 lb-mole/Bbl

= 60.6 scf/Bbl

Total hydrogen consumption rate = 430.5 scf/Bbl oil fed

APPENDIX F

EXPERIMENTAL DATA

Five different types of catalysts were tested during the eight experimental runs. Numerous samples were collected to study the effects of the reactor operating conditions. The reactor conditions selected for each of the samples are listed in Table XXXVII. The actual reactor temperature was held within $\pm$ 3 F (1.8 C) in the catalyst zone (see Figure 13 for a typical temperature profile, Experimental Procedure Chapter). Except for one experimental run, the actual reactor pressure was held within $\pm$ 20 psi of the desired value. During one run, the reactor pressure was mistakenly set a 1,060 psig instead of 1,000 psig. However, the run was not repeated because of the apparent absence of influence of pressure on the sulfur removal capability of the catalyst tested in the previous run. The samples collected are identified by the series name and the order of collection of a particular sample in that series. The reactor space time is presented both as volume hourly (volume of catalyst/volume of oil per hour) and weight hourly (weight of catalyst/weight of oil per hour). The experimental conditions such as hydrogen rate, catalyst size that were held constant during all the runs are listed at the end of the table.

TABLE XXXVII

EXPERIMENTAL DATA

Sample Number	Temp.[a] F	Press.[b] psig	LVHST	LWHST	Hours[c] on Oil	%S[d] Avg.
SP 1	600	1000	2.500	1.173	4	0.133
SP 2	600	1000	2.500	1.173	8	0.102
SP 3	600	1000	2.500	1.173	12	0.072
SP 4	600	1000	2.500	1.173	16	0.076
SP 5	600	1000	2.500	1.173	18	0.067
SP 6	600	1000	1.250	0.587	20	0.082
SP 7	600	1000	1.250	0.587	21	0.103
SP 8	600	1000	0.625	0.294	24	0.152
SP 9	600	1000	0.625	0.294	25	0.177
SP10	600	1000	2.500	1.173	29	0.116
SP11	600	1000	2.500	1.173	31	0.110
SP12	650	1000	2.500	1.173	35	0.062
SP13	650	1000	2.500	1.173	37	0.067
SP14	650	1000	1.250	0.587	40	0.084
SP15	650	1000	1.250	0.587	41	0.100
SP16	650	1000	0.625	0.294	43	0.128
SP17	650	1000	0.625	0.294	44	0.128
SP18	650	1000	2.500	1.173	46	0.080
SP19	650	1000	2.500	1.173	48	0.055
SP20	750	1000	2.500	1.173	53	0.014
SP21	750	1000	2.500	1.173	55	0.013
SP22	750	1000	1.250	0.587	57	0.012
SP23	750	1000	1.250	0.587	58	0.007
SP24	750	1000	0.625	0.294	60	0.047
SP25	750	1000	0.625	0.294	61	0.044
SP26	750	1000	2.500	1.173	65	0.016
SP27	750	1000	2.500	1.173	67	0.017
ASP 1	700	1000	0.925	0.440	9	0.086
ASP 2	700	1000	0.925	0.440	14	0.112
ASP 3	700	1000	0.925	0.440	19	0.113
ASP 4	700	1000	0.925	0.440	25	0.120
ASP 5	700	1000	0.925	0.440	29	0.098
ASP 6	700	1000	0.925	0.440	34	0.115
ASP 7	700	1000	0.925	0.440	39	0.127
ASP 8	700	1000	0.925	0.440	44	0.116
ASP 9	700	1000	0.925	0.440	49	0.064
ASP10	700	1000	0.925	0.440	54	0.112
ASP11	700	1000	0.925	0.440	59	0.160
ASP12	700	1000	0.925	0.440	64	0.124
ASP13	700	1000	0.925	0.440	70	NA
ASP14	700	1000	0.925	0.440	75	0.098
ASP15	700	1000	0.925	0.440	80	0.099
ASP16	700	1000	0.925	0.440	85	0.134

TABLE XXXVII (Continued)

Sample Number	Temp.[a] F	Press.[b] psig	LVHST	LWHST	Hours[c] on Oil	%S[d] Avg.
ASP17	700	1000	0.925	0.440	90	0.108
ASP18	700	1000	0.925	0.440	95	0.104
ASP19	700	1000	0.925	0.440	100	0.103
ASP20	700	1000	0.925	0.440	105	0.118
ASP21	700	1000	0.925	0.440	110	0.110
ASP22	700	1000	0.925	0.440	115	0.135
ASP23	700	1000	0.925	0.440	120	0.077
ASP24	700	1000	0.925	0.440	125	0.103
ASP25	700	1000	0.925	0.440	130	0.054
ASP26	700	1000	0.925	0.440	135	0.121
ASP27	700	1000	0.925	0.440	140	0.072
ASP28	700	1000	0.925	0.440	145	0.157
ASP29	700	1000	0.925	0.440	150	0.124
ASP30	700	1000	0.925	0.440	155	0.101
ASP31	700	1000	0.925	0.440	160	0.104
ASP32	700	1000	0.925	0.440	165	0.108
ASP33	700	1000	0.925	0.440	170	0.059
ASP34	700	1000	0.925	0.440	175	0.110
ASP35	700	1000	0.925	0.440	180	0.069
ASP36	700	1000	0.925	0.440	185	0.130
ASP37	700	1000	0.925	0.440	190	0.112
ASP38	700	1000	0.925	0.440	195	0.120
ASP39	700	1000	0.925	0.440	200	0.113
ASP40	700	1000	0.925	0.440	205	0.087
ANA 1	700	1000	0.640	0.440	7	0.165
ANA 2	700	1000	0.640	0.440	10	0.156
ANA 3	700	1000	0.640	0.440	15	0.142
ANA 4	700	1000	0.640	0.440	20	0.155
ANA 5	700	1000	0.640	0.440	25	0.163
ANA 6	700	1000	0.640	0.440	30	0.189
ANA 7	700	1000	0.640	0.440	35	0.180
ANA 8	700	1000	0.640	0.440	40	0.123
ANA 9	700	1000	0.640	0.440	45	0.183
ANA10	700	1000	0.640	0.440	50	0.103
ANA11	700	1000	0.640	0.440	55	0.105
ANA12	700	1000	0.640	0.440	60	0.112
ANA13	700	1000	0.640	0.440	65	0.096
ANA14	700	1000	0.640	0.440	70	0.126
ANA15	700	1000	0.640	0.440	75	0.110
ANA16	700	1000	0.640	0.440	80	0.101
ANA17	700	1000	0.640	0.440	85	0.102
ANA18	700	1000	0.640	0.440	90	0.110
ANA19	700	1000	0.640	0.440	95	0.137
ANA20	700	1000	0.640	0.440	100	0.122
ANA21	700	1000	0.640	0.440	105	0.128

TABLE XXXVII (Continued)

Sample Number	Temp.[a] F	Press.[b] psig	LVHST	LWHST	Hours[c] on Oil	%S[d] Avg.
ANA22	700	1000	0.640	0.440	110	0.125
ANA23	700	1000	0.640	0.440	115	0.111
ANA24	700	1000	0.640	0.440	120	0.109
ANA25	700	1000	0.640	0.440	125	0.151
ANA26	700	1000	0.640	0.440	130	0.109
ANA27	700	1000	0.640	0.440	135	0.137
ANA28	700	1000	0.640	0.440	140	0.120
ANA29	700	1000	0.640	0.440	145	0.139
ANA30	700	1000	0.640	0.440	150	0.115
ANA31	700	1000	0.640	0.440	155	0.136
ANA32	700	1000	0.640	0.440	160	0.095
ANA33	700	1000	0.640	0.440	165	0.135
ANA34	700	1000	0.640	0.440	170	0.115
ANA35	700	1000	0.640	0.440	175	0.107
ANA36	700	1000	0.640	0.440	180	0.125
ANA37	700	1000	0.640	0.440	185	0.141
ANA38	700	1000	0.640	0.440	190	0.117
ANA39	700	1000	0.640	0.440	195	0.106
ANA40	700	1000	0.640	0.440	200	0.097
NLA 1	700	1000	0.616	0.440	6	0.118
NLA 2	700	1000	0.616	0.440	10	0.119
NLA 3	700	1000	0.616	0.440	15	0.081
NLA 4	700	1000	0.616	0.440	20	0.143
NLA 5	700	1000	0.616	0.440	25	0.084
NLA 6	700	1000	0.616	0.440	30	0.110
NLA 7	700	1000	0.616	0.440	35	0.115
NLA 8	700	1000	0.616	0.440	40	0.111
NLA 9	700	1000	0.616	0.440	45	0.107
NLA10	700	1000	0.616	0.440	50	0.107
NLA11	700	1000	0.616	0.440	55	0.115
NLA12	700	1000	0.616	0.440	60	0.117
NLA13	700	1000	0.616	0.440	65	0.080
NLA14	700	1000	0.616	0.440	70	0.098
NLA15	700	1000	0.616	0.440	75	0.075
NLA16	700	1000	0.616	0.440	80	0.100
NLA17	700	1000	0.616	0.440	85	0.081
NLA18	700	1000	0.616	0.440	90	0.096
NLA19	700	1000	0.616	0.440	95	0.093
NLA20	700	1000	0.616	0.440	100	0.089
NLA21	700	1000	0.616	0.440	105	0.080
NLA22	700	1000	0.616	0.440	110	0.074
NLA23	700	1000	0.616	0.440	115	0.081
NLA24	700	1000	0.616	0.440	120	0.070
NLA25	700	1000	0.616	0.440	125	0.072
NLA26	700	1000	0.616	0.440	130	0.101

TABLE XXXVII (Continued)

Sample Number	Temp.[a] F	Press.[b] psig	LVHST	LWHST	Hours[c] on Oil	%S[d] Avg.
NLA27	700	1000	0.616	0.440	135	0.075
NLA28	700	1000	0.616	0.440	140	0.107
NLA29	700	1000	0.616	0.440	145	0.087
NLA30	700	1000	0.616	0.440	150	0.081
NLA31	700	1000	0.616	0.440	155	0.088
NLA32	700	1000	0.616	0.440	160	0.088
NLA33	700	1000	0.616	0.440	165	0.074
NLA34	700	1000	0.616	0.440	170	0.076
NLA35	700	1000	0.616	0.440	175	0.099
NLA36	700	1000	0.616	0.440	180	0.095
NLA37	700	1000	0.616	0.440	185	0.078
NLA38	700	1000	0.616	0.440	190	0.096
NLA39	700	1000	0.616	0.440	195	0.098
NLA40	700	1000	0.616	0.440	200	0.086
NLA41	700	1000	0.616	0.440	205	0.059
HSW 1	650	1000	1.300	0.880	7	0.152
HSW 2	650	1000	1.300	0.880	10	0.154
HSW 3	650	1000	1.300	0.880	14	0.128
HSW 4	650	1000	1.300	0.880	18	0.135
HSW 5	650	1000	1.300	0.880	22	0.174
HSW 6	650	1000	1.300	0.880	26	0.160
HSW 7	650	1000	1.300	0.880	30	0.122
HSW 8	650	1000	1.300	0.880	34	0.149
HSW 9	650	1000	1.300	0.880	38	0.110
HSW10	650	1000	1.300	0.880	42	0.127
HSW11	650	1000	1.300	0.880	46	0.114
HSW12	650	1000	1.300	0.880	50	0.104
HSW13	650	1000	0.650	0.440	54	0.194
HSW14	650	1000	0.650	0.440	56	0.157
HSW15	650	1000	0.325	0.220	57	0.198
HSW16	650	1000	0.325	0.220	58	0.182
HSW17	650	1500	0.325	0.220	65	0.205
HSW18	650	1500	0.325	0.220	66	0.170
HSW19	650	1500	0.650	0.440	70	0.221
HSW20	650	1500	0.650	0.440	71	0.156
HSW21	650	1500	1.300	0.880	75	0.121
HSW22	650	1500	1.300	0.880	77	0.104
HSW23	650	500	1.300	0.880	82	0.141
HSW24	650	500	1.300	0.880	84	0.114
HSW25	650	500	0.650	0.440	87	0.175
HSW26	650	500	0.650	0.440	89	0.159
HSW27	650	500	0.325	0.220	92	0.217
HSW28	650	500	0.325	0.220	93	0.192
HSW29	650	1000	1.300	0.880	96	0.133
HSW30	650	1000	1.300	0.880	98	0.102

TABLE XXXVII (Continued)

Sample Number	Temp.[a] F	Press.[b] psig	LVHST	LWHST	Hours[c] on Oil	%S[d] Avg.
HSW31	700	1000	1.300	0.880	106	0.089
HSW32	700	1000	1.300	0.880	108	0.086
HSW33	700	1000	0.650	0.440	114	0.140
HSW34	700	1000	0.650	0.440	116	0.119
HSW35	700	1000	0.325	0.220	121	0.156
HSW36	700	1000	0.325	0.220	122	0.124
HSW37	700	1500	0.325	0.220	127	0.175
HSW38	700	1500	0.325	0.220	128	0.112
HSW39	700	1500	0.650	0.440	135	0.116
HSW40	700	1500	0.650	0.440	137	0.088
HSW41	700	1500	1.300	0.880	144	0.160
HSW42	700	1500	1.300	0.880	146	0.049
HSW43	700	500	1.300	0.880	150	0.059
HSW44	700	500	1.300	0.880	152	0.060
HSW45	700	500	0.650	0.440	155	0.087
HSW46	700	500	0.650	0.440	156	0.126
HSW47	700	500	0.325	0.220	161	0.116
HSW48	700	500	0.325	0.220	162	0.143
HSW49	700	1000	1.300	0.880	166	0.091
HSW50	700	1000	1.300	0.880	168	0.045
HSW51	750	1000	1.300	0.880	175	0.071
HSW52	750	1000	1.300	0.880	177	0.085
HSW53	750	1000	0.650	0.440	181	0.064
HSW54	750	1000	0.650	0.440	183	0.038
HSW55	750	1000	0.325	0.220	186	0.083
HSW56	750	1000	0.325	0.220	187	0.094
HSW57	750	1500	0.325	0.220	194	0.123
HSW58	750	1500	0.325	0.220	195	0.091
HSW59	750	1500	0.650	0.440	199	0.114
HSW60	750	1500	0.650	0.440	201	0.065
HSW61	750	1500	1.300	0.880	208	0.050
HSW62	750	1500	1.300	0.880	210	0.050
HSW63	750	500	1.300	0.880	215	0.064
HSW64	750	500	1.300	0.880	219	0.032
HSW65	750	500	0.650	0.440	223	0.063
HSW66	750	500	0.650	0.440	225	0.057
HSW67	750	500	0.325	0.220	228	NA
HSW68	750	500	0.325	0.220	229	NA
HSW69	750	1000	1.300	0.880	234	NA
HSW70	750	1000	1.300	0.880	236	NA
HRW 1	700	1000	0.650	0.440	8	0.177
HRW 2	700	1000	0.650	0.440	15	0.136
HRW 3	700	1000	0.650	0.440	18	0.165
HRW 4	700	1000	0.650	0.440	21	0.197
HRW 5	700	1000	0.650	0.440	25	0.182

TABLE XXXVII (Continued)

Sample Number	Temp.[a] F	Press.[b] psig	LVHST	LWHST	Hours[c] on Oil	%S[d] Avg.
HRW 6	700	1000	0.650	0.440	30	0.173
HRW 7	700	1000	0.650	0.440	35	0.131
HRW 8	700	1000	0.650	0.440	40	0.156
HRW 9	700	1000	0.650	0.440	45	0.151
HRW10	700	1000	0.650	0.440	50	0.155
HRW11	700	1000	0.650	0.440	55	0.145
HRW12	700	1000	0.650	0.440	60	0.149
HRW13	700	1000	0.650	0.440	65	0.153
HRW14	700	1000	0.650	0.440	70	0.148
HRW15	700	1000	0.650	0.440	75	0.142
HRW16	700	1000	0.650	0.440	80	0.131
HRW17	700	1000	0.650	0.440	85	0.138
HRW18	700	1000	0.650	0.440	90	0.123
HRW19	700	1000	0.650	0.440	95	0.149
HRW20	700	1000	0.650	0.440	100	0.140
HRW21	700	1000	0.650	0.440	105	0.131
HRW22	700	1000	0.650	0.440	110	0.150
HRW23	700	1000	0.650	0.440	115	0.141
HRW24	700	1000	0.650	0.440	120	0.142
HRW25	700	1000	0.650	0.440	125	0.133
HRW26	700	1000	0.650	0.440	130	0.140
HRW27	700	1000	0.650	0.440	135	0.135
HRW28	700	1000	0.650	0.440	140	0.136
HRW29	700	1000	0.650	0.440	145	0.133
HRW30	700	1000	0.650	0.440	150	0.135
HRW31	700	1000	0.650	0.440	155	0.128
HRW32	700	1000	0.650	0.440	160	0.121
HRW33	700	1000	0.650	0.440	165	0.127
HRW34	700	1000	0.650	0.440	170	0.128
HRW35	700	1000	0.650	0.440	175	0.128
HRW36	700	1000	0.650	0.440	180	0.124
HRW37	700	1000	0.650	0.440	185	0.123
HRW38	700	1000	0.650	0.440	190	0.137
HRW39	700	1000	0.650	0.440	195	0.125
HRW40	700	1000	0.650	0.440	200	0.159
NAL 1	650	1000	1.480	0.880	7	0.152
NAL 2	650	1000	1.480	0.880	9	0.112
NAL 3	650	1000	1.480	0.880	12	0.107
NAL 4	650	1000	1.480	0.880	16	0.109
NAL 5	650	1000	1.480	0.880	20	0.143
NAL 6	650	1000	1.480	0.880	24	0.122
NAL 7	650	1000	1.480	0.880	28	0.134
NAL 8	650	1000	1.480	0.880	32	0.185
NAL 9	650	1000	1.480	0.880	36	0.115
NAL10	650	1000	1.480	0.880	40	0.088

TABLE XXXVII (Continued)

Sample Number	Temp.[a] F	Press.[b] psig	LVHST	LWHST	Hours[c] on Oil	%S[d] Avg.
NAL11	650	1000	1.480	0.880	44	0.139
NAL12	650	1000	1.480	0.880	48	0.108
NAL13	650	1000	0.740	0.440	50	0.143
NAL14	650	1000	0.740	0.440	52	0.163
NAL15	650	1000	0.740	0.440	54	0.173
NAL16	650	1000	0.370	0.220	55	0.175
NAL17	650	1000	0.370	0.220	56	0.202
NAL18	650	1000	0.370	0.220	57	0.215
NAL19	650	1000	1.480	0.880	59	0.130
NAL20	650	1000	1.480	0.880	61	0.108
NAL21	650	1000	1.480	0.880	63	0.118
NAL22	700	1000	1.480	0.880	67	0.069
NAL23	700	1000	1.480	0.880	69	0.048
NAL24	700	1000	1.480	0.880	71	0.092
NAL25	700	1000	0.740	0.440	73	0.142
NAL26	700	1000	0.740	0.440	75	0.066
NAL27	700	1000	0.740	0.440	77	0.068
NAL28	700	1000	0.370	0.440	78	0.105
NAL29	700	1000	0.370	0.440	79	0.111
NAL30	700	1000	0.370	0.440	80	0.102
NAL31	700	1000	1.480	0.880	82	0.096
NAL32	700	1000	1.480	0.880	84	0.041
NAL33	700	1000	1.480	0.880	86	0.064
NAL34	750	1000	1.480	0.880	90	0.042
NAL35	750	1000	1.480	0.880	92	0.025
NAL36	750	1000	1.480	0.880	94	0.040
NAL37	750	1000	0.740	0.440	96	0.121
NAL38	750	1000	0.740	0.440	98	0.044
NAL39	750	1000	0.740	0.440	100	0.183
NAL40	750	1000	0.493	0.294	101	0.108
NAL41	750	1000	0.493	0.294	102	0.050
NAL42	750	1000	0.493	0.294	103	0.039
NAL43	750	1000	1.480	0.880	105	0.038
NAL44	750	1000	1.480	0.880	107	0.034
NAL45	750	1000	1.480	0.880	109	0.062
NAC 1	700	1000	0.740	0.440	8	0.100
NAC 2	700	1000	0.740	0.440	12	0.077
NAC 3	700	1000	0.740	0.440	15	0.064
NAC 4	700	1000	0.740	0.440	20	0.071
NAC 5	700	1000	0.740	0.440	25	0.077
NAC 6	700	1000	0.740	0.440	30	0.073
NAC 7	700	1000	0.740	0.440	35	0.086
NAC 8	700	1000	0.740	0.440	40	0.108
NAC 9	700	1000	0.740	0.440	45	0.083
NAC10	700	1000	0.740	0.440	50	0.086

TABLE XXXVII (Continued)

Sample Number	Temp.[a] F	Press.[b] psig	LVHST	LWHST	Hours[c] on Oil	%S[d] Avg.
NAC11	700	1000	0.740	0.440	55	0.081
NAC12	700	1000	0.740	0.440	60	0.072
NAC13	700	1000	0.740	0.440	65	0.128
NAC14	700	1000	0.740	0.440	70	0.073
NAC15	700	1000	0.740	0.440	75	0.078
NAC16	700	1000	0.740	0.440	80	0.078
NAC17	700	1000	0.740	0.440	85	0.083
NAC18	700	1000	0.740	0.440	90	0.076
NAC19	700	1000	0.740	0.440	95	0.065
NAC20	700	1000	0.740	0.440	100	0.094
NAC21	700	1000	0.740	0.440	105	0.089
NAC22	700	1000	0.740	0.440	110	0.086
NAC23	700	1000	0.740	0.440	115	0.086
NAC24	700	1000	0.740	0.440	120	0.070
NAC25	700	1000	0.740	0.440	125	0.083
NAC26	700	1000	0.740	0.440	130	0.070
NAC27	700	1000	0.740	0.440	135	0.090
NAC28	700	1000	0.740	0.440	140	0.075
NAC29	700	1000	0.740	0.440	145	0.089
NAC30	700	1000	0.740	0.440	150	0.059
NAC31	700	1000	0.740	0.440	155	0.053
NAC32	700	1000	0.740	0.440	160	0.059
NAC33	700	1000	0.740	0.440	165	0.053
NAC34	700	1000	0.740	0.440	170	0.060
NAC35	700	1000	0.740	0.440	175	0.065
NAC36	700	1000	0.740	0.440	180	0.054
NAC37	700	1000	0.740	0.440	185	0.096
NAC38	700	1000	0.740	0.440	190	0.063
NAC39	700	1000	0.740	0.440	195	0.079
NAC40	700	1000	0.740	0.440	200	0.073

[a] Nominal reactor temperature.

[b] Nominal reactor pressure.

[c] Total hours which the catalyst has been in contact with oil.

[d] Average weight percent sulfur in the product oil.

The hydrogen flow rate to the reactor was held steady at 1500 SCF/Bbl during all the experimental runs.

The particle sizes of catalyst and inert were 8-10 mesh during all the experimental runs.

APPENDIX G

ESTIMATION OF PARTICLE PECLET NUMBER

The particle Peclet number (Pe_m) for the cocurrent flow in a trickle bed reactor is estimated using the model developed by Hockman and Effron (40). The model is applicable to the condition when the liquid side Reynolds number (Re_L) is between 4 and 100. The liquid side Reynolds number is needed to estimate the Peclet number.

Reynolds number estimation:

$$Re_L = \frac{d_p \cdot V_L \cdot \rho_L}{\mu_L}$$

for the experiments in this study,

average catalyst particle diameter = 0.2 cm = d_p

average liquid flow rate = 40 cc/hr

cross-section area available for the flow of liquid = 0.296 cm^2

average liquid density = 1.1365 gm/cc = ρ_L

average liquid velocity = 135.1 cm/hr = V_L

average liquid viscosity = 0.05 cp = 1.8 gm/cm-hr = μ_L

These values are then substituted in the above equation to give

$$Re_L = \frac{0.2 \times 135.1 \times 1.1365}{1.8}$$

$$Re_L = 17.06$$

Peclet number estimation:

The Hockman and Effron model to estimate Peclet number is -

$$Pe_m = 0.042 \times Re_L^{0.5}$$

$$Pe_m = 0.042 \times (17.06)^{0.5}$$

$$Pe_m = 0.1735$$

APPENDIX H

DIFFUSION COEFFICIENTS OF THE REACTANTS

The principal reactants involved in the HDS reaction were hydrogen and sulfur containing compounds. Greenwood (94) determined that the most frequently occurring sulfur containing compound (about 74%) in the anthracene feedstock was dibenzothiophene. Therefore, dibenzothiophene is considered here to represent the sulfur containing compounds. The diffusion coefficients of the reactants are calculated from a correlation developed by Wilke (124) for diffusion in liquids. The correlation is as follows:

$$D_L = 7.4 \times 10^{-8} \times \frac{(A \times M)^{0.5} \times T}{\mu \times (V_b)^{0.6}}$$

where, D_L = diffusion coefficient of the solute, cm^2/sec

A = "association parameter" for solvent

M = molecular weight of the solvent

μ = viscosity of the solvent, cp

V_b = molar volume of the solute, cc/gm-mole

T = temperature, K

For the present study, these variables have the magnitudes as shown.

M = 208

μ = 0.05 cp (by extrapolation)

T = 644.4 K (700 F)

$A = 1.0$

(i) Diffusion coefficient of hydrogen

$V_b = 14.3$

$$D_L = \frac{7.4 \times 10^{-8} \times (1 \times 208)^{0.5} \times 644.4}{0.05 \times (14.3)^{0.6}}$$

$D_L = 2.788 \times 10^{-3}$ cm^2/sec

(ii) Diffusion coefficient of dibenzothiophene

$V_b = 191.3$

$$D_L = \frac{7.4 \times 10^{-8} \times (1 \times 208)^{0.5} \times 644.4}{0.05 \times (191.3)^{0.6}}$$

$D_L = 5.881 \times 10^{-4}$cm^2/sec

APPENDIX I

ESTIMATION OF Φ AND η

$$\Phi = \frac{R}{3}\left[\frac{k \cdot C_s^{m-1}}{D_{eff}}\right]^{0.5}$$

where, R = particle diameter, cm

k = reaction rate constant, 1/(hr x conc.)

C_s = % S in feed oil

D_{eff} = diffusivity of the sulfur compound, cm^2/sec

Therefore,

$$\Phi = \frac{0.2}{3}\left[\frac{10 \times 0.47}{3600 \times 5.881 \times 10^{-4}}\right]^{0.5}$$

$$\Phi = \frac{0.2}{3} \times (2.200)^{0.5}$$

$$\Phi = 0.09933$$

$$\eta = \frac{1}{3\Phi^2} \times (3\Phi \ \text{Coth}\ 3\Phi - 1)$$

$$\eta = \frac{1}{3(0.09933^2} \left[3 \times (0.09933) \times \text{Coth}\ (3 \times 0.09933) - 1\right]$$

$$\eta = \frac{1}{0.02960} \ 0.2980 \times \text{Coth}\ (0.2980) - 1$$

$$\eta = \frac{1}{0.02960} \times (0.2980 \times 3.4529 - 1)$$

$$\eta = \frac{1}{0.02966} \times (1.028964 - 1)$$

$$\eta = 0.979$$

APPENDIX J

CALCULATION OF TEMPERATURE GRADIENT IN CATALYST PORES

The temperature in the catalyst pores has a bearing on the diffusion of the reactants, and thereby, on the overall HDS reaction rate. Drastic deviations of temperature in the catalyst pores could lead to erroneous temperature effect conclusions. The internal temperature of the catalyst pores can be calculated from the heat of reaction effects.

Satterfield (90) developed a correlation to estimate the temperature gradient in the catalyst pores. The correlation is:

$$(T_c - T_s) = \frac{(-\Delta H)(D_{eff})}{\lambda} (C_s - C_c)$$

where, ΔH = heat of reaction = -28,730 cal/mole

D_{eff} = effective diffusivity of sulfur containing compounds = 5.881×10^{-4} cm^2/sec

λ = thermal conductivity of alumina = 6.2×10^{-4} cal/sec cm C

C_s = concentration of sulfur at surface = 0.0048×10^{-2} mole/cc

C_c = concentration of sulfur at center = 0

Substituting all these values in the above equation,

$$T_c - T_s = \frac{(28730)\ (5.881 \times 10^{-4})}{6.2 \times 10^{-4}} \times (0.0048 \times 10^{-2})$$

$$= 1.26\ C = 2.3\ F$$

This gradient was no greater than the temperature variations in the other sections of the reactor. Therefore, the temperature gradient in the catalyst pores was not considered to have any noticeable effect on the overall HDS reaction rate.

APPENDIX K

CALCULATION OF ACTIVATION ENERGY

The calculations for a typical case are shown here. The values for k and T are from Table XXIX for MCM 4 catalyst at 1,000 psig.

Temp., F	k
650	5.787 (cu ft)^2/mole hr
700	7.563
750	12.430

It is assumed that the relation between k and T can be represented by the Arrhenius expression.

$$k = A \cdot e^{-E/RT}$$

$$\text{or } \ln k = \ln A - E/RT$$

The activation energy is computed from the above data and linear regression technique

$$E = 20{,}302 \text{ Btu/lb mole}$$

VITA 2

Dhirendra Chhotalal Mehta

Candidate for the Degree of

Doctor of Philosophy

Thesis: CATALYST AGING TESTS AND THE ROLE OF CATALYST WETTING ON HYDRODESULFURIZATION OF A COAL DERIVED LIQUID

Major Field: Chemical Engineering

Biographical:

Personal Data: Born in Bombay, India, on December 2, 1948, to Mangla and Chhotalal Mehta.

Education: Graduated from S. M. C. High School in Poona, India, in 1964; received Bachelor of Science degree in Chemical Engineering from Banaras Hindu University, Varanasi, India in March, 1970; received Master of Science degree in Chemical Engineering from Oklahoma State University, Stillwater, Oklahoma in July, 1972; completed requirements for the Doctor of Philosophy degree at Oklahoma State University in May, 1978.

Professional Experience: Engineering trainee at Excel Industries Ltd., Bombay, India, summer 1969; Graduate Teaching Assistant, Oklahoma State University, Stillwater, Oklahoma, January, 1972 to May, 1973; Graduate Research Assistant, Oklahoma State University, June, 1973 to October, 1975; Employed at Combustion Equipment Associates, Inc., from October, 1975 to present.